MIT-2344-7
MITNE-73

MASSACHUSETTS INSTITUTE OF TECHNOLOGY
DEPARTMENT OF NUCLEAR ENGINEERING
Cambridge, Massachusetts 02139

USE OF A PULSED NEUTRON SOURCE TO DETERMINE NUCLEAR PARAMETERS OF LATTICES OF PARTIALLY ENRICHED URANIUM RODS IN HEAVY WATER

by
H. E. Bliss, I. Kaplan, T. J. Thompson

September 1966

Contract AT (30-1) 2344
U.S. Atomic Energy Commission

MASSACHUSETTS INSTITUTE OF TECHNOLOGY

DEPARTMENT OF NUCLEAR ENGINEERING

Cambridge 39, Massachusetts

USE OF A PULSED NEUTRON SOURCE TO DETERMINE NUCLEAR PARAMETERS OF LATTICES OF PARTIALLY ENRICHED URANIUM RODS IN HEAVY WATER

by

H. E. Bliss, I. Kaplan, T. J. Thompson

September 1966

MIT - 2344 - 7

MITNE - 73

AEC Research and Development Report

UC - 34 Physics

(TID - 4500, 47th Edition)

Contract AT(30-1)2344

U. S. Atomic Energy Commission

DISTRIBUTION

MIT-2344-7 MITNE-73

AEC Research and Development Report

UC-34 Physics

(TID-4500, 47th Edition)

1. USAEC, New York Operations Office (D. Richtmann)
2. USAEC, Division of Reactor Development (P. Hemmig)
3-5. USAEC, Division of Reactor Development (I. Zartman)
6. USAEC, Division of Reactor Development (S. Strauch)
7. USAEC, Division of Reactor Development (H. Honeck)
8. USAEC, New York Patents Office (H. Potter)
9. USAEC, New York Operations Office (H. Fish)
10. USAEC, New York Operations Office, Research and Development Division
11. USAEC, Maritime Reactors Branch
12. USAEC, Civilian Reactors Branch
13. USAEC, Army Reactors Branch
14. USAEC, Naval Reactor Branch
15. Advisory Committee on Reactor Physics (E. R. Cohen)
16. ACRP (G. Dessauer)
17. ACRP (D. de Bloisblanc)
18. ACRP (M. Edlund)
19. ACRP (R. Ehrlich)
20. ACRP (I. Kaplan)
21. ACRP (J. Chernick)
22. ACRP (F. C. Maienschein)
23. ACRP (R. Avery)
24. ACRP (P. F. Zweifel)
25. ACRP (P. Gast)
26. ACRP (G. Hansen)
27. ACRP (S. Krasik)
28. ACRP (L. W. Nordheim)
29. ACRP (T. M. Snyder)
30. ACRP (J. J. Taylor)
31-33. O.T.I.E., Oak Ridge, for Standard Distribution
34-150. Internal Distribution

ABSTRACT

The pulsed neutron technique has been used to determine the nuclear parameters of a number of subcritical lattices of slightly enriched uranium metal rods in heavy water. Experimental values of the fundamental mode decay constant λ and geometric buckling B^2 have been related to the multiplication factor k_∞ and the absorption cross section $\overline{v\Sigma}_a$ by a two-group model. The thermal diffusion area ($L^2 \equiv \overline{vD}_o/\overline{v\Sigma}_a$) has also been obtained with calculated values of $\overline{vD}_o$. The values of k_∞ are generally in agreement, within experimental uncertainties, with values obtained with the method of added absorbers, with the four-factor formula, and with the two-group critical equation. The values of $\overline{v\Sigma}_a$ and L^2 are in agreement with the values computed with the THERMOS code.

The overall uncertainties in the values of k_∞ vary from 1.5% to 4.5% with the larger values attributed to statistical fluctuations in the experimental data. Known systematic sources of error presently limit the accuracy of the pulsed neutron method to between 1.0% and 1.5%.

Measurements have been made in two-region assemblies; the values of k_∞ obtained in the test region agree, within experimental uncertainties, with those obtained with the four-factor formula in lattices composed entirely of the test region medium.

Values of k_∞ and $\overline{v\Sigma}_a$ in lattices successively modified by the addition of a distributed neutron absorber have been obtained which are more accurate than those determined from pulsed neutron measurements on the unmodified lattices alone.

A value of 0.44 ± 0.05 has been determined for the return coefficient of thermal neutrons from the graphite-lined cavity below the M. I. T. Lattice Facility experimental tank.

ACKNOWLEDGEMENTS

The success of the M. I. T. Heavy Water Lattice Project has been due to the contributions of a number of individuals. The results of this report are due primarily to the work of the principal author, Henry Edison Bliss, who has submitted substantially this same report in partial fulfillment of the requirements for the Sc. D. degree at M. I. T. He has been assisted by other graduate students as well as by those mentioned below.

Overall direction of the project during the period of this research was shared by Professors I. Kaplan, T. J. Thompson, D. D. Lanning, and M. J. Driscoll. Messrs. Joseph Barch, Albert Supple, and Norman Berube have provided great assistance in the experimental work. Dr. B. K. Malaviya worked closely with the author in the early phases of this endeavor.

The staffs of the M. I. T. Reactor, the Reactor Machine Shop, the Radiation Protection Office, and the Reactor Electronics Shop have given advice and assistance throughout the experimental portion of this work. Mr. David Gwinn designed the pulsed neutron equipment and has been very helpful in keeping it in operating condition. Mrs. Mary Bosco has ably typed the final manuscript. The reduction of data was done in part at the M. I. T. Computation Center.

The encouragement and support of the author's wife and parents have been instrumental to the success and completion of this work.

The author would like to thank the U. S. Atomic Energy Commission through its Special Fellowship Program in Nuclear Science and Engineering and the Fannie and John Hertz Foundation for financial support during the period of this work.

TABLE OF CONTENTS

LIST OF FIGURES

LIST OF TABLES

CHAPTER I

INTRODUCTION

1.1 THE M. I. T. HEAVY WATER LATTICE PROJECT

The Department of Nuclear Engineering at M. I. T., with the support of the United States Atomic Energy Commission, has undertaken a program of experimental and theoretical studies of the physics of D_2O-moderated lattices of slightly enriched uranium rods.

The primary purpose of this program is to improve the understanding of the physics of heavy water lattices. The emphasis of the program has therefore been on the adaptation of existing methods and, where possible, the development of new methods for determining basic lattice parameters; on the comparison of experimental results with theoretical predictions; and on the refinement and extension of existing theoretical models.

The results of the program have been summarized in annual progress reports and in individual reports. Bibliographies of the Lattice Project publications may be found in Refs. H4 (prior to September, 1965) and H5 (after September, 1965).

1.2 IMPORTANCE OF THE PULSED NEUTRON SOURCE TECHNIQUE

Low power critical assemblies and subcritical (exponential) facilities have been used extensively for obtaining basic reactor physics data. These facilities are not encumbered by the difficulties which usually are inherent in the use of operating power reactors for this purpose, and they offer the advantage of versatility in the types of reactor core configurations which may be examined. Experimental methods have been adapted or developed at M. I. T. for research on buckling (P1), fast fission (W4), resonance capture (W2, D3), and thermal capture (B3, S2). These methods may be supplemented by research in areas of single rod measurements (P5), miniature lattice work (P3, S1), studies of lattices with distributed neutron absorber (H1), measurements of fast neutron distributions (W5), two-region lattice studies (G6), and pulsed neutron

source methods (M1).

The pulsed neutron method, therefore, represents one of the methods which can be applied to the study of subcritical neutron-multiplying assemblies. The basic technique in the method consists of introducing a short burst of high energy neutrons into a medium of interest and then following the variation of the neutron density with time after the end of the burst. Values of the prompt neutron decay constant obtained from measurements of the neutron density as a function of time have been used to evaluate lattice parameters of subcritical systems. Two of the most important are the parameters k_∞ and L^2 which are difficult to measure in steady-state experiments in subcritical assemblies. In addition, pulsed neutron experiments can be used to obtain the prompt neutron lifetime and absolute reactivity of a subcritical lattice.

The pulsed neutron source technique is attractive as a means for studying subcritical assemblies because it is relatively simple to apply; it provides its own supply of neutrons and, hence, does not require a reactor thermal column or other driving source; and it yields results of reasonable accuracy.

1.3 OBJECTIVES OF THE PRESENT WORK

The first objective in the present work is to measure, with the pulsed neutron source technique, the basic parameters of interest in subcritical lattices also studied by steady-state techniques at the M.I.T. Lattice Facility. Malaviya (M1) showed that such measurements are feasible and reported values of lattice parameters for one lattice. The aim, therefore, is to extend these measurements to several new lattices in order to build up a backlog of information against which the several theoretical models may be tested.

The second objective is to improve the experimental techniques and methods of data analysis where possible. Included in this objective is determining the limits on the accuracy to which the various lattice parameters can be measured by the pulsed source method.

The final objective is to set up techniques for making pulsed neutron measurements in two-region lattices and in lattices with distributed neutron absorbers. Such lattices have been studied by steady-

state methods, and pulsed neutron measurements in these lattices are attractive as refinements to the standard subcritical techniques. A part of the effort has been devoted to developing a method for analyzing the pulsed neutron experiments in these lattices and to comparing the results with those obtained by the steady-state methods.

1.4 CONTENTS OF THE REPORT

Chapter II contains the theoretical treatment of the pulsed neutron source experiment as applied to the configurations investigated in this work. The experimental methods are discussed in Chap. III. Chapter IV describes the analysis of the data and Chap. V gives the results of this work. The main body of the report concludes in Chap. VI which summarizes the results and offers suggestions for the future. The appendices contain, in order, a description of computer codes, the methods for calculating theoretical values of lattice parameters, measurement of higher mode decay constants and coefficients, and bibliography.

CHAPTER II

THEORETICAL METHODS

The theoretical basis of the pulsed neutron source experiments is discussed in this chapter. The basic features of the slowing down and diffusion processes are described, first qualitatively, and then quantitatively, on a Fermi age-diffusion model. Next, the treatment is extended to two-region and absorber-modified lattices. In the final sections of this chapter, the assumptions made in developing the model are investigated and, where possible, eliminated.

2.1 QUALITATIVE DESCRIPTION OF THE KINETICS OF AN ASSEMBLY IRRADIATED BY A BURST OF FAST NEUTRONS

The basic process in the pulsed neutron source technique begins with the introduction of a short burst of neutrons into the medium of interest. First, consider the medium to be non-multiplying. The neutrons interact with the nuclei of the medium and lose energy through elastic and inelastic collisions. During this slowing down phase, some of the neutrons are removed from the medium by leakage and absorption. Eventually, the remaining neutrons reach an asymptotic energy distribution characteristic of the scattering, absorption, and leakage properties of the medium. Recent theoretical work (C1) indicates that, for very small assemblies, the neutron distribution should not reach an asymptotic state. This feature will not be discussed further because the assemblies considered in this report are well above the maximum size at which the effect is predicted to occur.

Once the neutron population has thermalized (e. g., become asymptotic), the shape of the energy distribution remains constant with time while its amplitude decays at a rate ultimately controlled by the lowest eigenvalue characterizing the medium. The process terminates when the thermalized neutrons have all undergone adsorption by the medium or leakage from the medium.

If the medium under consideration possesses multiplying properties, the preceding description needs modification to include the effects

of multiplication. One must consider lattice produced neutrons as well as source produced neutrons. Those source neutrons which escape leakage and capture during the slowing down phase constitute the "zeroth" generation of thermal neutrons. Some of these thermal neutrons induce fission and produce further fast neutrons which, along with those neutrons produced in fast and epithermal fission, thermalize and constitute the first generation of thermal neutrons. This process continues, with the ratio of thermal neutrons in the $(n+1)^{st}$ generation to those in the n^{th} generation equal (by definition) to the effective multiplication factor (k_{eff}) of the medium. For a subcritical assembly, the effective multiplication factor is less than unity and the overall neutron population decreases with time.

In the succeeding sections of this chapter, the above described processes are put in quantitative form. The emphasis in this paper is placed on adapting the treatment to fit the various configurations investigated experimentally as well as examining the validity of several assumptions usually made in the analysis of pulsed neutron source experiments.

2.2 QUANTITATIVE TREATMENT OF THE KINETICS OF AN ASSEMBLY IRRADIATED BY A BURST OF FAST NEUTRONS

In this section, the basic equations describing the kinetics of an assembly irradiated by a burst of fast neutrons are developed. The model used for the description is Fermi age-diffusion theory, although other models, such as two-group or multigroup theory, may also be applied. The expressions obtained from these latter treatments are compared with that of the Fermi age-diffusion result in the last section of this chapter.

The assumptions made in the treatment are:

1) the neutrons from the pulsed source appear in the assembly instantaneously as fast neutrons,

2) the system is bare and homogeneous,

3) the effect of delayed neutrons is neglected except as applied to neutron multiplication,

4) fission during the neutron slowing down process is neglected, and

5) the slowing down time for neutrons arising from thermal fission is assumed negligible.

The effect of these assumptions is examined in the last section of this chapter and, where possible, the development is repeated with the assumption relaxed. All five assumptions are made in the treatment of multiplying media; only the first two are required for moderating media.

The development takes place in four steps. First, the spatial distribution of fast neutrons, in the assembly, from the pulsed source is derived. Next, the slowing down of the source neutrons in the medium is examined under the assumption of a continuous slowing down model. The third and fourth steps describe the diffusion of thermal neutrons in non-multiplying and multiplying media, respectively.

2.2.1 Spatial Distribution of Neutrons from the Pulsed Neutron Source

A knowledge of the spatial distribution of neutrons from the pulsed source is important because it provides an insight into the problem of determining the thermal neutron distribution as a function of time following the injection of the fast neutron burst. A "first collision" model is used to describe the source distribution. In other words, a neutron begins the slowing down process at the location (in space and time) of its first collision and not at its point of production (the pulsed neutron source). This procedure is reasonable when one considers that the mean free path of 14.7 Mev neutrons in heavy water is approximately 30 centimeters. Thus, the source neutrons are distributed over a large volume of the medium when they begin the slowing down process.

Although a more detailed description of the M. I. T. Lattice Facility and associated pulsed neutron source equipment is given in Chap. III, certain features of the Facility are shown schematically in Fig. 2.1. The assembly being irradiated is cylindrical, with height H and radius R. The pulsed neutron source is located at a distance b above the top of the assembly, is centered on the axis (to achieve azimuthal symmetry), and emits isotropically S_o neutrons per burst.

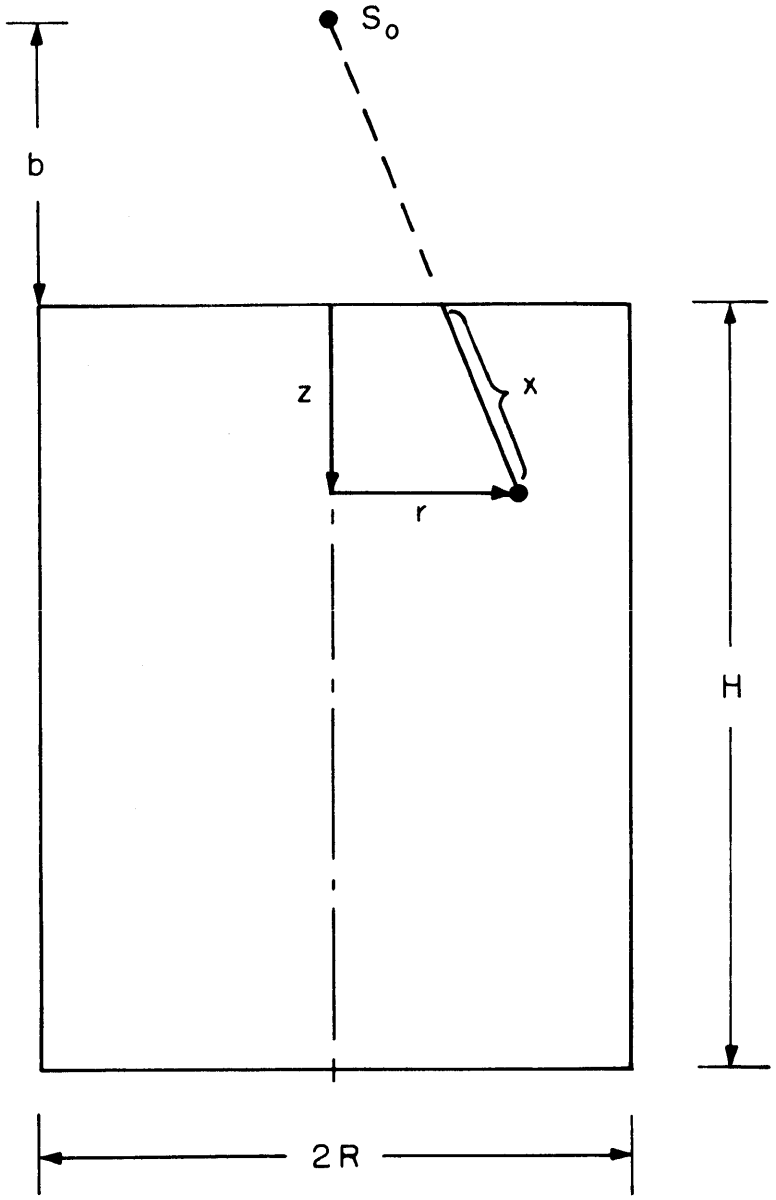

FIG. 2.1 SCHEMATIC DRAWING OF SUBCRITICAL ASSEMBLY AND PULSED NEUTRON SOURCE

The number of source neutrons reaching the location (r, z) in the absence of interaction with nuclei in the assembly is:

$$S''(r,z) = \frac{S_o}{4\pi(r^2+(b+z)^2)} . \tag{2.1}$$

In view of the fact that some of these neutrons interact with assembly nuclei before reaching (r, z), Eq. (2.1) should be multiplied by the probability that a neutron travels a distance x through the assembly and then suffers a collision in the distance dx:

$$P(x)dx = \Sigma e^{-\Sigma x}\, dx, \tag{2.2}$$

where Σ is the macroscopic removal cross section of the assembly for source neutrons. It can easily be shown that x is related to r and z:

$$x = z\sqrt{1 + (r/(b+z))^2} . \tag{2.3}$$

Hence, one obtains:

$$\begin{aligned} S(r,z) &= S''(r,z)P(r,z) \\ &= S_o\left(\frac{\Sigma}{4\pi}\right) \frac{e^{-\Sigma z\sqrt{1+(r/(b+z))^2}}}{r^2 + (b+z)^2} \\ &= S_o S'(r,z). \end{aligned} \tag{2.4}$$

This expression for the spatial distribution of source neutrons, when multiplied by appropriate terms governing time and energy dependence, is the source term to be used in the slowing down equation which is treated in the next section.

2.2.2 Slowing Down Phase

In this section, the Fermi age model for neutron transport is solved for a non-multiplying, weakly absorbing medium irradiated by a burst of fast neutrons. This model is chosen because it offers a clear description of the neutron behavior during the slowing down phase and provides a logical transition to the thermal diffusion phase which is the subject of the next two sections. A discussion of the restrictions involved in the use of Fermi age theory is given in Ref. G1. A more

complete treatment of the material presented here may be found in Ref. M1.

The basic time-dependent Fermi age equation may be written as:

$$\nabla^2\chi(\vec{r},\tau,t) - \frac{\partial}{\partial\tau}\chi(\vec{r},\tau,t) + \frac{S(\vec{r},\tau,t)}{p(0,\tau)} = \frac{1}{vD(\tau)}\frac{\partial}{\partial t}\chi(\vec{r},\tau,t), \tag{2.5}$$

where $\chi(\vec{r},\tau,t)$ is the slowing down density without absorption, τ is the Fermi age (G4), $p(0,\tau)$ is the infinite medium resonance escape probability, and the source term, $S(\vec{r},\tau,t)$, is given by:

$$S(\vec{r},\tau,t) = S(r,z)\delta(\tau)\delta(t). \tag{2.6}$$

The delta function representation in Eq. (2.6) is reasonably accurate because all source neutrons have the same energy (14.7 Mev) and leave the source at the same time (the difference in flight time between top and bottom of the assembly for 14.7 Mev neutrons is on the order of 20 nanoseconds which is negligible, compared to the slowing down scale of microseconds). The slowing down density with absorption, $q(\vec{r},\tau,t)$, is obtained by the transformation:

$$q(\vec{r},\tau,t) = p(0,\tau)\chi(\vec{r},\tau,t). \tag{2.7}$$

Equation (2.5) is solved with the aid of the Laplace Transform Technique (H7). Denoting the transform variable by s and a transformed quantity by a bar, the transform of Eq. (2.5) is written as:

$$\nabla^2\bar{\chi}(\vec{r},\tau,s) - \frac{\partial}{\partial\tau}\bar{\chi}(\vec{r},\tau,s) + \frac{\bar{S}(\vec{r},\tau,s)}{p(0,\tau)} = \frac{1}{vD(\tau)}\left[s\bar{\chi}(\vec{r},\tau,s) - \chi(\vec{r},\tau,0)\right]. \tag{2.8}$$

The second term of the right side of Eq. (2.8) is taken as zero on physical grounds:

$$\chi(\vec{r},\tau,0) = 0. \tag{2.9}$$

The spatial dependence of the functions $\bar{\chi}(\vec{r},\tau,s)$ and $\bar{S}(\vec{r},\tau,s)$ is expressed in terms of an infinite sum of eigenfunctions generated by the Helmholtz equation:

$$\nabla^2 F_n(\vec{r}) + B_n^2 F_n(\vec{r}) = 0, \tag{2.10}$$

where the functions $F_n(\vec{r})$ are required to vanish at the boundaries of

the medium. The subscript n is a composite subscript representing the same number of subscripts as there are spatial variables in the system. Then, we can write:

$$\bar{\chi}(\vec{r}, \tau, s) = \sum_n \bar{A}_n(\tau, s) F_n(\vec{r}), \tag{2.11a}$$

$$\bar{S}(\vec{r}, \tau, s) = S_o \sum_n C_n \delta(\tau) F_n(\vec{r}). \tag{2.11b}$$

In general, $F_n(\vec{r})$ is known when the boundaries of the medium are specified, the coefficients C_n are determined (after invoking the orthogonality of the functions $F_n(\vec{r})$) by:

$$C_n = \frac{\int_{\vec{r}} d\vec{r}\, S'(\vec{r}) F_n(\vec{r})}{\int_{\vec{r}} d\vec{r}\, F_n^2(\vec{r})}, \tag{2.12}$$

and the coefficients $\bar{A}_n(\tau, s)$ are unknown. If Eqs. (2.10), (2.11a), and (2.11b) are inserted in Eq. (2.5), a linear, first-order differential equation in the unknown coefficient $\bar{A}_n$ is obtained for which the solution is:

$$\bar{A}_n(\tau, s) = u(\tau) S_o C_n \exp\left[- \int_0^\tau \left(B_n^2 + \frac{S}{vD} \right) d\tau \right], \tag{2.13}$$

where $u(\tau)$ is the Heaviside function (M5). Equation (2.13) is easily inverted and the resultant expression for $q(\vec{r}, \tau, t)$, the slowing down density with absorption, is:

$$q(\vec{r}, \tau, t) = u(\tau) \delta\left(t - \frac{\tau}{\langle vD \rangle} \right) S_o \sum_n C_n F_n(\vec{r}) e^{-\left(B_n^2 + \left\langle \frac{\Sigma_a}{D} \right\rangle \right) \tau}, \tag{2.14}$$

where:

$$\left\langle \frac{\Sigma_a}{D} \right\rangle = \frac{1}{\tau} \int_0^\tau \frac{\Sigma_a(\tau')}{D(\tau')} d\tau', \tag{2.15a}$$

$$\left\langle \frac{1}{vD} \right\rangle = \frac{1}{\tau} \int_0^\tau \frac{d\tau'}{vD(\tau')}. \tag{2.15b}$$

The interpretation of Eq. (2.14) provides additional insight into the behavior of fast neutrons during slowing down. The monoenergetic source of fast neutrons excites an infinite series of spatial modes, i.e., $S_n \sim C_n F_n$. If we define:

$$T = \frac{\tau}{\langle vD \rangle}, \tag{2.16}$$

where T is the slowing down time to age τ, the exponential term in Eq. (2.14) may be written as:

$$e^{-\left(B_n^2 + \left\langle \frac{\Sigma_a}{D} \right\rangle\right)\tau} = e^{-\left(\langle vD \rangle B_n^2 + \langle vD \rangle \left\langle \frac{\Sigma_a}{D} \right\rangle\right)T} = e^{-\Lambda_n T}, \tag{2.17}$$

where Λ_n can be considered as the "slowing down decay constant" for the n^{th} mode. Thus, each source excited mode decays as it slows down because of leakage and absorption. Furthermore, the delta function in Eq. (2.14) indicates that the slowing down density to age τ is zero unless $t = T$.

In the following two sections, the thermal neutron diffusion equation for non-multiplying and multiplying media, respectively, is solved with the source taken as the slowing down density to the age at thermal energy ($\tau = \tau_o$) in Eq. (2.14).

2.2.3 Thermal Neutron Diffusion in Non-Multiplying Media

The main objective in this study is the determination of parameters (of non-multiplying and multiplying media) from experimentally observed values of the prompt neutron decay constant. The development of an appropriate expression relating the decay constant to parameters of the medium is undertaken in this section for a non-multiplying medium, and in the next section for a multiplying medium.

The time-dependent diffusion equation for the thermal neutron density is:

$$\overline{vD}\nabla^2 n(\vec{r}, t) - \overline{v\Sigma}_a n(\vec{r}, t) + q(\vec{r}, \tau_o, t) = \frac{\partial}{\partial t} n(\vec{r}, t), \tag{2.18}$$

where the bars over $\overline{vD}$ and $\overline{v\Sigma}_a$ indicate averages over the neutron density:

$$\overline{vD} = \frac{\int_v dv\ \overline{vD}(v)\, n(v)}{\int_v dv\ n(v)}, \tag{2.19a}$$

$$\overline{v\Sigma_a} = \frac{\int_v dv\ \overline{v\Sigma}_a(v)\, n(v)}{\int_v dv\ n(v)}. \tag{2.19b}$$

The Laplace Transform of Eq. (2.18) is:

$$\overline{vD}\nabla^2\bar{n}(\vec{r}, s) - \overline{v\Sigma}_a\,\bar{n}(\vec{r}, s) + \bar{q}(\vec{r}, \tau_o, s) = s\bar{n}(\vec{r}, s). \tag{2.20}$$

If we write:

$$\bar{n}(\vec{r}, s) = \sum_n \bar{Q}_n(s) F_n(\vec{r}), \tag{2.21}$$

and substitute Eq. (2.21) in Eq. (2.20), the result, after simplification, is:

$$(\lambda_n + s)\bar{Q}_n(s) = S_o C_n e^{-\Lambda_n T_o} e^{-sT_o}, \tag{2.22}$$

where:

$$\lambda_n = \overline{v\Sigma}_a + \overline{vD} B_n^2. \tag{2.23}$$

If Eq. (2.22) is solved for $\bar{Q}_n(s)$, we obtain:

$$\bar{Q}_n(s) = S_o C_n e^{-\Lambda_n T_o} \frac{e^{-sT_o}}{\lambda_n + S}. \tag{2.24}$$

The transform in Eq. (2.24) may be inverted with the help of the Convolution Theorem (H7) and, finally, we obtain:

$$n(\vec{r}, t) = S_o \sum_n C_n F_n(\vec{r})\, e^{-(\Lambda_n - \lambda_n)T_o} e^{-\lambda_n t}, \tag{2.25}$$

as the desired expression for the time and spatial dependent thermal neutron density in a non-multiplying medium. The familiar exponential time behavior of a thermalized burst of fast neutrons appears in the last term of Eq. (2.25). The quantities B_n^2 in Eq. (2.23) are the eigenvalues arising in the solution of the Helmholtz equation (Eq. (2.10)),

and they increase with increasing values of n. The smallest value of B_n^2 ($B_1^2 \equiv B^2$; the subscript 1 will be suppressed except when more than one spatial mode is involved) is the geometric buckling and, when inserted in Eq. (2.23), yields:

$$\lambda = \overline{v\Sigma}_a + \overline{vD}B^2, \tag{2.26}$$

which is the expression for the fundamental mode decay constant. After a sufficiently long time, Eq. (2.25) contains only the first term in the summation (corresponding to the fundamental mode (n=1) since the higher order terms decay more quickly, and we have:

$$n(\vec{r}, t) = S_o CF(\vec{r})\, e^{-(\Lambda-\lambda)T_o}\, e^{-\lambda t}. \tag{2.27}$$

Before turning to a description of thermal diffusion in multiplying media, a brief discussion of the quantity $\overline{vD}$ appearing in Eq. (2.23) should be undertaken. A one velocity group treatment such as the one leading to Eq. (2.25) cannot account for the interaction of thermal neutrons with nuclei of the moderator. In a finite system, some of the neutrons are lost during the diffusion process by leakage. Since the diffusion coefficient ($\overline{vD}$) increases with increasing neutron energy, neutrons with higher energies will preferentially escape from the system. This preferential leakage results in a "softening" of the neutron spectrum and a corresponding decrease in the value of $\overline{vD}$ from its value in an infinite medium (no leakage). This effect has been treated by von Dardel (D1) on the assumption that the deviation of the neutron spectrum from its value in an infinite medium can be characterized by the variation of the average neutron energy. His treatment indicates that the diffusion coefficient depends linearly on the geometric buckling (B^2). Additional theoretical (N1, N2) and experimental (K2) investigations suggest a second-order dependence when the system dimensions become quite limited. Hence, the diffusion coefficient is written as:

$$\overline{vD} = \overline{vD}_o - CB^2 \pm FB^4, \tag{2.28}$$

where $\overline{vD}_o$ is the infinite medium diffusion coefficient and C is commonly called the diffusion "cooling" coefficient. Inserting Eq. (2.28) in

Eq. (2.26), we obtain (to terms in B^4):

$$\lambda = \overline{v\Sigma}_a + \overline{vD}_o B^2 - CB^4, \tag{2.29}$$

as the expression for the fundamental mode decay constant in a non-multiplying medium.

2.2.4 Thermal Neutron Diffusion in Multiplying Media

The time-dependent diffusion equation for thermal neutrons in a multiplying medium is:

$$\overline{vD}\nabla^2 n(\vec{r}, t) - \overline{v\Sigma}_a n(\vec{r}, t) + \overline{v\Sigma}_a(1-\beta)k_\infty P_1(B^2)n(\vec{r}, t-T_o)$$

$$+ q(\vec{r}, \tau_o, t) = \frac{\partial}{\partial t} n(\vec{r}, t), \tag{2.30}$$

where β is the effective delayed neutron fraction, $P_1(B^2)$ is the fast non-leakage probability,* T_o is the slowing down time to thermal energies, and the rest of the terms have their usual meanings. In this derivation, delayed neutrons are neglected (except for the effect on neutron multiplication) and the slowing down time of fission neutrons is neglected ($T_o = 0$).

The Laplace Transform of Eq. (2.30) is:

$$\overline{vD}\nabla^2 \bar{n}(\vec{r}, s) - \overline{v\Sigma}_a \bar{n}(\vec{r}, s) + \overline{v\Sigma}_a(1-\beta)k_\infty P_1(B^2)\bar{n}(\vec{r}, s)$$

$$+ \bar{q}(\vec{r}, \tau_o, s) = s\bar{n}(\vec{r}, s). \tag{2.31}$$

Recalling that $\nabla^2 F_n(\vec{r}) = -B_n^2 F_n(\vec{r})$ and writing:

$$\bar{n}(\vec{r}, s) = \sum_n \bar{Q}_n(s) F_n(\vec{r}), \tag{2.32}$$

Eq. (2.31) is written as:

$$\left(\overline{v\Sigma}_a + \overline{vD}B_n^2 - \overline{v\Sigma}_a(1-\beta)k_\infty P_1(B_n^2) + s\right)\bar{Q}_n(s) = S_o C_n e^{-(\Lambda_n + s)T_o}. \tag{2.33}$$

---

* Following the usual practice, the subscript 1 denotes the fast energy group and the subscript 2 denotes the thermal energy group. If no subscript is used, the thermal energy group is implied.

If we define:

$$\lambda_n = \overline{v\Sigma}_a + \overline{vD}B_n^2 - \overline{v\Sigma}_a(1-\beta)k_\infty P_1(B_n^2), \tag{2.34}$$

and solve Eq. (2.33) for $\overline{Q}_n(s)$, the result is:

$$\overline{Q}_n(s) = S_o C_n e^{-\Lambda_n T_o} \frac{e^{-sT_o}}{\lambda_n + s}. \tag{2.35}$$

Equation (2.35) can be inverted with the help of the Convolution Theorem and the expression for the thermal neutron density is:

$$n(\vec{r}, t) = S_o \sum_n C_n F_n(\vec{r})\, e^{-(\Lambda_n - \lambda_n)T_o}\, e^{-\lambda_n t}. \tag{2.36}$$

After a sufficiently long time, all modes but the fundamental have decayed and only one term is left in the summation (2.36), for which the decay constant is:

$$\lambda = \overline{v\Sigma}_a + \overline{vD}B^2 - \overline{v\Sigma}_a(1-\beta)k_\infty P_1(B^2). \tag{2.37}$$

If the thermal neutron lifetime is defined as:

$$\ell_2 = \frac{1}{\overline{v\Sigma}_a + \overline{vD}B^2} = \frac{1}{\overline{v\Sigma}_a[1+L^2B^2]}, \tag{2.38}$$

Equation (2.37) may be rewritten:

$$\lambda = \frac{1}{\ell_2}\left[1 - \frac{(1-\beta)k_\infty P_1(B^2)}{1 + L^2B^2}\right] = \frac{1 - (1-\beta)k}{\ell_2}. \tag{2.39}$$

Equation (2.37) is the basic Fermi age-diffusion model expression for the prompt neutron, fundamental mode decay constant subject to the assumptions listed at the beginning of Sec. 2.2. The use of this equation in conjunction with experimental data to obtain values of lattice parameters is described in Chap. IV.

2.3 TREATMENT OF TWO-REGION LATTICES

The fact that the construction and operation of critical and subcritical facilities are often expensive has stimulated research into more economical means for determining lattice parameters while still retaining satisfactory accuracy. One such method consists in removing a small section from the center of a lattice whose properties are well known and inserting in the vacancy a test lattice whose properties are to be determined. An objective of the pulsed neutron source research reported here has been to develop a method to treat such assemblies and compare the experimental results with those obtained from steady-state measurements (G6).

In this section, a one velocity group model is developed to treat a two-region assembly irradiated by a burst of fast neutrons. The development is similar to that of Sec. 2.2, although it is necessary to examine the spatial dependence of the neutron density as well as the time dependence.

The usual treatment of the time behavior of a chain reacting system is based on the assumption that the time dependence of a particular spatial mode is the same at all locations within the system. The validity of this assumption has been seriously questioned in connection with studies of large reactor systems, and a great deal of effort in recent years has been devoted to the field of space-dependent reactor kinetics (see, for example, Ref. F1). The assumption of separability is well justified, however, in small assemblies of the type investigated in this work, and that it can be extended to two-region assemblies, may be seen by the following argument. Consider the properties of a medium to be functions of position, and write the diffusion equation as:

$$\nabla \cdot \overline{vD}(\vec{r})\nabla n(\vec{r},t) - \overline{v\Sigma}_a(\vec{r})n(\vec{r},t) + K(\vec{r})n(\vec{r},t) = \frac{\partial}{\partial t} n(\vec{r},t), \tag{2.40}$$

where,

$$K(\vec{r}) = \overline{v\Sigma}_a(\vec{r})\,[\,1-\beta(\vec{r})\,]\,k_\infty(\vec{r})P_1(\vec{r}). \tag{2.41}$$

We assume:

$$n(\vec{r},t) = \sum_n Q_n(t)F_n(\vec{r}), \tag{2.42}$$

and, substituting Eq. (2.42) in Eq. (2.40), the result is (for the n^{th} mode):

$$\frac{1}{F_n(\vec{r})}\left[\nabla\cdot\overline{vD}(\vec{r})\nabla F_n(\vec{r})+\left(K(\vec{r})-\overline{v\Sigma}_a(\vec{r})\right)F_n(\vec{r})\right]=\frac{1}{Q_n(t)}\frac{\partial}{\partial t}Q_n(t). \tag{2.43}$$

Since the right side of Eq. (2.43) is a function only of $\vec{r}$ and the left side is a function only of t, each side is separately equal to the same constant. Therefore, we have:

$$\frac{1}{Q_n(t)}\frac{\partial}{\partial t}Q_n(t) = -\lambda_n, \tag{2.44}$$

which yields:

$$Q_n(t) = Q_{no}e^{-\lambda_n t}. \tag{2.45}$$

Thus, the familiar exponential decay of each modal component of the thermal neutron density results when the parameters of the medium are functions of position. This result is now applied to the particular case of a two radial-region, cylindrical assembly whose properties are constant along the axial direction.

In the following analysis, the subscript b refers to the outer region of the assembly whose properties are assumed known (reference region), and the subscript x refers to the inner region of the assembly whose properties are to be determined (test region). To avoid confusion, the modal subscript n is omitted although the derivation applies equally well to any and all spatial modes. In addition, the following boundary conditions are stipulated:

1) the neutron density vanishes at the extrapolated boundaries of the assembly ($z = (0, H)$; $r = R_b$),

2) the neutron density is finite everywhere,

3) an effective source distribution appears at $t = 0$ ($n(\vec{r}, 0) = n_o(\vec{r})$),

4) the neutron flux and current are continuous across the boundary ($r = R_x$) between the two regions.

The thermal neutron diffusion equation for either region is:

$$\overline{vD}_{b,x}\nabla^2 n_{b,x}(\vec{r},t) - \overline{v\Sigma}_{ab,x}n_{b,x}(\vec{r},t)+K_{b,x}n_{b,x}(\vec{r},t) = \frac{\partial}{\partial t}n_{b,x}(\vec{r},t). \tag{2.46}$$

Substituting Eq. (2.42) in Eq. (2.46), the result is:

$$\overline{vD}_{b,x} \frac{\nabla^2 F_{b,x}(\vec{r})}{F_{b,x}(\vec{r})} + \left(K_{b,x} - \overline{v\Sigma}_{ab,x}\right) = \frac{1}{Q(t)} \frac{\partial}{\partial t} Q(t), \tag{2.47}$$

and, after introduction of Eq. (2.44), we get:

$$\frac{\nabla^2 F_{b,x}(\vec{r})}{F_{b,x}(\vec{r})} = - \frac{\lambda + K_{b,x} - \overline{v\Sigma}_{ab,x}}{\overline{vD}_{b,x}} = - B^2_{b,x}. \tag{2.48}$$

The solutions of Eq. (2.48) in each region are:

$$F_b(r,z) = A_b \operatorname{Sin}\left(\frac{\pi z}{H}\right) \left[Y_o(\alpha_b r) - \frac{Y_o(\alpha_b R_b)}{J_o(\alpha_b R_b)} J_o(\alpha_b r) \right], \tag{2.49a}$$

$$F_x(r,z) = A_x \operatorname{Sin}\left(\frac{\pi z}{H}\right) J_o(\alpha_x r), \tag{2.49b}$$

where,

$$B^2_b = \alpha^2_b + \left(\frac{\pi}{H}\right)^2, \tag{2.50a}$$

$$B^2_x = \alpha^2_x + \left(\frac{\pi}{H}\right)^2. \tag{2.50b}$$

The boundary conditions (4) state that:

$$F_b(R_x, z) = F_x(R_x, z), \tag{2.51a}$$

$$\overline{vD}_b F'_b(R_x, z) = \overline{vD}_x F'_x(R_x, z). \tag{2.51b}$$

If Eq. (2.51b) is divided by Eq. (2.51a) and Eqs. (2.49a) and (2.49b) are substituted into the result, we obtain:

$$\overline{vD}_x \alpha_x \left[\frac{J_1(\alpha_x R_x)}{J_o(\alpha_x R_x)} \right] = \overline{vD}_b \alpha_b \left[\frac{Y_1(\alpha_b R_x) - \frac{Y_o(\alpha_b R_b)}{J_o(\alpha_b R_b)} J_1(\alpha_b R_x)}{Y_o(\alpha_b R_x) - \frac{Y_o(\alpha_b R_b)}{J_o(\alpha_b R_b)} J_o(\alpha_b R_x)} \right], \tag{2.52}$$

which is the so-called secular equation in which both α_b and α_x are unknown. However, additional information is available for the determination of these quantities. From Eq. (2.48), we have:

$$\lambda = \overline{v\Sigma}_{ab} + \overline{vD}_b B_b^2 - \overline{v\Sigma}_{ab}(1-\beta_b)k_{\infty b}P_1(B_b^2), \qquad (2.53a)$$

$$\lambda = \overline{v\Sigma}_{ax} + \overline{vD}_x B_x^2 - \overline{v\Sigma}_{ax}(1-\beta_x)k_{\infty x}P_1(B_x^2). \qquad (2.53b)$$

Since the properties of the reference region are known, a value for B_b^2 can be obtained from Eq. (2.53a), once an experimental determination of λ is available. Then, a value of α_b is evaluated from Eq. (2.50a) and inserted in the secular equation (Eq. (2.52)). If it is assumed that the difference $\overline{vD}_b - \overline{vD}_x$ is negligible or can be calculated, a value of α_x is obtained from the solution of the secular equation. The relation between α_x^2 and B_x^2 (Eq. (2.50b)) is next used to obtain a value for B_x^2. Finally, values of λ and B_x^2 are used in conjunction with Eq. (2.53b) to evaluate the lattice parameters of the test region.

The analysis of data taken in two-region assemblies is described in Chap. IV and the results of exploratory measurements in two such assemblies are presented in Chap. V.

2.4 TREATMENT OF ABSORBER-MODIFIED LATTICES

The continuing search for more accurate determinations of reactor parameters – in particular, the infinite medium multiplication factor – has led to the development of several experimental procedures with this purpose in mind. The technique of adding thermal neutron absorber to a test section of a critical reactor, to the point where the reactivity effect of the test section is the same as that of an equal volume of void, is well documented (H6, D8). This technique has recently been extended to subcritical lattices by J. Harrington (H1) in an attempt to obtain an estimate of k_∞ more precise than that obtainable by other methods used in subcritical assemblies. An objective of this work has been to make pulsed neutron measurements in absorber-modified lattices and explore possible methods for analyzing the data with the ultimate aim of comparing the results with those obtained by steady-state techniques.

The expression for the prompt neutron, fundamental mode decay constant, as derived in Sec. 2.2.4, is:

$$\lambda = \overline{v\Sigma}_a + \overline{vD}B^2 - \overline{v\Sigma}_a(1-\beta)k_\infty P_1(B^2). \qquad (2.37)$$

One approach to the analysis of pulsed neutron source experiments, to be discussed more fully in Chap. IV, begins by rewriting Eq. (2.37):

$$\lambda' = r - sP', \tag{2.54}$$

where

$$\lambda' = \lambda - \overline{vD}B^2, \tag{2.55a}$$

$$P' = P_1(B^2) - 1, \tag{2.55b}$$

$$r = \overline{v\Sigma}_a[1-(1-\beta)k_\infty], \tag{2.55c}$$

$$s = \overline{v\Sigma}_a(1-\beta)k_\infty. \tag{2.55d}$$

Then, assuming that $\overline{vD}$ can be calculated or determined in a separate experiment and that an appropriate expression for $P_1(B^2)$ is selected, we can determine the coefficients r and s by least squares fitting the measured values of λ and B^2 to a function of the form given by Eq. (2.54). Finally, k_∞ and $\overline{v\Sigma}_a$ may be evaluated from the fit values of r and s by using a calculated value of β.

If successive amounts of a distributed thermal neutron absorber are now added uniformly to the medium and a set of pulsed neutron measurements made on each configuration, additional information is available which may improve the accuracy to which k_∞ is determined. This possibility was originally pointed out by D. D. Lanning (L2). If the lattice thermal utilization, f, and the absorption cross section, $\overline{v\Sigma}_a$, are written in terms of summations over the unit cell:

$$f = \frac{\overline{v\Sigma}_{ao}\bar{n}_o V_o}{\sum_{i=0}^{3} \overline{v\Sigma}_{ai}\bar{n}_i V_i}, \tag{2.56a}$$

$$\overline{v\Sigma}_a = \frac{\sum_{i=0}^{3} \overline{v\Sigma}_{ai}\bar{n}_i V_i}{\sum_{i=0}^{3} \bar{n}_i V_i}, \tag{2.56b}$$

where the subscripts 0, 1, 2, and 3 represent fuel, moderator, cladding, and added thermal absorber, respectively, and V_i is the volume of the i^{th} constituent, then:

$$\overline{v\Sigma}_a(1-\beta)k_\infty = (1-\beta)\eta\epsilon p \frac{\overline{v\Sigma}_{ao}}{1 + \sum_{i=1}^{3} \frac{\bar{n}_i V_i}{\bar{n}_o V_o}} . \tag{2.57}$$

The coefficient s in Eq. (2.54), therefore, changes only because of changes in volume fractions and disadvantage factors on the addition of a thermal absorber. (This assumes that the absorber is a pure thermal absorber so that ϵ and p remain constant and that spectral changes are small enough so that η remains constant.) The coefficient r, on the other hand, increases as absorber is added because $\overline{v\Sigma}_a$ increases and, therefore, is a measure of the amount of absorber added. If sufficient absorber is added to make $(1-\beta)k_\infty = 1$, a null state, corresponding to r = 0, results. Furthermore:

$$\frac{r}{s} = \frac{1}{(1-\beta)k_\infty} - 1, \tag{2.58}$$

so that in the neighborhood of r=0, a sensitive measure of k_∞ is obtained.

In order to quantify the effect of adding absorber, consider the following two situations: a) the clean (or no absorber added) lattice — denoted by the superscript c — and b) the "null state" lattice — denoted by the superscript y. Then:

$$(1-\beta)k_\infty^c = (1-\beta)\eta^c\epsilon^c p^c f^c, \tag{2.59a}$$

$$(1-\beta)k_\infty^y = (1-\beta)\eta^y\epsilon^y p^y f^y = 1.0, \tag{2.59b}$$

and

$$\frac{(1-\beta)k_\infty^c}{(1-\beta)k_\infty^y} = (1-\beta)k_\infty^c = \left(\frac{\eta^c}{\eta^y}\right)\left(\frac{\epsilon^c}{\epsilon^y}\right)\left(\frac{p^c}{p^y}\right)\left(\frac{f^c}{f^y}\right) . \tag{2.60}$$

The ratio (f^c/f^y) may be written (H1):

$$\frac{f^c}{f^y} = 1 + f^c A_3^y + f^c\left[A_1^y - A_1^c + A_2^y - A_2^c\right], \tag{2.61}$$

where,

$$f^c = \frac{1}{1 + A_1^c + A_2^c} , \tag{2.62a}$$

$$A_i = \frac{\int d\vec{r}_i \int dv\ \overline{v\Sigma}_{ai}(v) n(\vec{r}, v)}{\int d\vec{r}_o \int dv\ \overline{v\Sigma}_{ao}(v) n(\vec{r}, v)} = \frac{\overline{v\Sigma}_{ai} \bar{n}_i V_i}{\overline{v\Sigma}_{ao} \bar{n}_o V_o} . \qquad (2.62b)$$

The last term in Eq. (2.61) accounts for changes in the relative absorption rates in moderator and cladding caused by spectral and volume displacement effects of the added absorber. If it is neglected, one may write:

$$\frac{f^c}{f^y} = 1 + f^c A_3^y = 1 + \left(\frac{\overline{v\Sigma}_{ao}^c \bar{n}_o^c V_o}{\overline{v\Sigma}_{ao}^y \bar{n}_o^y V_o} \right) \left(\frac{\overline{v\Sigma}_{a3}^y}{\overline{v\Sigma}_a^c} \right) \left(\frac{\bar{n}_3^y V_3}{\sum_{i=0}^{2} \bar{n}_i^c V_i} \right) . \qquad (2.63)$$

Substituting Eq. (2.63) in Eq. (2.60) and defining:

$$\gamma_1 = \left(\frac{\eta^c}{\eta^y} \right) \left(\frac{\epsilon^c}{\epsilon^y} \right) \left(\frac{p^c}{p^y} \right) , \qquad (2.64a)$$

$$\gamma_2 = \left(\frac{\overline{v\Sigma}_{ao}^c \bar{n}_o^c V_o}{\overline{v\Sigma}_{ao}^y \bar{n}_o^y V_o} \right) , \qquad (2.64b)$$

$$\gamma_3 = \left(\frac{\bar{n}_3^y V_3}{\sum_{i=0}^{2} \bar{n}_i^c V_i} \right) , \qquad (2.64c)$$

the result is:

$$\frac{(1-\beta)k_\infty^c}{1.0} = \gamma_1 \left[1 + \gamma_2 \gamma_3 \left(\frac{\overline{v\Sigma}_{a3}^y}{\overline{v\Sigma}_a^c} \right) \right] , \qquad (2.65)$$

and, on recalling the definition of r^c, we get:

$$r^c = \overline{v\Sigma}_a^c \left[1-(1-\beta)k_\infty^c \right] = (1-\gamma_1)\overline{v\Sigma}_a^c - \gamma_1\gamma_2\gamma_3 \overline{v\Sigma}_{a3}^y . \qquad (2.66)$$

If the changes in the neutron spectrum and constituent volume fractions caused by the added absorber are small, then $\gamma_1 \approx 1$; $\gamma_2 \approx 1$; and Eq. (2.66) reduces to:

$$r^c = -\gamma_3 \overline{v\Sigma}^y_{a3} . \tag{2.67}$$

Therefore, once the amount of added absorber required to achieve the null state is ascertained, the coefficient r^c is known; and Eq. (2.54) has only one unknown, namely, s^c. This should reduce the uncertainty in the fit value of s^c and, consequently, the uncertainty in the value of k_∞ which is derived from values of r^c and s^c.

In addition to improving the accuracy in k_∞, a knowledge of the null state condition may also yield an estimate of τ_o for the lattice. To this end, it is assumed that the fast non-leakage probability can be expressed by a Fermi slowing down kernel:

$$P' = P_1(B^2) - 1 = e^{-B^2\tau_o} - 1 \approx -B^2\tau_o + \frac{1}{2} B^4\tau_o^2 . \tag{2.68}$$

Inserting Eq. (2.68) in Eq. (2.54) and collecting terms corresponding to like powers of B^2, one obtains:

$$\lambda' = r + sB^2\tau_o - \frac{1}{2} sB^4\tau_o^2$$

$$= r + tB^2 - uB^4, \tag{2.69}$$

where

$$r = \overline{v\Sigma}_a[\,1-(1-\beta)k_\infty], \tag{2.55c}$$

$$t = \overline{v\Sigma}_a(1-\beta)k_\infty\tau_o, \tag{2.70a}$$

$$u = \frac{1}{2} \overline{v\Sigma}_a(1-\beta)k_\infty\tau_o^2. \tag{2.70b}$$

Thus, it is also possible to fit the values of λ for different values of B^2 data to a second-order power series in B^2 and determine the coefficients r, t, and u. For the null state, we have:

$$t^y = \overline{v\Sigma}^y_a(1-\beta)k^y_\infty\tau_o = \overline{v\Sigma}^y_a\tau_o, \tag{2.71}$$

and, therefore:

$$\tau_o = \frac{t^y}{\overline{v\Sigma}^y_a} . \tag{2.72}$$

Equation (2.72) states that an estimate for τ_o may be derived from the

ratio of the coefficient t to the absorption cross section in the null state lattice.

Hence, this series of experiments may improve the accuracy in k_∞ over that which is obtainable from pulsed neutron source measurements on the clean lattice alone and may also yield an estimate for the age in the clean lattice.

2.5 INVESTIGATION OF THE ASSUMPTIONS MADE IN THE TREATMENT OF THE KINETICS OF AN ASSEMBLY IRRADIATED BY A BURST OF FAST NEUTRONS

In this section, the assumptions listed at the beginning of Sec. 2.2 are investigated in order to determine if they have a significant effect on the expression for the prompt neutron decay constant in a subcritical, multiplying assembly. Further discussion may be found in Chap. IV (analysis of data) and Chap. V (results).

2.5.1 Effect of a Finite Source Burst Width

The assumption that the neutron source may be represented as a delta function in time is generally applied to theoretical treatments of pulsed neutron kinetics. However, the expression for the fundemantal mode decay constant is not changed if the burst width is finite. Consider the source shape to be a square wave of height H_o and width Δ:

$$S(\vec{r}, \tau, t) = H_o S(r, z)\delta(\tau)[u(t)-u(t-\Delta)], \tag{2.73}$$

where u(t) is the unit Heaviside or step function having a value of unity for times greater than t = 0 and a value of zero otherwise. If Eq. (2.73) is substituted in Eq. (2.5) (the basic time-dependent Fermi age equation) and the solution developed along the lines indicated in Sec. 2.2.2, the resulting expression for the slowing down density with absorption is similar to that derived in Sec. 2.2.2 (Eq. 2.14)):

$$q(\vec{r}, \tau, t) = u(\tau)[u(t-T)-u(t-T-\Delta)]H_o \sum_n C_n F_n(\vec{r})\, e^{-\Lambda_n T}, \tag{2.74}$$

where, as before,

$$T = \frac{\tau}{\langle vD \rangle}. \tag{2.16}$$

Physically, Eq. (2.74) states that, on the Fermi age model of neutron slowing down, the slowing down density to age τ is zero for all time before $t = T$ and after $t = T + \Delta$ and has a constant value over the time interval between.

The thermal neutron diffusion equation is solved in a manner analogous to that in Sec. 2.2.4 with the source given by Eq. (2.74). The result is:

$$n(\vec{r},t) = H_o \sum_n C_n F_n(\vec{r})\, e^{-\Lambda_n T_o} \left\{ \frac{1 - e^{\lambda_n T_o} e^{-\lambda_n t}}{\lambda_n} \right\} \qquad (T_o \leq t \leq T_o + \Delta), \tag{2.75a}$$

$$= H_o \sum_n C_n F_n(\vec{r})\, e^{-(\Lambda_n - \lambda_n) T_o} \left\{ \frac{e^{\lambda_n \Delta} - 1}{\lambda_n} \right\} e^{-\lambda_n t} \qquad (t \leq T_o + \Delta). \tag{2.75b}$$

The interpretation of Eq. (2.75) is as follows. For a very long burst width (e.g., a steady-state source in the limit), Eq. (2.75a) states that the n^{th} modal component of the thermal neutron density approaches a constant value. After the source is terminated and all neutrons have slowed down to thermal velocities ($t \geq T_o + \Delta$), then Eq. (2.75b) states that the n^{th} modal component of the neutron density decays exponentially with the same decay constant λ_n as derived in Sec. 2.2.4. Therefore, a finite source burst width is not, in itself, a limitation to the observation of a fundamental mode decay constant.

The limitation manifests itself in two experimental difficulties. First, bursts of fast neutrons are introduced repetitively into the assembly, so it is essential that the neutron density following one burst not be overlapped by the density from the succeeding burst. Second, the nature of pulsed neutron sources is such that the area under the burst shape is approximately constant ($H_o \Delta \cong S_o$), so that the longer the burst width, the smaller the effective neutron density (per burst) as measured by a neutron counter. This is seen by taking the ratio of the fundamental mode component of the neutron density given by Eq. (2.36) (instantaneous burst) to that given by Eq. (2.75b) (finite burst width):

$$R = \frac{S_o CF(\vec{r})\, e^{-(\Lambda-\lambda)T_o} e^{-\lambda t}}{H_o CF(\vec{r})\, e^{-(\Lambda-\lambda)T_o \left\{\frac{e^{\Delta\lambda}-1}{\lambda}\right\}} e^{-\lambda t}}$$

$$= \frac{S_o}{H_o \Delta \left(1 + \frac{\lambda\Delta}{2} + \ldots\right)}$$

$$\approx \frac{1}{1 + \frac{\lambda\Delta}{2}} . \qquad (2.76)$$

Hence, to a first approximation, the effective neutron density is not decreased until the quantity $\frac{\lambda\Delta}{2}$ in Eq. (2.76) becomes significant.

2.5.2 Effect of a Non-Black Boundary Condition

A bare system is usually approximated experimentally by isolating the system from its surroundings by distance or by wrapping it with an absorbing material such as cadmium. The latter method is employed at the M. I. T. Lattice Facility with the exception of the bottom of the lattice tank through which the thermal neutron source enters the assembly during steady-state experiments. However, the derivation leading to Eq. (2.36) assumed that the entire assembly is bare, and, to this end, a cadmium plate has been inserted at the bottom of the lattice tank whenever pulsed neutron source experiments have been made. The installation of this plate is not desirable from an experimental standpoint because the lattice must be withdrawn from the tank to insert the plate. Withdrawing the lattice has several effects: (1) it exposes a radiation source of fairly high intensity, 0.05 to 0.5 r/hr, depending on the recent operating history of the Facility; (2) it results in partial degradation of 1 to 2 gallons of heavy water per experiment which must be removed before the Facility can be operated again and which eventually must be reprocessed; and (3) it consumes time while the system is being dried before further use.

If pulsed neutron source experiments are made without the cadmium plate at the bottom of the tank, there may be a discernable return of thermal neutrons from the graphite-lined cavity below the lattice tank. This return, which decreases the fundamental mode decay constant

relative to that which would be observed with the cadmium plate in the tank, may be taken into account by modifying the usual expression for the extrapolation distance d (G4).

A certain fraction of the thermal neutrons leaving the assembly through the bottom of the tank will be reflected back into the tank by the graphite. This fraction, which is called the albedo, is written as the ratio of return to outgoing neutron currents:

$$\beta_a = \frac{J_{in}}{J_{out}} = \frac{\frac{\phi}{4} + \frac{D}{2}\phi'}{\frac{\phi}{4} - \frac{D}{2}\phi'}, \tag{2.77}$$

where, because of continuity of flux and current at an interface between the two media, the quantities ϕ and $D\phi'$ may be regarded as referring to either medium. If Eq. (2.77) is solved for the ratio ϕ/ϕ', the result is:

$$\frac{\phi}{\phi'} = -\frac{2}{3}\lambda_{tr}\left(\frac{1+\beta_a}{1-\beta_a}\right), \tag{2.78}$$

where

$$\lambda_{tr} = 3D . \tag{2.79}$$

According to simple diffusion theory, the linear extrapolation distance is given by:

$$d' = -\frac{\phi}{\phi'}, \tag{2.80}$$

so that, inserting Eq. (2.78) in Eq. (2.80), we have:

$$d' = \frac{2}{3}\lambda_{tr}\left(\frac{1+\beta_a}{1-\beta_a}\right). \tag{2.81}$$

According to the more exact transport theory, the numerical constant in Eq. (2.81) should be 0.71, and, hence:

$$d' = 0.71\,\lambda_{tr}\left(\frac{1+\beta_a}{1-\beta_a}\right) = d\left(\frac{1+\beta_a}{1-\beta_a}\right), \tag{2.82}$$

where d is the extrapolation distance for a completely bare system.

The expression for the geometric buckling of a bare cylindrical system is:

$$B^2 = \left(\frac{2.405}{R_o + d}\right)^2 + \left(\frac{\pi}{H_o + 2d}\right)^2, \tag{2.83}$$

where R and H are the physical radius and height, respectively, of the system. To account for the return of neutrons through the bottom of the tank, Eq. (2.82) is introduced into Eq. (2.83):

$$(B')^2 = \left(\frac{2.405}{R_o + d}\right)^2 + \left(\frac{\pi}{H_o + d + d'}\right)^2. \tag{2.84}$$

Finally, the measured values of the decay constant can be related to the lattice parameters of interest by replacing B^2 with $(B')^2$ in Eq. (2.37) (the fast non-leakage probability is not affected because it refers to neutrons with energies above the cadmium cutoff):

$$\lambda = \overline{v\Sigma}_a + \overline{vD}(B')^2 - \overline{v\Sigma}_a(1-\beta)k_\infty P_1(B^2). \tag{2.85}$$

The experimental determination of an effective return coefficient for the M. I. T. Lattice Facility is described in Chap. IV.

2.5.3 Effect of Delayed Neutrons

In this section, the effect of delayed neutrons on the kinetics of an assembly irradiated by a burst of fast neutrons is examined, and conditions under which this effect may be neglected are postulated. One group of delayed neutrons is assumed; the treatment can be extended to include any arbitrary number of groups.

The conservation equations for thermal neutrons and delayed neutron precursors, respectively, are:

$$\overline{vD}\nabla^2 n(\vec{r}, t) - \overline{v\Sigma}_a n(\vec{r}, t) + \overline{v\Sigma}_a(1-\beta)k_\infty P_1(B^2)n(\vec{r}, t)$$

$$+ p\omega P_1(B^2)C(\vec{r}, t) + q(\vec{r}, \tau_o, t) = \frac{\partial}{\partial t} n(\vec{r}, t), \tag{2.86}$$

and

$$-\omega C(\vec{r}, t) + \frac{\beta}{p}\overline{v\Sigma}_a k_\infty n(\vec{r}, t) = \frac{\partial}{\partial t} C(\vec{r}, t), \tag{2.87}$$

where ω is the decay constant for the delayed neutron precursors, $C(\vec{r}, t)$ is the concentration of delayed neutron precursors, and the other terms have been defined previously. These equations are

solved by the Laplace Transform technique in a manner similar to that of Sec. 2.2. Assuming that:

$$\bar{n}(\vec{r}, s) = \sum_n \bar{Q}_n(s) F_n(\vec{r}), \tag{2.88a}$$

$$\bar{C}(\vec{r}, s) = \sum_n \bar{Q}'_n(s) F_n(\vec{r}), \tag{2.88b}$$

where

$$\nabla^2 F_n(\vec{r}) = -B_n^2 F_n(\vec{r}), \tag{2.10}$$

and substituting Eqs. (2.88a), (2.88b), and (2.10) into the transforms of Eqs. (2.86) and (2.87), there follows, after eliminating the precursor concentration between the two equations:

$$\bar{Q}_n(s) = \frac{(\omega+s)\bar{q}(\vec{r}, \tau_o, s)}{\left(\overline{v\Sigma}_a + \overline{vD}B_n^2 - \overline{v\Sigma}_a(1-\beta)k_\infty P_1(B_n^2) + s\right)(\omega+s) - \beta\overline{v\Sigma}_a k_\infty P_1(B_n^2)\omega}. \tag{2.89}$$

We are interested in the time behavior of the thermal neutron density, which is governed by the zeros of the denominator of Eq. (2.89). Hence:

$$n_n(\vec{r}, t) = \left[A_{np} e^{-\lambda_{np} t} + A_{nd} e^{-\lambda_{nd} t}\right] F_n(\vec{r}), \tag{2.90}$$

where the subscripts p and d refer to the prompt and delayed portions of the neutron density, respectively. If we let:

$$\alpha_n = \overline{v\Sigma}_a + \overline{vD}B_n^2 - \overline{v\Sigma}_a(1-\beta)k_\infty P_1(B_n^2), \tag{2.91}$$

and solve for the zeros of the denominator of Eq. (2.89), the result is:

$$\lambda_{np} = -\left(\frac{\alpha_n+\omega}{2}\right)\left[1 + \sqrt{\frac{1 - 4\left(\alpha_n\omega - \beta\overline{v\Sigma}_a k_\infty P_1(B_n^2)\omega\right)}{(\alpha_n+\omega)^2}}\right], \tag{2.92a}$$

$$\lambda_{nd} = -\left(\frac{\alpha_n+\omega}{2}\right)\left[1 - \sqrt{\frac{1 - 4\left(\alpha_n\omega - \beta\overline{v\Sigma}_a k_\infty P_1(B_n^2)\omega\right)}{(\alpha_n+\omega)^2}}\right]. \tag{2.92b}$$

If $(\omega/\alpha_n) \ll 1$, Eqs. (2.92a) and (2.92b) may be approximated by:

$$\lambda_{np} \approx \frac{(\alpha_n+\omega)^2 - \alpha_n\omega + \beta\overline{v\Sigma}_a k_\infty P_1(B_n^2)\omega}{(\alpha_n+\omega)} \approx \alpha_n, \tag{2.93a}$$

$$\lambda_{nd} \approx \frac{\alpha_n\omega - \beta\overline{v\Sigma}_a k_\infty P_1(B_n^2)\omega}{\alpha_n + \omega} \approx \omega. \tag{2.93b}$$

The quantity α_n in Eq. (2.91) is identical to the expression previously obtained for the n^{th} mode decay constant when delayed neutron effects were neglected. Therefore, if the inequality:

$$\left(\frac{\omega}{\alpha_n}\right) \ll 1, \tag{2.94}$$

is satisfied, the prompt and delayed neutron decay constants are adequately described by Eqs. (2.93a) and (2.93b); furthermore, if the time interval over which the neutron density is measured is short compared to $1/\omega$, the delayed neutron contribution may be considered as a constant background superimposed on a sum of exponentially decaying functions.

2.5.4 Effect of Epithermal Fission

The treatment presented in Sec. 2.2 assumed that all multiplied neutrons were produced by thermal fission. Non-thermal fissions may be of two types: epithermal 1/v-fission and resonance fission. Contributions of the former type are automatically included in the preceding treatment since the quantities $\overline{v\Sigma}_a$, $\overline{vD}$, and k_∞ are suitably averaged over the neutron spectrum. However, for systems with high enrichment or low moderator-to-fuel ratios, the contribution of fissions induced by resonance energy neutrons may become significant. Malaviya (M1) has treated the problem by a modified two-group model in which two multiplication factors are defined:

$$k_\infty = \eta\epsilon p_{28} p_{25}^f, \tag{2.95a}$$

$$k_r = \eta_r \epsilon p_{28}(1-p_{25}), \tag{2.95b}$$

where the subscript r refers to the resonance region, p_{28} and p_{25} are the resonance escape probabilities for U^{238} and U^{235}, respectively, and the other symbols have their usual meaning. Since the thermal neutron lifetime is defined by the relation:

$$\ell_2 = \frac{1}{\overline{v\Sigma}_a(1+L^2B^2)}, \tag{2.38}$$

the expression for the observed prompt neutron, fundamental mode decay constant in the presence of resonance fission becomes:

$$\lambda_r = \frac{1}{\ell_2}\left[1 - \frac{(1-\beta)k_\infty P_1(B^2)}{(1+L^2B^2)\left(1 - \frac{(1-\beta_r)k_r}{P_1(B^2)}\right)}\right]. \tag{2.96}$$

In the absence of resonance fission, we obtained earlier:

$$\lambda = \frac{1}{\ell_2}\left[1 - \frac{(1-\beta)k_\infty P_1(B^2)}{1 + L^2B^2}\right], \tag{2.39}$$

so that for small k_r ($p_{25} \approx 1$), Eq. (2.96) reduces to the result given in Eq. (2.39). Furthermore, if we define:

$$k'_\infty = \frac{k_\infty}{1 - \frac{(1-\beta_r)k_r}{P_1(B^2)}},$$

Eq. (2.96) is identical in form to Eq. (2.39).

2.5.5 Effect of Fission Neutron Slowing Down Time

In reactor kinetics calculations based on the one-group model, it is customary to neglect the slowing down time for fission neutrons produced in the assembly. This assumption is well justified in most non-steady state treatments because the change in the neutron density during a time interval equal to the neutron slowing down time is negligible. The decay constant for a far subcritical assembly, however, may be large enough so that this assumption is not valid for the purposes of evaluating pulsed neutron source experiments. Hence, in this section, the

assumption that neutrons produced from thermal fission slow down instantaneously is removed. An age-diffusion analysis will be given first, to be followed by a multigroup treatment.

The diffusion equation for thermal neutrons is repeated here:

$$\overline{vD}\nabla^2 n(\vec{r},t) - \overline{v\Sigma}_a n(\vec{r},t) + \overline{v\Sigma}_a(1-\beta)k_\infty P_1(B^2) n(\vec{r},t-T_o) + q(\vec{r},\tau_o,t) = \frac{\partial}{\partial t} n(\vec{r},t), \tag{2.30}$$

where the notation $n(\vec{r}, t-T_o)$ indicates that the source of fission neutrons at time t is actually due to fast neutrons which were produced at time T_o earlier. It should be recalled that the continuous slowing down model assumes that all neutrons require the same time to slow down. If $n(\vec{r}, t-T_o)$ is expanded in a Taylor Series about $(\vec{r}, t)$, the result is:

$$n(\vec{r}, t-T_o) = n(\vec{r}, t) - T_o \left.\frac{\partial n(\vec{r}, t)}{\partial t}\right)_t + \frac{T_o^2}{2!} \left.\frac{\partial^2 n(\vec{r}, t)}{\partial t^2}\right)_t - \ldots . \tag{2.97}$$

Inserting Eq. (2.97) in Eq. (2.30) and taking the Laplace Transform of the result, we have:

$$\overline{vD}\nabla^2 \bar{n} - \overline{v\Sigma}_a \bar{n} + \overline{v\Sigma}_a(1-\beta)k_\infty P_1(B^2)\left[1 - sT_o + \frac{s^2T_o^2}{2!} - \ldots\right]\bar{n} + \bar{q} = s\bar{n}. \tag{2.98}$$

The series in Eq. (2.98) can be truncated after two terms if $sT_o \ll 1$ and, solving for $\bar{n}_n$, the result is:

$$\bar{n}_n = \frac{\bar{q}_n}{\lambda_n + s\left(1 + T_o\overline{v\Sigma}_a(1-\beta)k_\infty P_1(B_n^2)\right)}, \tag{2.99}$$

where λ_n has previously been defined as the n^{th} mode decay constant in the Fermi age-diffusion treatment:

$$\lambda_n = \overline{v\Sigma}_a + \overline{vD}B_n^2 - \overline{v\Sigma}_a(1-\beta)k_\infty P_1(B_n^2). \tag{2.34}$$

The time behavior of the n^{th} mode of the neutron density is governed by the zeros in the denominator of Eq. (2.99) and, hence, the decay constant is given by:

$$\lambda_n' = \frac{\lambda_n}{1 + T_o \overline{v\Sigma}_a (1-\beta) k_\infty P_1 (B_n^2)} \quad . \tag{2.100}$$

If the slowing down time, T_o, is neglected, Eq. (2.100) reduces to Eq. (2.34) of Sec. 2.2 ($\lambda_n' = \lambda_n$). The physical interpretation of Eq. (2.100) is as follows. The Fermi age-diffusion expression for the decay constant, λ_n, underestimates the contribution of the multiplied neutrons because it assumes these neutrons were produced instantaneously rather than at an earlier time when the neutron density was higher by a factor $e^{\lambda T_o}$. The modified Fermi age-diffusion treatment leading to Eq. (2.100) corrects this deficiency by decreasing the non-modified value of the decay constant which, in effect, prolongs the decay time of the neutron density.

Another approach to the problem of a finite slowing down time is afforded by the use of multigroup theory. Suppose that the energy range between fission and thermal energies is divided into I groups spaced so that equal time is spent in each group during the slowing down process; then, for a sufficient number of groups, the change in the amplitude of the neutron density over the time interval spanned by a particular group may be neglected. This effect is first treated by a two-group model and then extended to an arbitrary number of groups in a straightforward manner.

The two-group diffusion equations are:

$$\overline{v_1 D_1} \nabla^2 n_1 - \overline{v_1 \Sigma}_1 n_1 + \frac{\overline{v_2 \Sigma}_2}{p} (1-\beta) k_\infty n_2 + \overline{v_o \Sigma}_o n_o \delta(t) = \frac{\partial n_1}{\partial t} \quad , \tag{2.101a}$$

$$\overline{v_2 D_2} \nabla^2 n_2 - \overline{v_2 \Sigma}_2 n_2 + p \overline{v_1 \Sigma}_1 n_1 = \frac{\partial n_2}{\partial t} \quad , \tag{2.101b}$$

where the subscripts 0, 1, and 2 refer to the source group (assumed to appear in the system instantaneously at t = 0), the fast group, and the thermal group, respectively. It will be noted that $\overline{v_2 D}_2 \equiv \overline{vD}$; $\overline{v_2 \Sigma}_2 \equiv \overline{v\Sigma}_a$; and $n_2(\vec{r}, t) \equiv n(\vec{r}, t)$ in accordance with the definitions of these quantities given in Sec. 2.2.

The solution of Eqs. (2.101a) and (2.101b) is obtained with the aid of the Laplace Transformation. If the initial conditions:

$$n_1(\vec{r}, 0) = 0,$$

$$n_2(\vec{r}, 0) = 0,$$

are assumed and the spatial dependence is determined, as usual, by the Helmholtz equation:

$$\nabla^2 n_{1,2}(\vec{r}, t) = -B^2 n_{1,2}(\vec{r}, t),$$

the transformed equations become:

$$-(\overline{v_1 D}_1 B_n^2 + \overline{v_1 \Sigma}_1 + s)\bar{n}_{1n} + \frac{\overline{v_2 \Sigma}_2}{p}(1-\beta)k_\infty \bar{n}_{2n} = -\overline{v_o \Sigma}_o \bar{n}_{on}, \quad (2.102a)$$

$$p\overline{v_1 \Sigma}_1 \bar{n}_{1n} - \left(\overline{v_2 D}_2 B_n^2 + \overline{v_2 \Sigma}_2 + s\right)\bar{n}_{2n} = 0. \quad (2.102b)$$

If we define:

$$\ell_{1n} = \frac{1}{\overline{v_1 \Sigma}_1 + \overline{v_1 D}_1 B_n^2} = \frac{1}{\overline{v_1 \Sigma}_1 (1+\tau B_n^2)}, \quad (2.103a)$$

$$\ell_{2n} = \frac{1}{\overline{v_2 \Sigma}_2 + \overline{v_2 D}_2 B_n^2} = \frac{1}{\overline{v_2 \Sigma}_2 (1+L^2 B_n^2)}, \quad (2.103b)$$

and eliminate $\bar{n}_{1n}$ between Eqs. (2.102a) and (2.102b), the result is:

$$\left[(1+s\ell_{1n})(1+s\ell_{2n}) - (1-\beta)k_\infty \overline{v_1 \Sigma}_1 \ell_{1n} \overline{v_2 \Sigma}_2 \ell_{2n}\right]\bar{n}_{2n}$$

$$= p\overline{v_o \Sigma}_o \overline{v_1 \Sigma}_1 \ell_{1n} \ell_{2n} \bar{n}_{on}. \quad (2.104)$$

The time behavior of the thermal neutron density is characterized by those values of s for which the quantity in brackets on the left-hand side of Eq. (2.104) vanishes. Hence, we require:

$$s^2 + s\left(\frac{1}{\ell_{1n}} + \frac{1}{\ell_{2n}}\right) + \frac{1-\gamma_n}{\ell_{1n}\ell_{2n}} = 0, \quad (2.105)$$

where

$$\gamma_n = (1-\beta)k_\infty \overline{v_1 \Sigma}_1 \ell_{1n} \overline{v_2 \Sigma}_2 \ell_{2n}. \quad (2.106)$$

The two roots of Eq. (2.105) are:

$$\lambda_{1n} = \frac{\ell_{1n} + \ell_{2n}}{2\ell_{1n}\ell_{2n}} \left[1 + \sqrt{\frac{1 - 4(1-\gamma_n)\ell_{1n}\ell_{2n}}{(\ell_{1n}+\ell_{2n})^2}} \right], \tag{2.107a}$$

$$\lambda_{2n} = \frac{\ell_{1n} + \ell_{2n}}{2\ell_{1n}\ell_{2n}} \left[1 - \sqrt{\frac{1 - 4(1-\gamma_n)\ell_{1n}\ell_{2n}}{(\ell_{1n}+\ell_{2n})^2}} \right]. \tag{2.107b}$$

Since $\frac{\ell_{1n}\ell_{2n}}{(\ell_{1n}+\ell_{2n})^2} \ll 1$, we have:

$$\sqrt{\frac{1 - 4(1-\gamma_n)\ell_{1n}\ell_{2n}}{(\ell_{1n}+\ell_{2n})^2}} \approx 1 - \frac{2(1-\gamma_n)\,\ell_{1n}\ell_{2n}}{(\ell_{1n}+\ell_{2n})^2}, \tag{2.108}$$

and, substituting Eq. (2.108) in Eqs. (2.107a) and (2.107b), the result is:

$$\lambda_{1n} \approx \frac{(\ell_{1n}+\ell_{2n})^2 - (1-\gamma_n)\ell_{1n}\ell_{2n}}{\ell_{1n}\ell_{2n}(\ell_{1n}+\ell_{2n})} = \frac{1}{\ell_{1n}} + \frac{1}{\ell_{2n}} - \frac{1-\gamma_n}{\ell_{1n}+\ell_{2n}} \approx \frac{1}{\ell_{1n}}, \tag{2.109a}$$

$$\lambda_{2n} \approx \frac{1-\gamma_n}{\ell_{1n}+\ell_{2n}} = \frac{1-\gamma_n}{\ell_{2n}\left(1+\frac{\ell_{1n}}{\ell_{2n}}\right)}. \tag{2.109b}$$

The asymptotic time behavior of the thermal neutron density is governed by the smaller decay constant which is λ_{2n}. Furthermore, if Eqs. (2.106) and (2.103b) are inserted in Eq. (2.109b) and it is noted that:

$$\overline{v_1\Sigma}_1\ell_{1n} = \frac{1}{1+\tau_o B_n^2} = P_1(B_n^2), \tag{2.110}$$

then:

$$\lambda_{2n} = \frac{\overline{v_2\Sigma}_2 + \overline{v_2 D}_2 B_n^2 - \overline{v_2\Sigma}_2(1-\beta)k_\infty P_1(B_n^2)}{1+\frac{\ell_{1n}}{\ell_{2n}}}, \tag{2.111}$$

which is identical to the expression derived in Sec. 2.2.4 (Eq. 2.34) based on the Fermi age-diffusion model provided the ratio ℓ_{1n}/ℓ_{2n} is neglected. Thus, it is evident that neglect of the fast neutron lifetime

in two-group theory is, in a sense, equivalent to neglect of the slowing down time in Fermi age-diffusion theory.

The extension of the above development to an arbitrary number of groups, insofar as comparison of asymptotic decay constants is concerned, is straightforward. The characteristic polynomial equation in s for I groups is:

$$s^I + s^{I-1}\left(\sum_{i=1}^{I}\frac{1}{\ell_{in}}\right) + \ldots s\frac{\sum_{i=1}^{I}(\ell_{in})}{\prod_{i=1}^{I}(\ell_{in})}$$

$$+\frac{1-(1-\beta)k_\infty\prod_{i=1}^{I}(\overline{v_i\Sigma}_i\ell_{in})}{\prod_{i=1}^{I}(\ell_{in})} = 0, \tag{2.112}$$

or

$$s^I + a_1 s^{I-1} + \ldots + a_{I-1}s + a_I = 0. \tag{2.113}$$

The smallest root of Eq. (2.113) is given approximately by:

$$\lambda_{In} = \frac{a_I}{a_{I-1}}, \tag{2.114}$$

and, hence:

$$\lambda_{In} = \frac{1-(1-\beta)k_\infty\prod_{i=1}^{I}(\overline{v_i\Sigma}_i\ell_{in})}{\sum_{i=1}^{I}(\ell_{in})}. \tag{2.115}$$

If we write:

$$\sum_{i=1}^{I}(\ell_{in}) = \sum_{i=1}^{I-1}(\ell_{in}) + \ell_{In}, \tag{2.116a}$$

$$\prod_{i=1}^{I}(\overline{v_i\Sigma}_i\ell_{in}) = \overline{v_I\Sigma}_I\ell_{In}\prod_{i=1}^{I-1}\left(P_i(B_n^2)\right), \tag{2.116b}$$

and revert to the notation used in the two-group treatment:

$$\sum_{i=1}^{I-1} (\ell_{in}) + \ell_{In} \equiv \ell_{1n} + \ell_{2n}, \tag{2.117a}$$

$$\overline{\nu_I \Sigma}_I \ell_{In} \prod_{i=1}^{I-1} P_i(B_n^2) \equiv \overline{\nu_2 \Sigma}_2 \ell_{2n} P_1(B_n^2), \tag{2.117b}$$

$$\lambda_{In} \equiv \lambda_{2n}, \tag{2.117c}$$

the expression for the decay constant becomes:

$$\lambda_{2n} = \frac{1 - (1-\beta)k_\infty \overline{\nu_2 \Sigma}_2 \ell_{2n} P_1(B_n^2)}{\ell_{1n} + \ell_{2n}}$$

$$= \frac{\overline{\nu_2 \Sigma}_2 + \overline{\nu_2 D}_2 B_n^2 - \overline{\nu_2 \Sigma}_2 (1-\beta)k_\infty P_1(B_n^2)}{1 + \dfrac{\ell_{1n}}{\ell_{2n}}} . \tag{2.119}$$

Equation (2.119) is identical to Eq. (2.111) which was derived on the basis of two-group theory. Thus, to first-order, the two-group and multigroup treatments yield the same result provided the neutron lifetimes and fast non-leakage probabilities are suitably defined in each case.

Several expressions for the fundamental mode decay constant have been derived in this chapter. Although each assumption or condition has been investigated separately, the resulting expressions are such that any combination can be applied to fit the experimental situation. Table 2.1 contains a summary of the various expressions In Chap. IV, the evaluation of lattice parameters using several of the above expressions is discussed, and in Chap. V, the results and conclusions are given.

TABLE 2.1

Expressions for the Fundamental Mode Decay Constant

Model	Expression	Remarks
1) Age-Diffusion	$\overline{v\Sigma}_a + \overline{vD}B^2 - \overline{v\Sigma}_a(1-\beta)k_\infty P_1(B^2)$	Includes all assumptions given in Sec. 2.2
2) Age-Diffusion	$\overline{v\Sigma}_a + \overline{vD}(B')^2 - \overline{v\Sigma}_a(1-\beta)k_\infty P_1(B^2)$	Removes black boundary assumption $\left[(B')^2 = \left(\frac{2.405}{R+d}\right)^2 + \left(\frac{\pi}{H+d+d'}\right)^2\right]$
3) Age-Diffusion	$\overline{v\Sigma}_a + \overline{vD}B^2 - \overline{v\Sigma}_a(1-\beta)k_\infty P_1(B^2)$	Includes delayed neutrons: $(\omega/\lambda) \ll 1$
4) Modified Two-Group	$\overline{v\Sigma}_a + \overline{vD}B^2 - \dfrac{\overline{v\Sigma}_a(1-\beta)k_\infty P_1(B^2)}{1 - \dfrac{(1-\beta_r)k_r}{P_1(B^2)}}$	Includes resonance fission
5) Modified Age-Diffusion	$\dfrac{\overline{v\Sigma}_a + \overline{vD}B^2 - \overline{v\Sigma}_a(1-\beta)k_\infty P_1(B^2)}{1 + T_o\overline{v\Sigma}_a(1-\beta)k_\infty P_1(B^2)}$	Includes finite slowing down time (T_o)
6) Two-Group	$\dfrac{\overline{v\Sigma}_a + \overline{vD}B^2 - \overline{v\Sigma}_a(1-\beta)k_\infty P_1(B^2)}{1 + \dfrac{\ell_1}{\ell_2}}$	Includes finite fast neutron lifetime
7) Multigroup	$\dfrac{\overline{v\Sigma}_a + \overline{vD}B^2 - \overline{v\Sigma}_a(1-\beta)k_\infty \prod_{i=1}^{I-1} P_i(B^2)}{1 + \dfrac{\sum_{i=1}^{I-1} \ell_i}{\ell_I}}$	Includes effective finite fast neutron lifetime

CHAPTER III

EXPERIMENTAL EQUIPMENT

3.1 THE M.I.T. LATTICE FACILITY

A detailed description of the M. I. T. Exponential Lattice Facility and its ancillary equipment has been given in an earlier report (H2). Cross-sectional drawings of the Facility are shown in Figs. 3.1 and 3.2. Neutrons from the thermal column of the M. I. T. Reactor enter a graphite-lined cavity or "hohlraum" and are reflected upward through a graphite pedestal into a cylindrical tank. The tank is 67-1/4 inches high and either 36 or 48 inches in diameter, depending on the lattice being studied.

In all cases, the lattices studied consisted of uranium metal rods clad in Type 1100 aluminum, located on a triangular spacing, and immersed in heavy water. The absorber-modified lattices contained, in addition, thin OFHC (oxygen-free, high conductivity) copper rods which served as the distributed thermal neutron absorber. The lattices investigated are summarized in Table 3.1.

The active length of the fuel rods was 48 inches, and the rods were supported by aluminum adapters positioned in girders at the top of the tank. An aluminum grid plate with appropriately spaced holes served to position the rods at the bottom of the tank. A blanket of nitrogen gas was kept over the high purity (approximately 99.5 mole per cent) heavy water to prevent degradation by atmospheric light water.

3.2 PULSED NEUTRON SOURCE EQUIPMENT

The modification of the M. I. T. Lattice Facility for pulsed neutron source measurements and the additional equipment required for these experiments have been described in detail in an earlier report (M1). Since the experimental equipment used in this work differs very little from that used previously, only those features which have changed will be described in detail. A brief summary of the unchanged features will be given. A block diagram of the experimental arrangement and data

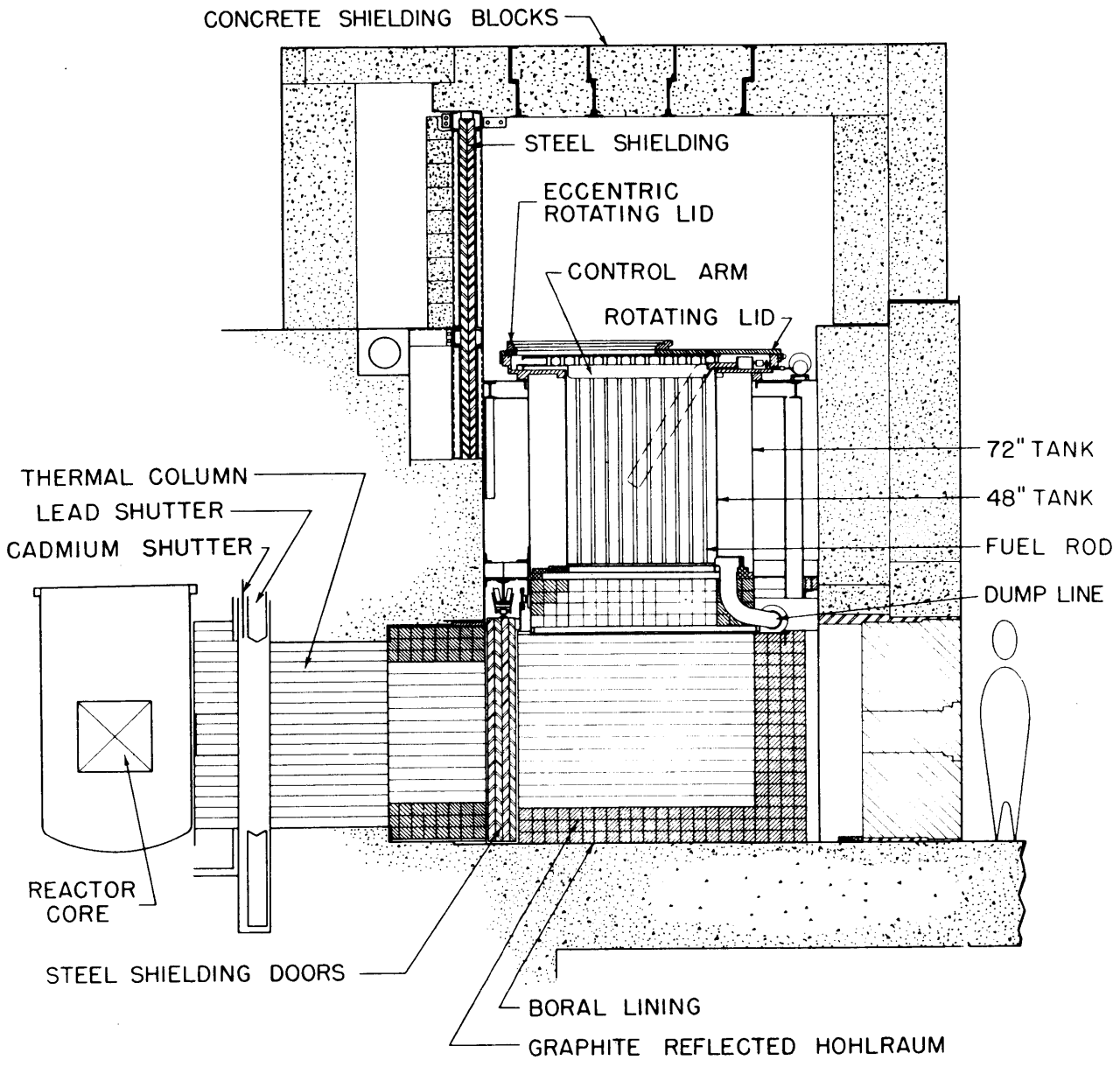

FIG. 3.1. VERTICAL SECTION OF THE SUBCRITICAL ASSEMBLY

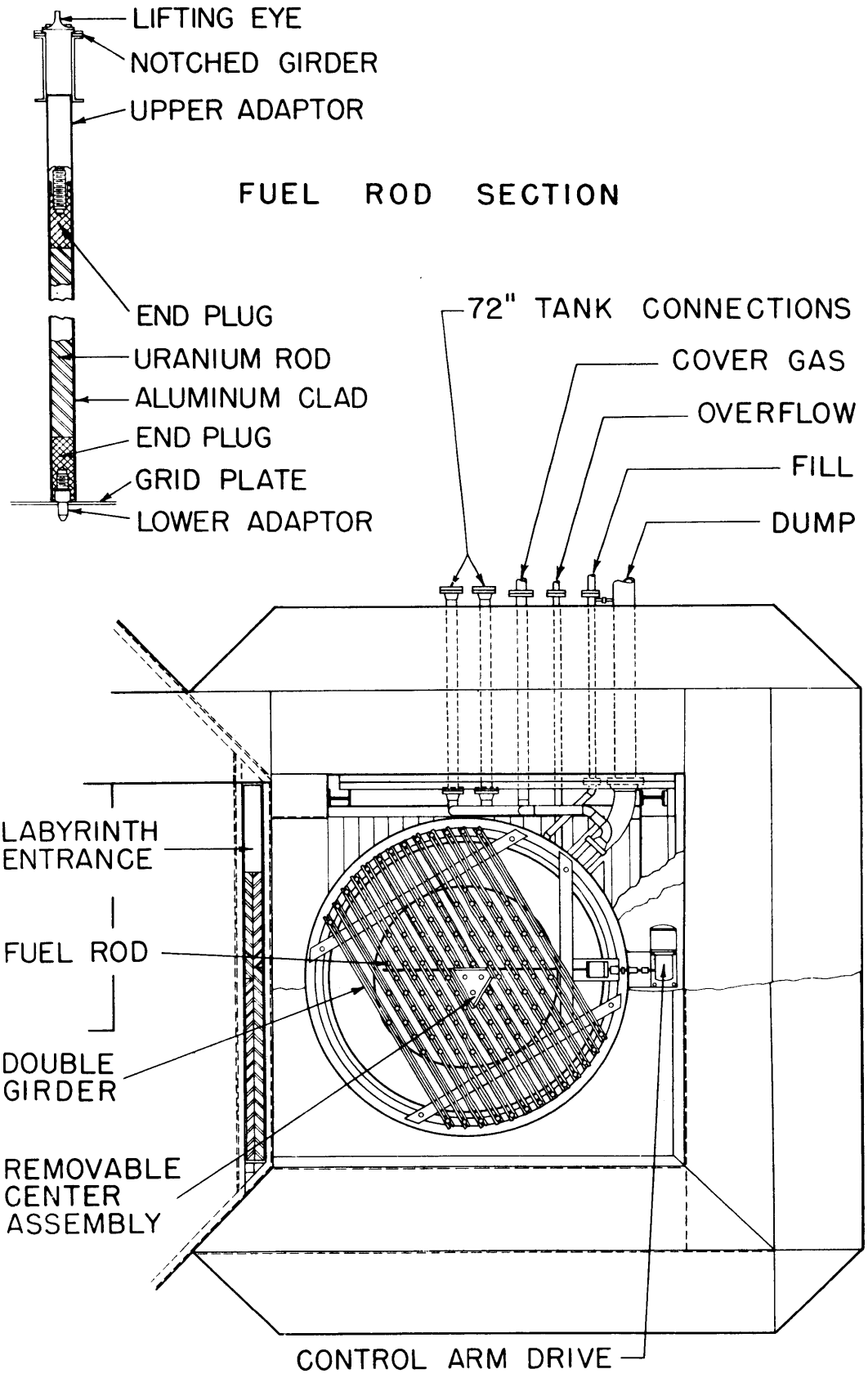

FIG. 3.2. PLAN VIEW OF THE SUBCRITICAL ASSEMBLY

TABLE 3.1

Description of Lattices Studied

Lattice Designator	Lattice Spacing (inches)	Fuel Slug Diameter (inches)	Air Gap (inches)	Clad Thickness (inches)	Fuel Rod Outer Diameter (inches)	Uranium Enrichment (weight %)	D_2O Purity (mole %)	Cross Sectional Area of Added Absorber per Fuel Rod (inches^2)
125	1.25	0.250	0.006	0.028	0.318	1.143	99.60	–
175	1.75	0.250	0.006	0.028	0.318	1.143	99.53	–
175A1[a]	1.75	0.250	0.006	0.028	0.318	1.143	99.53	0.0278
175A1B1	1.75	0.250	0.006	0.028	0.318	1.143	99.53	0.0441
250	2.50	0.250	0.006	0.028	0.318	1.143	99.56	–
250B1[a]	2.50	0.250	0.006	0.028	0.318	1.143	99.56	0.0163
250B2	2.50	0.250	0.006	0.028	0.318	1.143	99.56	0.0326
253	2.50	0.750	0.004	0.028	0.814	0.947	99.51	–
253A2B1	2.50	0.750	0.004	0.028	0.814	0.947	99.51	0.0718
350	3.50	0.750	0.004	0.028	0.814	0.947	99.47	–
500	5.00	0.750	0.004	0.028	0.814	0.947	99.47	–
175(2R)[b]	1.75	0.250	0.006	0.028	0.318	1.027	99.53	–
	1.75	0.250	0.006	0.028	0.318	1.143	99.53	–
500(2R)	5.00	1.010	0.014	0.028	1.094	0.710	99.47	–
	5.00	0.750	0.004	0.028	0.814	0.947	99.47	–
MOD[c]	∞	–	–	–	–	–	99.47	–

[a] The symbol A1 refers to one 0.188-inch-diameter copper rod per unit cell; the symbol B1 refers to one 0.144-inch-diameter copper rod per unit cell.

[b] Two region assembly; the first set of values refers to the test lattice and the second set refers to the reference lattice.

[c] Pure moderator.

recording system is given at the end of this section.

3.2.1 Description of the Assembly

The normal arrangement and operation of the Lattice Facility had to be modified to accept pulsed neutron source experiments. The black boundary condition, essential to the definition of the geometric buckling eigenvalue, was completed at the bottom of the exponential tank by the presence of a 0.020-inch-thick cadmium plate of the same diameter as the tank and clad with 0.0625-inch-thick aluminum (Type 6106-T6). This plate, which blocked the bottom of the tank from the thermal column source, was inserted when pulsed source experiments were made and removed when steady-state measurements were made. The installation of the plate was undesirable for experimental reasons (described in Sec. 2.5.2) and experiments were made with and without the plate in an attempt to obviate the need for the plate.

A second modification was made in order to insert a neutron detector. The detector was located at the point $r = 0; z = H/2$, where H was the variable height of the moderator. This location was chosen to achieve maximum suppression of higher mode contributions to the observed thermal neutron density. The central fuel rod was replaced with a 1.125-inch-O.D. aluminum thimble (Type 1100) in which the detector could move axially. A lead plug at the bottom of the thimble prevented the thimble from floating and a thin cadmium disk inserted in the bottom of the thimble helped reduce thermal neutron streaming up the thimble.

The third modification was necessitated by the proximity of the M. I. T. Reactor. When the reactor was operating and the Lattice Facility was blocked from the thermal column source, there was still an appreciable neutron background in the assembly caused by photo-neutrons resulting from gamma rays leaking from the reactor. It was found that this background was too high for the achievement of satisfactory results; consequently, pulsed source experiments were made only on weekends when the reactor was shut down.

3.2.2 Pulsed Neutron Source

The pulsed neutron source used for all experiments at the M. I. T. Lattice Facility was a Type A-810 neutron generator built by Kaman Nuclear of Colorado Springs, Colorado. A description of its operation follows. The actual neutron source is situated in a sealed tube approximately 2 inches in diameter by 4-1/2 inches in length. Deuterium ions are produced in a Penning cold cathode ion source and are accelerated toward a tritiated titanium target by application of a short duration, large negative voltage pulse. Neutrons (approximately 10^7 per burst) are thus produced by the D-T reaction. The supply of deuterium gas is continually replenished from a zirconium wire which releases adsorbed deuterium when heated. The entire sealed tube is mounted in a sealed cylindrical enclosure (5-inch diameter by 11-inch length) filled with insulating oil. A schematic diagram of the tube and its components is shown in Fig. 3.3.

The negative target voltage pulse was provided by a step-up (1:25) transformer and was variable between 0 and 150 kilovolts. The pulse width was approximately 10 microseconds and therefore was short enough to meet the instantaneous burst width requirement discussed in Sec. 2.5.1. A 7-foot shielded, flexible, high voltage cable carried the voltage pulse from the step-up transformer to the target. The sealed tube assembly and step-up transformer were located in the Lattice Room above the exponential tank while the main control unit, which provided a variable (0 to 6 kv) pulse voltage to the step-up transformer, was located on the reactor floor, 18 feet below the Lattice Room.

3.2.3 Detection System

The thermalized neutrons were detected by a small BF_3 neutron counter centered axially and radially in the assembly. The counter was a N. Wood model (active volume 0.50-inch diameter by 4.0-inch length, 40 cms Hg filling pressure, B^{10} enrichment 96%) and was guided by the aluminum thimble (Sec. 3.2.1) mounted along the axis of the tank. A shielded cable ran from the counter to a small pre-amplifier through an airtight stopper plugged in a hole on the side of the exponential tank. The associated amplifier-scaler (RIDL Models 30-19 and 49-30,

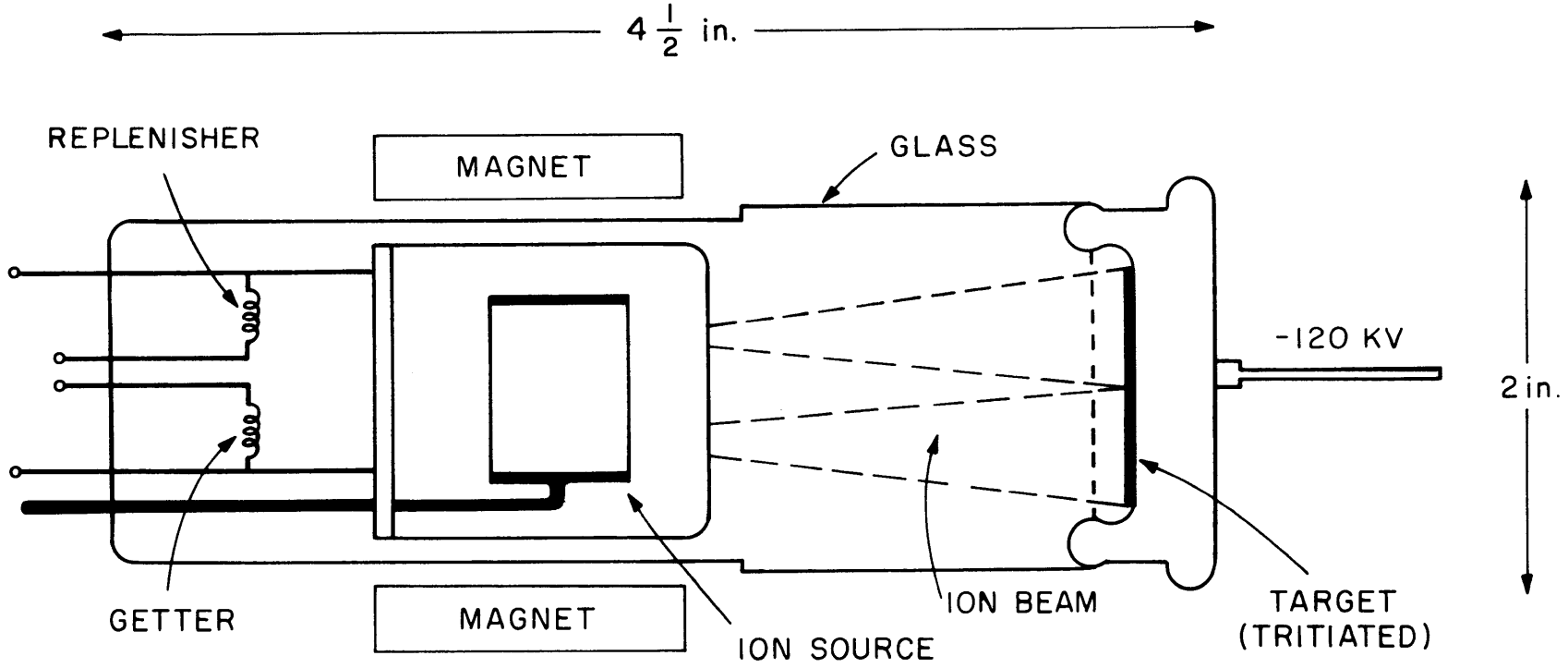

FIG. 3.3 ELEMENTS OF THE PULSED NEUTRON SOURCE

respectively) and counter high voltage supply (RIDL Model 40-9) were located near the main control unit on the reactor floor.

The dead time of the detection system was determined by the double pulse generator method and was on the order of 2 microseconds (M1). The output of the amplifier was monitored by an oscilloscope to insure that the observed count rates corresponded to detected neutrons and not to an external source of noise.

3.2.4 Data Recording System

The counts from the amplifier were sent to an analyzer whose purpose was to map a time profile of the decaying neutron density by recording numbers proportional to the density at preset intervals of time. The analyzer used in this work was a TMC-256 channel analyzer with a Model CN-110 digital computer and a Type 212 Pulsed Neutron plug-in unit.

The system operates in the following way. The 255 channels (2-256) are time analysis channels of equal duration Δ (adjustable from 10 to 2560 microseconds in multiples of 2). Each channel is separated from its neighbors by a dead time gap of 10 microseconds, during which accumulated counts are stored in memory. The first channel records a pre-burst background and its width is independently variable as $2^n\Delta(n = 1, 2, 3, \ldots 8)$.

The time sequence of the logic operation begins with a signal from the main control rack to the Type 212 plug-in unit which opens the pre-burst background channel. At the close of the background channel, the Type 212 plug-in unit sends a signal back to the main control rack which, in turn, sends out a signal to the pulsed voltage source. This causes the negative voltage pulse to be applied to the pulsed neutron source target. At the same time, a variable delay of duration $2^n\Delta(n = 1, 2, 3, \ldots 8)$ is initiated in the time analyzer while the neutron burst thermalizes in the assembly. There is also a pre-set target delay time continuously variable between 0 and 100 microseconds, so that the overall delay time is reduced by the pre-set target delay time. Thereafter, the remaining 255 channels open in succession to receive counts from the detector. After the close of the last channel, the

system is dead until another signal is received from the main control unit by the Type 212 plug-in unit.

This sequence was repeated at a pre-set repetition rate (variable from 1 pulse per second (pps) to 10 pps in steps of 1 pps) until a desired number of counts was stored in the memory of the analyzer. At the end of the run, the data were available in the form of punched tape and printed tape.

A block diagram of the experimental arrangement and the data recording system is shown in Fig. 3.4.

3.3 EXPERIMENTAL PROCEDURES

In this section, the experimental procedures of particular importance to the performance of pulsed neutron source experiments are summarized. The operation of the pulsed source, itself, has been described in detail in Ref. M1 and is not repeated here.

The modifications of the Lattice Facility described in Sec. 3.2.1 were usually made on Friday night, to allow for a full day (Saturday) of experiments. After the electronic equipment was fully warmed up, the pulsed source was placed on the lid of the lattice tank and centered. Then, the moderator was raised to its lowest level and the pulsed source turned on.

Approximately 10 runs (at 10 different moderator heights) could be made in a single day operation with the changes in moderator level geared to give equal changes in the geometric buckling. The ranges of moderator levels and corresponding geometric bucklings for the 3- and 4-foot-diameter tanks are listed in Table 3.2.

TABLE 3.2

Ranges of the Moderator Heights and Geometric Bucklings

Tank Diameter (ft)	Moderator Height H_o, cm	Geometric Buckling B^2, cm^{-2}
3	57.5 - 130.7	0.0052 - 0.0031
4	57.0 - 129.9	0.0042 - 0.0020

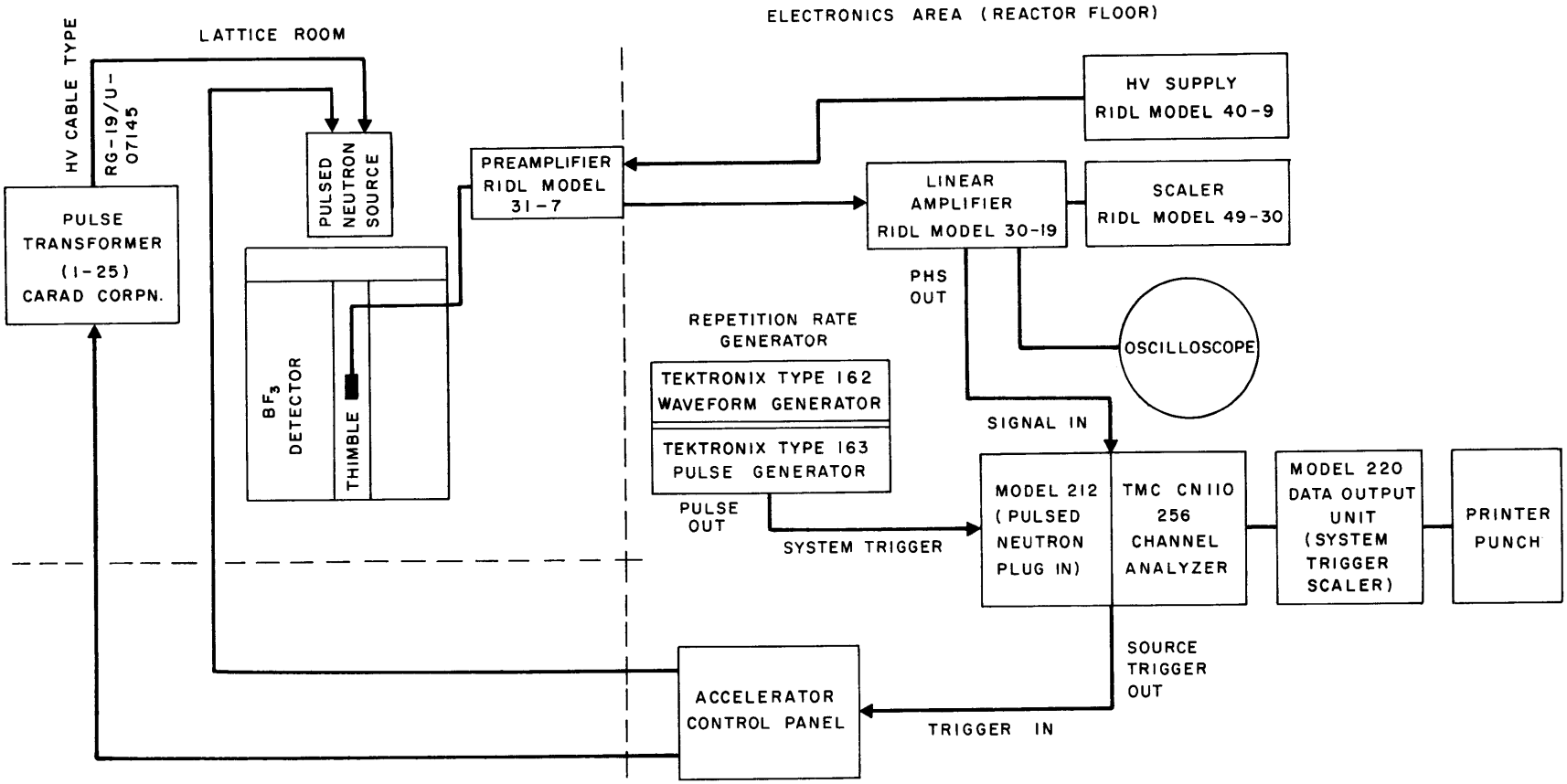

FIG. 3.4 SCHEMATIC OF OVERALL PULSING, DETECTION AND ANALYSIS CIRCUITRY

An accurate determination of the moderator height was essential to a precise definition of the geometric buckling of the system. The relative moderator level could be read to an accuracy of ± 0.05 cm on a graduated sight glass attached to the outside of the assembly shielding. However, a sight glass reading of zero did not correspond to a moderator level of zero so that it was necessary to determine a correction factor to convert sight glass readings to moderator heights. This was accomplished by measuring the distance from the bottom of the tank (or cadmium plate) to the overflow line on the tank and subtracting it from the full height sight glass reading. The correction factors obtained (both with and without the cadmium plate in the bottom of the tank) are listed in Table 3.3. These correction factors should be remeasured each time the tank is changed in the future, since the tank location relative to that of the sight glass may change.

TABLE 3.3

Values of the Sight Glass Correction Factor

Tank Diameter (ft)	With Cd. Plate (cm)	Without Cd. Plate (cm)
3	28.9	28.3
4	30.2	28.6

The variables in the data recording system were set as follows. For expected values of the decay constant greater than approximately 1500 sec^{-1}, a channel width of Δ = 40 microseconds was used. A width of Δ = 80 microseconds was used for expected values less than 1500 sec^{-1}. A minimum of 2000 counts in the most active channel was found to give a statistical accuracy of 1% or better in the fit value of the decay constant when a channel width of 40 microseconds was employed (4000 counts in the case of an 80-microsecond channel width). The background channel was set at 256 $\times \Delta$ to maximize the accumulation of

pre-burst background counts while the combination of the analyzer delay and the preset target delay were set to minimize the overall delay time.

CHAPTER IV

ANALYSIS OF DATA

This chapter deals with the means by which the desired values of lattice parameters are obtained from pulsed neutron measurements on subcritical assemblies. The extraction of a value for the fundamental mode decay constant (and, possibly, one for the next higher spatial mode decay constant) from a measurement of the neutron density as a function of time is treated first. Next, the relation between the parameters of a multiplying medium and the decay constant is developed. Then, the analysis of measurements in two-region assemblies, absorber-modified assemblies, and media with a non-black boundary (determination of the graphite cavity albedo) is described. The chapter concludes with a discussion of the errors associated with the parameters obtained from pulsed source measurements.

4.1 DETERMINATION OF DECAY CONSTANTS

The first step in the analysis of data from pulsed neutron experiments is the determination of decay constants from measurements of the neutron density as a function of time. In general, it is always possible to obtain a value for the fundamental mode decay constant, and under certain conditions, it is possible to obtain an estimate of the next higher mode decay constant.

4.1.1 Fundamental Mode Decay Constant

The data from pulsed source experiments are analyzed under the assumption that the observed neutron density can be represented by an infinite sum of exponential functions plus a constant background term:

$$n(t) = \sum_{n=1}^{\infty} A_n e^{-\lambda_n t} + b. \qquad (4.1)$$

The spatial dependence of the neutron density, which would normally appear in the coefficients A_n in Eq. (4.1), is omitted because the

neutron detector location is fixed during any particular measurement. The background term contains contributions from lattice photoneutrons (induced by gamma rays from the MITR and the lattice fuel elements) and delayed neutrons. As shown in Sec. 2.5.3, the assumption that the delayed neutron contribution is constant over the time interval of observation depends on the inequality:

$$(\omega/\lambda) \ll 1. \tag{2.94}$$

The largest value of (ω/λ) in this work is approximately 0.01, so that the assumption of a constant delayed neutron background is justified.

The decay constants λ_n increase with increasing values of the index n; hence, after a sufficient length of time, the summation in Eq. (4.1) has only one term (corresponding to the fundamental mode). Thus, Eq. (4.1) reduces to:

$$n(t) = A_1 e^{-\lambda_1 t} + b, \tag{4.2}$$

where the quantities A_1, λ_1, and b are to be determined.

One of the computer codes used in this work, EXPO (M1), makes a weighted, least-squares iterative analysis of the count rate data obtained from the data recording system described in Sec. 3.2.4 and calculates values of A_1, λ_1, and b. Since the data in early time channels may contain significant contributions from higher spatial modes (harmonics), the code has provisions to neglect the early channels, one by one, and repeat the analysis. This procedure effectively varies the waiting time between the introduction of the neutron pulse and the beginning of the data analysis. When the decaying neutron density is following only the fundamental mode, the fit values of A_1, λ_1, and b remain constant as a function of the waiting time. In this way, the waiting time for the establishment of the fundamental mode is ascertained along with the corresponding value of the fundamental mode decay constant.

A second code, STRIP, which has been written as a part of this program to provide an independent check on the results of EXPO, determines the parameters A_1, λ_1, and b in a slightly different manner. An initial guess for the background (obtained from the pre-burst background channel) is subtracted from the data and a least-squares fit

made on the natural logarithm of the difference:

$$\ell n[n(t_i)-b] = \ell n(A_1) - \lambda_1 t_i, \tag{4.3}$$

where the index i indicates channel number. However, the resulting values of A_1, λ_1, and b may not be the best fit to the data, owing to a poor guess for b and/or the presence of higher modes in the early time channels. These two difficulties are overcome by systematically varying the value of b subtracted from the data and the time range over which the fit to Eq. (4.3) is made (e.g., varying the initial and final channel numbers) until the variance of fit is a minimum. The variance of fit, which is a measure of how well the fitted parameters (A_1, λ_1, and b) agree with the experimental data, is defined by:

$$V = \frac{\sum_{i=1}^{N} W_i\left(n_i - A_1 e^{-\lambda_1 t_i} - b\right)^2}{N - 3}, \tag{4.4}$$

where W_i is the weight assigned to the i^{th} data point and the quantity N-3 represents the number of data points minus the number of degrees of freedom. That combination of values of A_1, λ_1, and b which yields the smallest value of V is the set which is the "best fit" to the experimental data. In this way, a value of λ_1 is obtained which can be compared to that obtained from EXPO.

4.1.2 Fundamental and Next Higher Mode Decay Constants

Under certain conditions, it may be possible to obtain an estimate of the next higher spatial mode decay constant. If λ_2 is sufficiently smaller than λ_n for all n greater than 2, then over a certain portion of the data, Eq. (4.1) can be simplified to:

$$n(t) = A_1 e^{-\lambda_1 t} + A_2 e^{-\lambda_2 t} + b. \tag{4.5}$$

The FRAUD code, also written as a portion of this work, fits the experimental data to the form given in Eq. (4.5) in much the same way that STRIP analyzes the data according to Eq. (4.3).

Initial estimates of $A_1 e^{-\lambda_1 t}$ and b (which can be obtained from the results of STRIP or EXPO) are subtracted from the data and a least-

squares fit made on the natural logarithm of the difference:

$$\ell n\left[n(t_i) - A_1^1 e^{-\lambda_1^1 t_i} - b \right] = \ell n\, A_2^1 - \lambda_2^1 t_i, \qquad (4.6)$$

where the superscript 1 indicates the first estimate. The quantities $A_2^1 e^{-\lambda_2^1 t_i}$ and b are then subtracted from the initial data and a similar least-squares fit made to obtain values of A_1^2 and λ_1^2 (the second estimate of these quantities). This process is continued until the changes in A_1, λ_1, A_2, and λ_2 from one iteration to the next satisfy predetermined convergence criteria.

The above procedure is repeated with systematically different values of b and the time ranges over which the least-squares fit to the two exponential functions is made. That set of values of the five unknown parameters in Eq. (4.5) which results in the smallest variance of fit is, as before, taken to be the "best fit" to the experimental data. Thus, a third value of λ_1 is obtained as well as an estimate for the next higher mode decay constant. Another advantage of FRAUD is that more of the experimental data are used in the analysis, which reduces the uncertainty in the fit values of A_1 and λ_1 relative to those obtained from STRIP and EXPO.

A more complete description of the operation and use of these three computer codes may be found in Appendix A. The values of the decay constants are listed in Sec. 5.1.

4.2 DETERMINATION OF LATTICE PARAMETERS

The second step in the analysis of pulsed source experiments involves relating the experimental values of the decay constant to the lattice parameters of interest. The evaluation of moderator parameters has been described in an earlier report (M1) and is not taken up here.

The expression for the decay constant in terms of the parameters of the medium for which the decay constant is measured is not unique. There appears to be no "a priori" reason dictating the preference of modified age-diffusion or two-group theories, each of which yields slightly different expressions for the decay constant. Furthermore, the values of the fast non-leakage probability differ by as much as 16%

between the two models. Thus, one of the goals of this work is to determine which, if either, of the two theories is the more appropriate.

In addition to the selection of a theoretical model, a decision must be made as to which lattice parameters to treat as unknown and which to treat as known. There are seven quantities appearing in the expressions for the decay constant which are to be determined: the absorption cross section, $\overline{v\Sigma}_a$; the diffusion coefficient, $\overline{vD}$; the infinite medium multiplication factor, k_∞; the neutron age to thermal, τ_o; the effective delayed neutron fraction, β; the fission neutron slowing down time, T_o; and the ratio of fast to thermal neutron lifetimes, (ℓ_1/ℓ_2). The remaining quantity, the geometric buckling:

$$B^2 = \left(\frac{2.405}{R_o + d}\right)^2 + \left(\frac{\pi}{H_o + 2d}\right)^2, \tag{2.83}$$

is the known independent invariable (the moderator height, H_o, is changed to vary the value of B^2) which can be measured to an estimated accuracy of 0.4%.

The last three quantities of the seven listed above are all small compared to the dominant term in the factor in which they appear; i. e., the quantity β appears only in the factor $(1-\beta)$, which is close to unity; the quantity T_o appears only in the factor $(1+T_o\overline{v\Sigma}_a(1-\beta)k_\infty P_1(B^2))$, which is usually between 1.01 and 1.10 in the assemblies studied; and the quantity (ℓ_1/ℓ_2) appears only in the factor $(1+\ell_1/\ell_2)$, which is also usually between 1.01 and 1.10. Thus, it is reasonable to assume that β, T_o, and (ℓ_1/ℓ_2) can be calculated because, although the uncertainty in the calculation may be relatively large, the overall contribution to the expressions for the decay constant is small. The calculation of these quantities is described in Appendix B.

The neutron age to thermal, τ_o, has been measured in heavy water to an accuracy of 2.5% (W1), and extensive theoretical treatments (G1) are available to correct this value for the small effects of lattice heterogeneity. The age to thermal is therefore taken as known.

These assumptions reduce the number of quantities to be determined experimentally from seven to three. Of these three, the diffusion coefficient:

$$\overline{vD} = \overline{vD}_o - CB^2, \tag{2.28}$$

is directly obtainable from the analysis of pulsed source experiments on pure moderator (see, for example, Ref. M1). However, as pointed out in Appendix B (see Sec. B.4), the introduction of fuel or other strong absorber into a weakly absorbing medium such as a moderator significantly hardens the neutron spectrum relative to that existing in pure moderator. Thus, the values of $\overline{vD}_o$ and C for heavy water cannot be applied directly to the analysis of pulsed source experiments on uranium, heavy water lattices. It is argued, nevertheless, that if the experimental values of $\overline{vD}_o$ and C in heavy water are corrected for the effects of spectral hardening by some theoretical model, valid estimates of these quantities in a lattice are obtained. A theoretical correction to account for spectral hardening, which is based on use of the THERMOS code (H9), is described in Appendix B and corrected values are tabulated there. This final assumption leaves two quantities, $\overline{v\Sigma}_a$ and k_∞, to be treated as unknown in the analysis of pulsed source experiments.

Both modified age-diffusion and two-group models are applied to the analysis of the experimental data. The age-diffusion treatment is presented first, followed by the two-group treatment.

The expression for the fundamental mode decay constant obtained from a modified age-diffusion model is transcribed from Chap. II:

$$\lambda_i = \frac{\overline{v\Sigma}_a + \overline{vD}B_i^2 - \overline{v\Sigma}_a(1-\beta)k_\infty P_1(B_i^2)}{1 + T_o\overline{v\Sigma}_a(1-\beta)k_\infty P_1(B_i^2)}, \tag{2.100}$$

where the subscript i refers to the discrete values of the experimental observables λ_i and B_i^2. The objective is to find values of $\overline{v\Sigma}_a$ and k_∞ which, in conjunction with the calculated value of $\overline{vD}$, β, τ_o, and T_o, give the best agreement with the experimental data.

To this end, Eq. (2.100) is rewritten:

$$\lambda_i' = \overline{v\Sigma}_a - \overline{v\Sigma}_a(1-\beta)k_\infty P_1(B_i^2), \tag{4.7}$$

where,

$$\lambda_i' = \lambda_i\left[1+\alpha_{FA}P_1(B_i^2)\right] - \overline{vD}B_i^2, \tag{4.8a}$$

$$\alpha_{FA} = T_o\overline{v\Sigma}_a(1-\beta)k_\infty. \tag{4.8b}$$

For a particular value of α_{FA}, the quantity λ_i' in Eq. (4.7) can be considered as a corrected experimental decay constant and, with $P_1(B_i^2) = e^{-B_i^2\tau_o}$ as the independent variable, a least-squares fit is made to obtain the "least-squares" coefficients $\overline{v\Sigma}_a$ and $\overline{v\Sigma}_a(1-\beta)k_\infty$. Hence, values of the parameters $\overline{v\Sigma}_a$ and k_∞ are obtained from the coefficients of the least-squares fit. Furthermore, since k_∞ is customarily close to unity, a smaller uncertainty in the derived value of k_∞ is obtained if the least-squares fit is made on a modified version of Eq. (4.7):

$$\lambda_i' = \overline{v\Sigma}_a[1-(1-\beta)k_\infty] - \overline{v\Sigma}_a(1-\beta)k_\infty[P_1(B_i^2) - 1] = r - sP_1' . \tag{4.9}$$

Then, k_∞ is derived as:

$$k_\infty = \frac{1}{(1-\beta)(1+r/s)} . \tag{4.10}$$

There is, however, a further equation to satisfy before the final values of $\overline{v\Sigma}_a$ and k_∞ are obtained; namely, Eq. (4.8b), which is rewritten as:

$$\frac{\alpha_{FA}}{T_o(1-\beta)} = \overline{v\Sigma}_a k_\infty . \tag{4.11}$$

If, for a particular choice of α_{FA} and for the calculated values of T_o and β, the product of the derived parameters $\overline{v\Sigma}_a$ and k_∞ does not agree with the right-hand side of Eq. (4.11), the least-squares fit to Eq. (4.7) is repeated with a different value of α_{FA} until Eq. (4.11) is satisfied. The corresponding values of $\overline{v\Sigma}_a$ and k_∞ are then the values of these parameters which yield the best agreement between the experimental data and Eq. (2.100). Finally, an experimental value of the thermal diffusion area ($L^2 \equiv \overline{vD}_o/\overline{v\Sigma}_a$) is obtained as the ratio of the infinite medium diffusion coefficient (tabulated in Table B.5) to the absorption cross section.

An IBM-7094 Computer code, LSQHEB, has been written as a part of this program to aid in the analysis. The code takes the experimental values of λ_i and B_i^2 and the calculated values of β, τ_o, and $\overline{vD}$ as input data, makes a least-squares fit to Eq. (4.7) for a specified range of values of α_{FA}, and computes values of $\overline{v\Sigma}_a$ and k_∞ and their standard deviations. A description of the use and operation of LSQHEB is given in Appendix A.

The two-group expression for the fundamental mode decay constant is derived in Chap. II:

$$\lambda_i = \frac{\overline{v\Sigma}_a + \overline{vD}B_i^2 - \overline{v\Sigma}_a(1-\beta)k_\infty P_1(B_i^2)}{1 + \ell_1/\ell_2} . \tag{2.111}$$

The use of Eq. (2.111) in conjunction with experimental data is similar to the procedure just described for the modified age-diffusion model. The ratio (ℓ_1/ℓ_2) is written as:

$$\frac{\ell_1}{\ell_2} = \frac{\overline{v\Sigma}_a(1+L^2B_i^2)}{\overline{v_1\Sigma}_1(1+\tau_o B_i^2)} = \alpha_{2G}(1+L^2B_i^2)P_1(B_i^2), \tag{4.12}$$

where:

$$\alpha_{2G} = \frac{\overline{v\Sigma}_a}{\overline{v_1\Sigma}_1} , \tag{4.13a}$$

$$P_1(B_i^2) = \frac{1}{1 + \tau_o B_i^2} . \tag{4.13b}$$

Then, substitution of Eq. (4.12) into Eq. (2.111) yields:

$$\lambda_i' = \lambda_i\left[1 + \alpha_{2G}(1+L^2B_i^2)P_1(B_i^2)\right] - \overline{vD}B_i^2$$

$$= \overline{v\Sigma}_a - \overline{v\Sigma}_a(1-\beta)k_\infty P_1(B_i^2). \tag{4.14}$$

The parameters $\overline{v\Sigma}_a$ and k_∞ are evaluated over a range of values of α_{2G}, with calculated values of β, τ_o, $\overline{vD}$, and L^2. When Eq. (4.13a) is satisfied (i. e., the least-squares value of $\overline{v\Sigma}_a$ equals the product of α_{2G} and the calculated value of $\overline{v_1\Sigma}_1$), the corresponding values of $\overline{v\Sigma}_a$ and k_∞ are taken to be the best values relating the experimental data to Eq. (2.111). Reference is again made to Appendix A where a description of LSQHEB, the computer code written to facilitate the analysis, is given.

This section is concluded with a brief summary of the method used by Malaviya (M1) to determine the parameters k_∞ and $\overline{v\Sigma}_a$. The age-diffusion model was used to develop the expression for λ, with the slowing down time T_o neglected in the derivation and the diffusion cooling coefficient set equal to zero. The resulting expression for λ was:

$$\lambda = \overline{v\Sigma}_a + \overline{vD}_o B^2 - \overline{v\Sigma}_a(1-\beta)k_\infty P_1(B^2). \tag{2.37}$$

The fast non-leakage probability was expanded in a power series in $B^2\tau_o$:

$$e^{-B^2\tau_o} = 1 - B^2\tau_o + \frac{1}{2}B^4\tau_o \ldots ,$$

and, after collecting terms in like powers of B^2, Malaviya obtained:

$$\lambda = r + tB^2 - uB^4, \tag{4.15}$$

where:

$$r = \overline{v\Sigma}_a[1 - (1-\beta)k_\infty], \tag{4.15a}$$

$$t = \overline{vD}_o + \overline{v\Sigma}_a(1-\beta)k_\infty\tau_o, \tag{4.15b}$$

$$u = \frac{1}{2}\overline{v\Sigma}_a(1-\beta)k_\infty\tau_o^2. \tag{4.15c}$$

A least-squares fit was made to obtain the coefficients r, t, and u (with calculated values of τ_o and β and with the value of $\overline{vD}_o$ obtained from experiments on moderator alone), and the parameters k_∞ and $\overline{v\Sigma}_a$ were evaluated from Eqs. (4.15a) and (4.15b). The results obtained from Malaviya's method of analysis are given in Sec. 5.2.2 for the 500 lattice for purposes of comparison with the method of analysis developed in this work.

4.3 ANALYSIS OF TWO-REGION LATTICES

The goal of pulsed neutron measurements in two-region assemblies is to obtain experimental values of lattice parameters in the inner (or test) region of the assembly. The properties of the outer (or reference) region of the assembly are presumed known from previous pulsed source measurements on a lattice composed entirely of the reference medium. The analysis is based on the two-group expression for the decay constant (for reasons to be given in Sec. 5.7) although the modified age-diffusion treatment could be used as well.

The measured value of the fundamental mode decay constant can be related to the parameters of the reference region (denoted, as in Chap. II, by the subscript b):

$$\lambda = \frac{\overline{v\Sigma}_{ab} + \overline{vD}_b B_b^2 - \overline{v\Sigma}_{ab}(1-\beta)k_{\infty b}P_1(B_b^2)}{1 + \alpha_{2Gb}(1+L_b^2 B_b^2)P_1(B_b^2)}, \tag{4.16}$$

where:

$$B_b^2 = \alpha_b^2 + \left(\frac{\pi}{H}\right)^2. \tag{2.50a}$$

The quantity α_b^2 is the radial geometric buckling of the reference region and is unknown. However, for a measured value of λ (corresponding to a particular extrapolated moderator height H), Eq. (4.16) can be solved for B_b^2 since the properties of the reference region are known. Then, a value of α_b^2 is obtained from Eq. (2.50a). This procedure is repeated for several sets of values of λ and H and, since the radial geometric buckling is independent of H, the several values of α_b^2 can be averaged to obtain α_b^2 for the reference region. The radial geometric buckling of the test region (denoted, as in Chap. II, by the subscript x) is next determined from the secular equation (Eq. (2.52)) which is transcribed from Chap. II in functional form:

$$g_b(\alpha_b, \overline{vD}_b, R_x, R_b) = g_x(\alpha_x, \overline{vD}_x, R_x, R_b), \tag{2.52}$$

where R_b is the outer radius of the assembly and R_x is the boundary separating the two regions. The quantity R_x is determined from:

$$\pi R_x^2 = N_x A_x, \tag{4.17}$$

where A_x is the cross-sectional area of a unit cell of the test region and N_x is the number of such unit cells. The left-hand side of Eq. (2.52) is a known quantity, once α_b is determined; hence, α_x can be obtained from the solution of Eq. (2.52). The geometric buckling of the test region at each moderator height H is then known:

$$B_x^2 = \alpha_x^2 + \left(\frac{\pi}{H}\right)^2. \tag{2.50b}$$

Finally, the parameters of the test lattice are related to the measured values of the decay constant:

$$\lambda = \frac{\overline{v\Sigma}_{ax} + \overline{vD}_x B_x^2 - \overline{v\Sigma}_{ax}(1-\beta)k_{\infty x}P_1(B_x^2)}{1 + \alpha_{2Gx}(1+L_x^2 B_x^2)P_1(B_x^2)}, \tag{4.18}$$

in a manner identical to that described in Sec. 4.2.

4.4 ANALYSIS OF ABSORBER-MODIFIED LATTICES

The uncertainty in the values of $\overline{v\Sigma}_a$ and k_∞ derived from a set of pulsed source measurements may be reduced by adding successive amounts of a thermal neutron absorber to the lattice and repeating the measurements.

Equation (4.9) is first recalled:

$$\lambda' = r - sP'_1, \tag{4.9}$$

where,

$$r = \overline{v\Sigma}_a[1-(1-\beta)k_\infty], \tag{4.19a}$$

$$s = \overline{v\Sigma}_a(1-\beta)k_\infty, \tag{4.19b}$$

$$P'_1 = P_1(B^2) - 1. \tag{4.19c}$$

Values of $\overline{v\Sigma}_a$ and k_∞ can be obtained for each lattice studied (e.g., the unmodified lattice and each absorber-modified lattice) from the coefficients r and s in the manner described in Sec. 4.2. However, as pointed out in Chap. II, the addition of a thermal absorber provides additional information. If sufficient absorber is added to make $(1-\beta)k_\infty = 1.0$, then r = 0 and a "null state" results. With the null state condition, a relation between the absorption cross section of the "null state" added absorber and the coefficient r in the unmodified lattice is derived in Chap. II:

$$r^c = (1-\gamma_1)\overline{v\Sigma}_a^c - \gamma_1\gamma_2\gamma_3\overline{v\Sigma}_{a3}^y, \tag{2.66}$$

where the superscripts c and y represent the unmodified and null state lattices, respectively; $\overline{v\Sigma}_{a3}$ is the added absorber cross section, and:

$$\gamma_1 = \left(\frac{\eta^c}{\eta^y}\right)\left(\frac{\epsilon^c}{\epsilon^y}\right)\left(\frac{p^c}{p^y}\right), \tag{2.64a}$$

$$\gamma_2 = \frac{\overline{v\Sigma}_{ao}^c \bar{n}_o^c V_o}{\overline{v\Sigma}_{ao}^y \bar{n}_o^y V_o}, \tag{2.64b}$$

$$\gamma_3 = \frac{\bar{n}_3^y V_3}{\sum_{i=0}^{2} \bar{n}_i^c V_i} \quad . \tag{2.64c}$$

Thus, Eq. (4.9) has only one unknown coefficient, s^c, which should reduce the uncertainty in the fit value of s^c and, consequently, the uncertainty in the values of $\overline{v\Sigma}_a^c$ and k_∞^c derived from r^c and s^c. The purpose of this section is to describe how the "null state" condition is determined since, in general, it is highly unlikely that the exact amount of absorber required can be determined in advance.

The null state is determined from the experimental values of the coefficient r and the theoretical results of THERMOS and TULIP (H1). First, Eqs. (2.56b) and (2.57) are substituted into Eq. (4.19):

$$r = \frac{\sum_{i=0}^{3} \overline{v\Sigma}_{ai} \bar{n}_i V_i}{\sum_{i=0}^{3} \bar{n}_i V_i} - (1-\beta)\eta\epsilon p \frac{\overline{v\Sigma}_{ao} \bar{n}_o V_o}{\sum_{i=0}^{3} \bar{n}_i V_i} \quad . \tag{4.20}$$

If Eq. (4.20) is multiplied by the ratio $\left(\sum_{i=0}^{3} \bar{n}_i V_i / \overline{v\Sigma}_{ao} \bar{n}_o V_o \right)$, the result is:

$$ar = q + X_3, \tag{4.21}$$

where:

$$a = \frac{\sum_{i=0}^{3} \bar{n}_i V_i}{\overline{v\Sigma}_{ao} \bar{n}_o V_o}, \tag{4.22a}$$

$$q = [1 - (1-\beta)\eta\epsilon p] + \frac{\sum_{i=0}^{2} \overline{v\Sigma}_{ai} \bar{n}_i V_i}{\overline{v\Sigma}_{ao} \bar{n}_o V_o}, \tag{4.22b}$$

$$X_3 = \frac{\overline{v\Sigma}_{a3} \bar{n}_3 V_3}{\overline{v\Sigma}_{ao} \bar{n}_o V_o} \quad . \tag{4.22c}$$

The quantities a and X_3 are obtained from the output of THERMOS

(unmodified lattice) and TULIP (absorber-modified lattices) , leaving the coefficient q as the only unknown quantity in Eq. (4.21). Hence, a least-squares fit to Eq. (4.21), with the experimental values of r, is used to obtain q. Furthermore, at the null state, r = 0; and, therefore:

$$(X_3)_{\substack{\text{null}\\ \text{state}}} = -q \equiv \frac{\overline{v\Sigma}^y_{a3}\,\bar{n}^y_3 V_3}{\overline{v\Sigma}^y_{ao}\,\bar{n}^y_o V_o} . \tag{4.23}$$

Finally, substitution of Eqs. (4.22a) and (4.23) into Eq. (2.66) and insertion of the definitions of γ_2 and γ_3 yields:

$$r^c = (1-\gamma_1)\overline{v\Sigma}^c_a - \frac{\gamma_1 q}{a^c} . \tag{4.24}$$

Values of the factors appearing in γ_1 (Eq. (2.64a)) have been tabulated in a recent report (H1).

It is also shown in Chap. II that an estimate of τ_o for the unmodified lattice can be obtained if a three-parameter least-squares fit is made on the decay constant as a function of geometric buckling data:

$$\lambda' = r + tB^2 - uB^4. \tag{2.69}$$

The expression for τ_o is:

$$\tau_o = \frac{t^y}{\overline{v\Sigma}^y_a} . \tag{2.72}$$

Since the variation of the coefficient t with increasing amounts of added absorber is small (see Eq. (2.57)), an adequate estimate of t^y can be obtained from a first-order least-squares fit to the experimental values of t as a function of $\overline{v\Sigma}_{a3}\bar{n}_3 V_3/\overline{v\Sigma}_{ao}\bar{n}_o V_o$. The absorption cross section of the null state lattice can be written in terms of a and q:

$$\overline{v\Sigma}^y_a = \frac{1}{a^y}\left[\frac{\sum_{i=0}^{2} \overline{v\Sigma}^y_{ai}\,\bar{n}^y_i V_i}{\overline{v\Sigma}^y_{ao}\,\bar{n}^y_o V_o} - q\right] . \tag{4.25}$$

Hence, provided the range and accuracy of the data justify a three-parameter fit, an estimate of τ_o for the lattice is obtained which can then be compared with the value calculated in Appendix B.

4.5 DETERMINATION OF EFFECTIVE RETURN COEFFICIENT

Pulsed source measurements have been made with and without a cadmium plate at the bottom of the lattice tank in an attempt to obviate the need for the plate. Both a moderating medium and a neutron-multiplying medium have been investigated. The analysis of the former condition is described first, followed by that for a multiplying medium.

The expression for the decay constant in a moderating medium is derived in Sec. 2.2.3:

$$\lambda = \overline{v\Sigma}_a + \overline{vD}_o B^2 - CB^4, \tag{2.29}$$

where B^2 is the geometric buckling for a bare cylindrical system:

$$B^2 = \left(\frac{2.405}{R_o + d}\right)^2 + \left(\frac{\pi}{H_o + 2d}\right)^2. \tag{2.83}$$

If the bottom of the lattice tank is not effectively bare, the expression for the buckling should be modified:

$$(B')^2 = \left(\frac{2.405}{R_o + d}\right) + \left(\frac{\pi}{H_o + d + d\left(\frac{1+\beta_a}{1-\beta_a}\right)}\right)^2, \tag{2.84}$$

where β_a is the return coefficient or albedo of the graphite-lined cavity below the lattice tank. For a measurement of the decay constant in the non-bare system:

$$\lambda = \overline{v\Sigma}_a + \overline{vD}_o (B')^2 - C(B')^4. \tag{4.26}$$

Thus, once the properties of the moderator (e. g., $\overline{v\Sigma}_a$, $\overline{vD}_o$, C) have been determined from pulsed neutron experiments on the bare system, $(B')^2$ is obtained as the smaller solution of Eq. (4.26) for a particular measured value of λ. Finally, the return coefficient is evaluated from Eq. (2.84). Since β_a should be independent of the moderator height H_o, the several values of β_a (one for each value of λ) are averaged to obtain a value for the entire set of measurements.

The above analysis can be extended to multiplying systems provided the distinction between fast and thermal neutrons is taken into account insofar as cadmium is concerned. The cadmium plate absorbs

practically all neutrons impinging on it with energies less than the cadmium cutoff and very few with energies above the cutoff. Hence, the terms in the expression for the decay constant which involve the fast non-leakage probability are not affected by the presence or absence of the cadmium plate. The expression for the decay constant in the non-bare system becomes, on the modified age-diffusion model:

$$\lambda = \frac{\overline{v\Sigma}_a + \overline{vD}(B')^2 - \overline{v\Sigma}_a(1-\beta)k_\infty P_1(B^2)}{1 + T_o\overline{v\Sigma}_a(1-\beta)k_\infty P_1(B^2)}, \qquad (4.27a)$$

or,

$$\lambda = \frac{\overline{v\Sigma}_a + \overline{vD}(B')^2 - \overline{v\Sigma}_a(1-\beta)k_\infty P_1(B^2)}{1 + \frac{\overline{v\Sigma}_a}{\overline{v_1\Sigma}_1}\left(1+L^2(B')^2\right)P_1(B^2)}, \qquad (4.27b)$$

on the two-group model. The determination of β_a from this point on is the same as that described for the non-multiplying medium.

4.6 ANALYSIS OF ERRORS

One of the objectives of this work is to determine how accurately the lattice parameters – in particular, k_∞ – can be measured with the pulsed source technique. There are two types of errors associated with the derived value of k_∞; statistical and systematic.

The statistical errors arise because of the random nature of neutron interactions. Thus, the data recorded by the time analyzer exhibit random fluctuations about the exponential form of the decay of the neutron density. The magnitudes of these fluctuations are reflected in the standard deviation of the decay constant which is computed by standard techniques (H8) as a part of the operation of each of the three computer codes described in Sec. 4.1. In theory, the standard deviation of a particular decay constant can be made negligibly small if enough data are collected.

After several different decay constants have been measured, a least-squares fit is made to obtain the coefficients r and s (Eqs. (4.19a) and (4.19b)) together with their standard deviations. The uncertainty in the value of k_∞ derived from r and s (denoted by δk_∞) then reflects the

uncertainties in r and s which, in turn, reflect the standard deviations of the decay constants used in the least-squares fit. This contribution to the error in k_∞, which arises solely from the statistical nature of neutron interactions, can, in theory, be made arbitrarily small if enough values of the decay constants are obtained.

However, in the absence of significant statistical errors, there are still systematic errors which contribute to the overall uncertainty in k_∞. For example, a change in the reported value of the age to thermal, τ_o, would shift all the values of the fast non-leakage probability by approximately the same percentage and, hence, change the derived value of k_∞. These systematic errors can be taken into account by solving the two-group (or modified age-diffusion) expression for the decay constant to obtain k_∞:

$$k_\infty = \frac{\overline{v\Sigma}_a + \overline{vD}B^2 - \lambda\left(1 + \frac{\overline{v\Sigma}_a}{\overline{v_1\Sigma}_1}(1+L^2B^2)P_1(B^2)\right)}{\overline{v\Sigma}_a(1-\beta)P_1(B^2)}, \tag{4.28}$$

and then applying the formula (F2):

$$(\Delta k_\infty)^2 = \sum_i \left(\frac{\partial k_\infty}{\partial X_i}\right)^2 (\Delta X_i)^2, \tag{4.29}$$

where X_i takes on successive values of all the parameters in Eq. (4.28) except those whose errors are part of the least-squares fitting process (i. e., λ and $\overline{v\Sigma}_a$) and do not affect k_∞ in a systematic way. The two parameters whose associated errors have the most pronounced effect on k_∞ are τ_o and $\overline{vD}_o$ (see Sec. 5.6). Their contributions to Eq. (4.29) are, respectively:

$$(\Delta k_\infty)_{\tau_o} \approx k_\infty B^2 P_1(B^2)\Delta\tau, \tag{4.30}$$

$$(\Delta k_\infty)_{\overline{vD}_o} = \frac{B^2}{\overline{v\Sigma}_a(1-\beta)P_1(B^2)}\Delta\overline{vD}_o. \tag{4.31}$$

The final error associated with k_∞ is then given by:

$$(\sigma k_\infty)^2 = (\delta k_\infty)^2 + (\Delta k_\infty)^2, \tag{4.32}$$

and reflects contributions from both systematic sources (Eq. (4.29)) and random sources (standard deviations in the least-squares coefficients arising from uncertainties in the fit values of the decay constants).

CHAPTER V

RESULTS AND CONCLUSIONS

The results of the investigation are given in this chapter. Section 5.1 contains values of the fundamental mode decay constants and corresponding geometric bucklings. The derived parameters for heavy water and for multiplying media are presented in Sec. 5.2. The results of two-region and absorber-modified lattice studies are dealt with in Secs. 5.3 and 5.4, respectively, while the measured values of the return coefficient are given in Sec. 5.5. The several systematic contributions to the total error in k_∞ are listed in Sec. 5.6. The final section discusses and compares the results, and, where appropriate, presents the conclusions drawn from this work.

5.1 FUNDAMENTAL MODE DECAY CONSTANTS

The determination of a value for the fundamental mode decay constant from a measurement of the neutron density as a function of time is described in Sec. 4.1. The results for heavy water are given in Table 5.1 and for the several lattices are given in Tables 5.2 - 5.12. The corresponding values of geometric buckling are also listed. Estimates of the next higher mode decay constants for the 500 lattice, which yielded the best results from the standpoint of statistical accuracy, are given in Appendix C based on the analysis with FRAUD. The lattices studied are described in Table 3.1.

Each set of data was analyzed with the three IBM-7094 Computer codes, FRAUD, EXPO, and STRIP. A typical example, based on the results of FRAUD, is given in Fig. 5.1 which illustrates the variation of λ as a function of B^2 for the 500 lattice.

The errors listed are the standard deviations arising from the least-squares fitting and reflect the statistical fluctuations in the observed data.

TABLE 5.1

Measured Fundamental Mode Decay Constant λ
as a Function of Geometric Buckling B^2
for 99.47% Heavy Water at 25°C

Geometric Buckling B^2, m^{-2}	Decay Constant λ, sec^{-1}		
	FRAUD	EXPO	STRIP
20.41	452.6 ± 4.2	443.6 ± 8.9	441.8 ± 4.7
22.29	487.7 ± 4.9	488.7 ± 9.1	486.6 ± 11.8
24.59	528.6 ± 5.3	539.2 ± 10.4	521.0 ± 5.7
26.82	588.6 ± 2.9	580.3 ± 5.4	581.2 ± 5.6
28.83	614.6 ± 5.8	608.2 ± 7.5	606.9 ± 10.5
31.10	669.1 ± 4.3	663.8 ± 5.6	663.9 ± 9.9
31.18	674.9 ± 2.9	664.5 ± 9.7	656.6 ± 7.3
33.43	728.5 ± 10.4	722.6 ± 7.6	720.2 ± 14.2
35.68	767.7 ± 5.8	762.1 ± 6.5	761.9 ± 8.8
38.13	809.4 ± 6.3	806.0 ± 17.2	800.6 ± 23.9
38.88	825.5 ± 5.8	829.6 ± 12.8	822.2 ± 14.9
40.21	867.4 ± 4.2	852.8 ± 13.8	847.6 ± 13.4
41.91	890.4 ± 4.9	890.2 ± 10.7	879.6 ± 23.5
42.57	899.6 ± 6.9	900.7 ± 19.2	895.7 ± 28.2
45.04	954.8 ± 4.6	952.4 ± 13.8	939.6 ± 11.1
48.97	1026.9 ± 4.9	1030.4 ± 14.9	1026.3 ± 27.5
54.71	1139.6 ± 13.7	1132.4 ± 13.8	1130.7 ± 19.0
57.48	1206.7 ± 13.2	1196.7 ± 10.8	1178.8 ± 11.3

TABLE 5.2

Measured Fundamental Mode Decay Constant λ
as a Function of Geometric Buckling B^2
for the 125 Lattice

Geometric Buckling B^2, m^{-2}	Decay Constant λ, sec^{-1}	
	EXPO	STRIP
30.94	950.7 ± 15.3	945.5 ± 21.8
33.01	1084.2 ± 14.6	1075.8 ± 20.4
34.55	1135.2 ± 20.7	1140.6 ± 24.3
36.60	1239.2 ± 20.8	1231.3 ± 21.8
39.30	1376.7 ± 26.4	1377.0 ± 32.3
43.21	1558.7 ± 17.6	1562.6 ± 18.3

TABLE 5.3

Measured Fundamental Mode Decay Constant λ
as a Function of Geometric Buckling B^2
for the 175 Lattice

Geometric Buckling B^2, m^{-2}	Decay Constant λ, sec^{-1}		
	FRAUD	EXPO	STRIP
31.00	676.6 ± 4.3	675.1 ± 5.9	672.3 ± 6.1
31.88	746.9 ± 6.3	745.0 ± 8.2	736.8 ± 7.7
33.03	747.5 ± 4.2	761.0 ± 9.3	755.8 ± 10.2
34.58	816.2 ± 3.7	814.2 ± 8.2	810.3 ± 6.6
36.62	922.5 ± 4.6	922.8 ± 10.5	921.4 ± 17.5
39.26	1009.8 ± 8.3	1014.3 ± 12.2	1003.4 ± 9.3
43.23	1125.1 ± 6.6	1133.8 ± 13.1	1121.0 ± 11.6
45.80	1207.8 ± 7.9	1202.8 ± 16.2	1204.6 ± 13.6
49.26	1309.0 ± 15.9	1284.0 ± 11.9	1286.0 ± 16.0
52.59	1449.5 ± 39.2	1440.0 ± 18.0	1452.2 ± 22.9
57.81	1591.6 ± 34.8	1579.0 ± 17.8	1577.8 ± 27.2

TABLE 5.4

Measured Fundamental Mode Decay Constant λ
as a Function of Geometric Buckling B^2
for the 175 A1 Lattice

Geometric Buckling B^2, m^{-2}	Decay Constant λ, sec^{-1}		
	FRAUD	EXPO	STRIP
30.96	1357.9 ± 8.1	1291.3 ± 32.6	1231.0 ± 40.8
31.88	1410.5 ± 14.1	1317.0 ± 22.5	1278.8 ± 47.5
33.04	1491.0 ± 21.5	1400.6 ± 42.1	1375.2 ± 37.0
34.57	1517.7 ± 11.2	1491.3 ± 26.2	1485.3 ± 35.1
36.56	1583.4 ± 10.7	1546.9 ± 26.3	1533.2 ± 26.6
39.40	1689.6 ± 34.8	1645.3 ± 29.5	1648.5 ± 37.2
43.29	1875.6 ± 23.7	1779.3 ± 42.3	1761.6 ± 59.7
49.31	2085.1 ± 54.2	1998.7 ± 37.4	2013.5 ± 78.3

TABLE 5.5

Measured Fundamental Mode Decay Constant λ
as a Function of Geometric Buckling B^2
for the 175 A1B1 Lattice

Geometric Buckling B^2, m^{-2}	Decay Constant λ, sec^{-1}		
	FRAUD	EXPO	STRIP
30.95	1761.8 ± 26.5	1707.6 ± 23.2	1686.0 ± 30.8
31.85	1792.8 ± 13.3	1738.0 ± 27.6	1720.5 ± 26.0
33.04	1832.6 ± 26.5	1783.6 ± 31.3	1739.4 ± 42.3
34.56	1894.9 ± 19.5	1824.1 ± 28.5	1823.8 ± 31.9
36.46	1978.4 ± 17.8	1940.7 ± 22.1	1967.1 ± 33.7
39.32	2068.9 ± 32.7	2011.8 ± 34.9	2030.7 ± 50.4
43.33	2188.8 ± 38.2	2154.0 ± 42.4	2158.7 ± 44.1
49.37	2397.2 ± 30.5	2396.9 ± 48.0	2381.3 ± 50.3

TABLE 5.6

Measured Fundamental Mode Decay Constant λ
as a Function of Geometric Buckling B^2
for the 250 Lattice

Geometric Buckling B^2, m^{-2}	Decay Constant λ, sec^{-1}		
	FRAUD	EXPO	STRIP
31.03	658.2 ± 2.9	654.8 ± 10.5	660.0 ± 6.9
31.03	665.1 ± 5.2	655.0 ± 9.4	670.4 ± 10.6
31.92	681.2 ± 2.4	682.2 ± 7.7	680.9 ± 7.2
33.20	705.6 ± 8.3	701.3 ± 8.8	696.6 ± 12.8
34.66	752.7 ± 13.5	748.4 ± 11.1	744.2 ± 14.6
36.69	802.9 ± 5.1	817.2 ± 17.2	801.6 ± 12.6
39.46	895.1 ± 7.0	880.0 ± 21.6	874.6 ± 12.5
43.54	994.9 ± 4.9	985.8 ± 14.4	980.1 ± 12.9
49.59	1204.5 ± 5.3	1170.0 ± 13.1	1163.7 ± 14.2

TABLE 5.7

Measured Fundamental Mode Decay Constant λ
as a Function of Geometric Buckling B^2
for the 250 B1 Lattice

Geometric Buckling B^2, m^{-2}	Decay Constant λ, sec^{-1}		
	FRAUD	EXPO	STRIP
31.02	829.1 ± 5.7	813.1 ± 11.1	810.2 ± 8.2
31.90	878.5 ± 2.3	844.8 ± 11.9	854.2 ± 16.3
33.10	904.4 ± 5.4	889.7 ± 9.1	890.3 ± 9.6
34.62	921.8 ± 4.5	919.1 ± 14.6	912.1 ± 13.2
36.64	985.9 ± 6.1	968.3 ± 15.3	970.5 ± 16.2
39.38	1079.6 ± 13.5	1048.0 ± 15.0	1039.5 ± 18.2
43.34	1174.0 ± 7.2	1143.2 ± 13.2	1149.9 ± 12.2
49.36	1336.6 ± 22.9	1309.9 ± 19.7	1309.9 ± 31.0

TABLE 5.8

Measured Fundamental Mode Decay Constant λ
as a Function of Geometric Buckling B^2
for the 250 B2 Lattice

Geometric Buckling B^2, m^{-2}	Decay Constant λ, sec^{-1}		
	FRAUD	EXPO	STRIP
31.02	1045.5 ± 5.5	1019.7 ± 15.6	1027.3 ± 18.5
31.96	--	--	1062.6 ± 24.7
33.13	1144.8 ± 8.9	1089.9 ± 16.3	1088.8 ± 20.4
34.63	1111.5 ± 28.1	1109.0 ± 39.6	1113.7 ± 66.5
36.66	1212.0 ± 21.7	1166.1 ± 53.0	1194.3 ± 75.9
39.25	1243.4 ± 6.9	1214.3 ± 16.5	1221.8 ± 23.8
43.44	1352.0 ± 11.3	1351.5 ± 17.4	1347.3 ± 16.4
49.51	1542.9 ± 20.3	1512.4 ± 26.8	1509.7 ± 26.7

TABLE 5.9

Measured Fundamental Mode Decay Constant λ
as a Function of Geometric Buckling B^2
for the 253 Lattice

Geometric Buckling B^2, m^{-2}	Decay Constant λ, sec^{-1}		
	FRAUD	EXPO	STRIP
30.90	1511.2 ± 8.9	1452.0 ± 21.4	1456.9 ± 42.1
30.90	1596.5 ± 12.1	1602.0 ± 33.3	1567.9 ± 33.6
33.40	1726.4 ± 14.3	1697.7 ± 41.1	1703.7 ± 44.8
35.87	1918.1 ± 24.1	1892.3 ± 28.1	1871.2 ± 28.5
38.83	2063.5 ± 26.8	1976.4 ± 27.7	1957.7 ± 27.5
41.97	2168.8 ± 39.0	2133.8 ± 37.4	2136.7 ± 44.3
45.20	2343.0 ± 17.6	2286.2 ± 30.2	2265.7 ± 42.9
48.38	2487.6 ± 32.4	2464.3 ± 41.1	2466.7 ± 123.5
51.63	2661.5 ± 73.6	2623.1 ± 37.6	2610.3 ± 50.6
55.30	2747.8 ± 39.5	2740.1 ± 88.3	2748.1 ± 78.8
57.61	2887.1 ± 32.9	2844.2 ± 49.4	2858.5 ± 47.7

TABLE 5.10

Measured Fundamental Mode Decay Constant λ
as a Function of Geometric Buckling B^2
for the 253 A2B1 Lattice

Geometric Buckling B^2, m^{-2}	Decay Constant λ, sec^{-1}		
	FRAUD	EXPO	STRIP
30.87	2237.0 ± 37.1	2338.5 ± 72.0	2286.5 ± 115.7
30.88	2537.3 ± 40.9	2460.9 ± 83.5	2383.4 ± 108.2
33.40	2479.8 ± 43.0	2525.5 ± 57.4	2456.2 ± 59.7
33.40	2805.5 ± 61.5	--	--
35.88	2779.2 ± 36.1	2664.8 ± 78.7	2608.3 ± 61.1
38.74	2902.3 ± 68.4	2819.3 ± 61.9	2772.6 ± 110.4
41.95	3040.3 ± 83.5	2975.5 ± 73.9	2928.2 ± 89.6
45.18	3365.7 ± 47.3	3175.2 ± 79.1	3143.6 ± 85.4
48.29	3297.8 ± 68.0	3233.4 ± 205.5	3226.9 ± 107.2
51.36	3352.1 ± 106.8	3316.1 ± 136.2	3259.1 ± 138.4
51.36	3728.0 ± 86.1	3417.9 ± 101.4	3375.2 ± 92.1

TABLE 5.11

Measured Fundamental Mode Decay Constant λ
as a Function of Geometric Buckling B^2
for the 350 Lattice

Geometric Buckling B^2, m^{-2}	Decay Constant λ, sec^{-1}		
	FRAUD[a]	EXPO[a]	STRIP[a]
20.18	332.1 ± 1.7	330.7 ± 2.0	330.6 ± 2.6
22.19	421.4 ± 5.1	418.6 ± 2.2	418.5 ± 4.6
24.01	491.3 ± 2.8	494.4 ± 3.4	490.0 ± 7.7
26.01	592.9 ± 5.1	587.5 ± 6.0	584.7 ± 7.0
27.93	665.9 ± 5.7	662.9 ± 4.7	662.6 ± 6.8
30.03	747.8 ± 12.6	743.6 ± 5.9	746.9 ± 11.2
32.15	817.1 ± 8.1	816.4 ± 6.1	816.8 ± 7.0
34.12	897.5 ± 9.0	888.9 ± 7.2	891.7 ± 7.8
36.31	961.9 ± 8.2	958.0 ± 9.4	958.6 ± 7.3
38.23	1030.1 ± 9.6	1029.9 ± 9.4	1030.4 ± 11.8
40.58	1094.6 ± 8.4	1076.7 ± 9.6	1077.4 ± 14.4

[a]These values were measured without the cadmium plate at the bottom of the tank.

TABLE 5.12

Measured Fundamental Mode Decay Constant λ
as a Function of Geometric Buckling B^2
for the 500 Lattice

Geometric Buckling B^2, m^{-2}	Decay Constant λ, sec^{-1}		
	FRAUD	EXPO	STRIP
20.36	324.3 ± 1.5	319.2 ± 5.4	321.6 ± 2.8
22.16	382.3 ± 3.7	380.1 ± 4.0	380.7 ± 3.6
24.34	450.6 ± 3.5	447.2 ± 3.8	447.1 ± 3.2
26.44	517.1 ± 3.9	519.8 ± 8.4	518.4 ± 5.2
28.49	587.5 ± 6.4	590.5 ± 7.1	591.2 ± 10.1
30.68	658.4 ± 9.0	647.0 ± 6.0	642.8 ± 5.5
33.02	723.7 ± 3.3	723.1 ± 10.0	722.5 ± 13.1
35.02	782.7 ± 6.8	774.7 ± 9.5	775.4 ± 11.7
37.43	857.1 ± 10.5	848.9 ± 9.0	842.5 ± 9.0
39.41	928.1 ± 4.6	926.6 ± 20.9	925.9 ± 18.2
41.66	969.3 ± 9.2	967.8 ± 14.0	967.4 ± 17.1

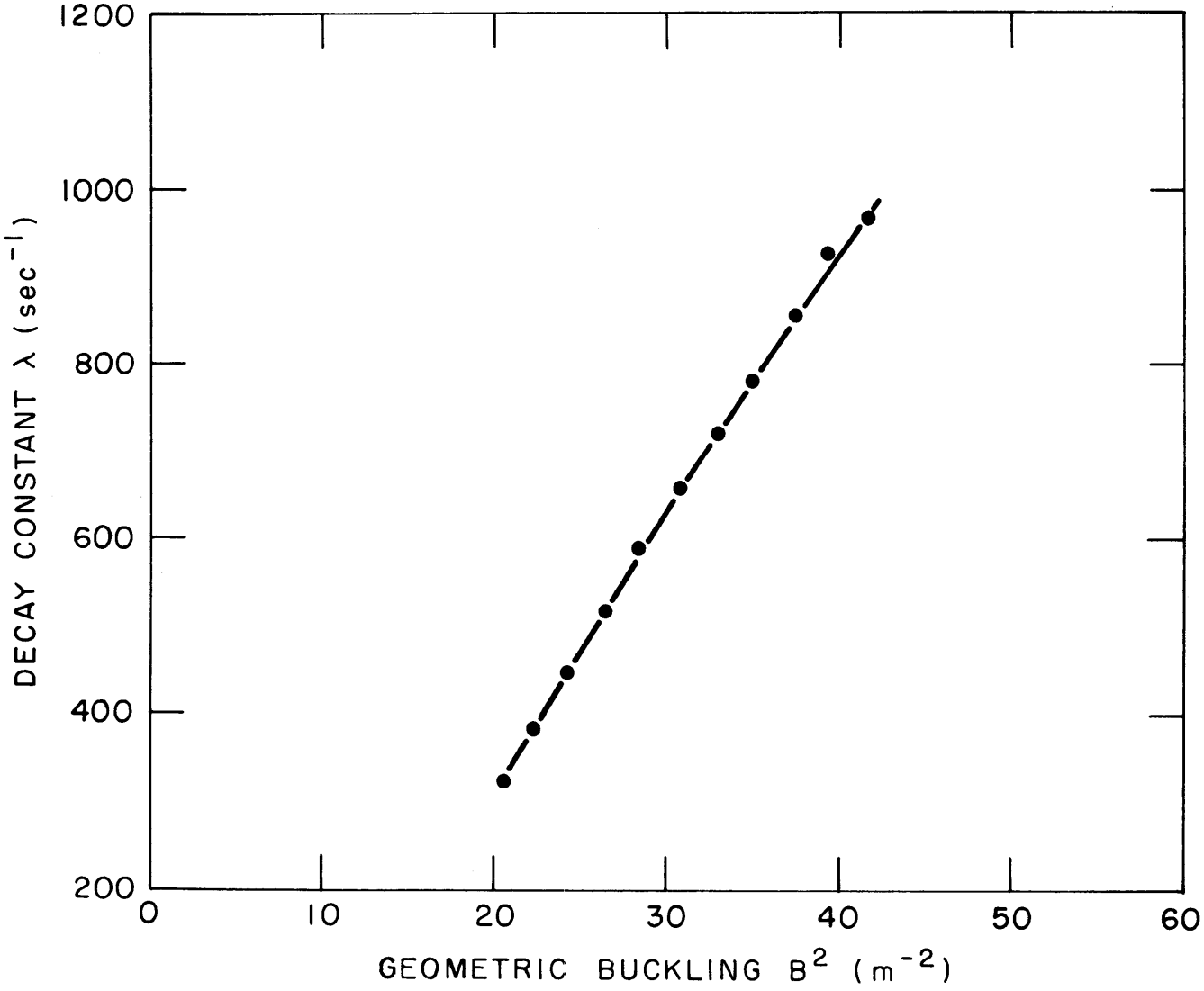

FIG. 5.1 MEASURED DECAY CONSTANT λ FOR THE 500 LATTICE AS A FUNCTION OF GEOMETRIC BUCKLING B^2

5.2 PARAMETERS OF HEAVY WATER AND OF MULTIPLYING MEDIA

5.2.1 Parameters of Heavy Water

The decay constants for heavy water listed in Table 5.1 were analyzed with the DEECEE code (M1) to determine the diffusion coefficient, $\overline{vD}_o$, and the diffusion cooling coefficient, C. The absorption cross section was computed according to the relation:

$$v\Sigma_a = 2.2 \times 10^5 N_{D_2O}\left[f\sigma_{D_2O} + (1-f)\sigma_{H_2O}\right] \text{ sec}^{-1},$$

where N_{D_2O} is the number density of heavy water molecules, f is the mole fraction of heavy water, and σ_{D_2O} and σ_{H_2O} are the 2200 meter/second microscopic absorption cross sections of D_2O and H_2O, respectively. With the following values:

$$N_{D_2O} = 0.0331 \times 10^{24}/\text{cc},$$

$$f = 0.9947,$$

$$\sigma_{D_2O} = 0.0012 \times 10^{-24} \text{ cm}^2,$$

$$\sigma_{H_2O} = 0.660 \times 10^{-24} \text{ cm}^2,$$

$\overline{v\Sigma}_a$ was determined to be 34.16 sec^{-1}.

The values of vD_o and C obtained for 99.47% D_2O at 25°C are given in Table 5.13 based on each of the three decay constant analysis codes.

TABLE 5.13

Measured Values of the Diffusion Coefficient $\overline{vD}_o$ and the Diffusion Cooling Coefficient C in 99.47% Heavy Water at 25°C

Computer Code	Diffusion Coefficient $\overline{vD}_o$, $\text{cm}^2\text{sec}^{-1} \times 10^{-5}$	Diffusion Cooling Coefficient C, $\text{cm}^4\text{sec}^{-1} \times 10^{-5}$
FRAUD	2.067 ± 0.018	5.18 ± 3.24
EXPO	2.039 ± 0.015	2.13 ± 2.58
STRIP	2.018 ± 0.017	1.94 ± 3.01

5.2.2 Parameters of Multiplying Media

The analysis of a series of measured decay constants as a function of geometric buckling to obtain values of k_∞ and $\overline{v\Sigma}_a$ is described in Sec. 4.2. Both a modified age-diffusion model and a two-group model have been used and, since there is no a priori reason to prefer one model to the other, the results of both treatments are given. The modified age-diffusion results are listed in Tables 5.14a and 5.14b and those from the two-group treatment in Tables 5.15a and 5.15b. Values of the parameters presumed known in the analysis, either from a calculation or from a previous experiment, are tabulated in Appendix B.

The errors listed are derived from the standard deviations of the coefficients of the least-squares fit and reflect only the statistical fluctuations in the data. The contribution of systematic errors to the total error is presented in Sec. 5.6.

Section 4.2 concludes with a brief summary of the method of Malaviya (M1) for determining k_∞ and $\overline{v\Sigma}_a$. The results obtained with his method are given here for the 500 lattice based on use of the decay constants from FRAUD.

The following values were obtained for the three coefficients of the least-squares fit:

$$r = \overline{v\Sigma}_a[1 - (1-\beta)k_\infty] = -354.9 \pm 26.7 \text{ sec}^{-1},$$

$$t = \overline{vD}_o + \overline{v\Sigma}_a(1-\beta)k_\infty\tau_o = (3.441 \pm 0.198) \times 10^5 \text{ cm}^2 \text{ sec}^{-1},$$

$$u = \frac{1}{2}\overline{v\Sigma}_a(1-\beta)k_\infty\tau_o^2 = (5.66 \pm 3.44) \times 10^6 \text{ cm}^4 \text{ sec}^{-1}.$$

With values of τ_o and β given in Appendix B:

$$\tau_o = 121 \pm 3 \text{ cm}^2,$$

$$\beta = (7.83 \pm 0.18) \times 10^{-3},$$

and the value of $\overline{vD}_o$ for heavy water listed in Table 5.13:

$$\overline{vD}_o = (2.067 \pm 0.018) \times 10^5 \text{ cm}^2 \text{ sec}^{-1},$$

the following values were obtained for k_∞ and $\overline{v\Sigma}_a$:

$$k_\infty = 1.466 \pm 0.064,$$

$$\overline{v\Sigma}_a = 1000.5 \pm 184.1 \text{ sec}^{-1}.$$

TABLE 5.14a

Measured Values of the Multiplication Factor k_∞
Derived from a Modified Age-Diffusion Analysis

Lattice Designator	Multiplication Factor k_∞		
	FRAUD	EXPO	STRIP
125	--	1.327 ± 0.042	1.330 ± 0.031
175	1.455 ± 0.092	1.440 ± 0.080	1.437 ± 0.068
175 A1	1.006 ± 0.030	1.016 ± 0.045	1.086 ± 0.071
175 A1B1	0.704 ± 0.020	0.796 ± 0.028	0.842 ± 0.040
250	1.452 ± 0.089	1.445 ± 0.075	1.412 ± 0.102
250 B1	0.983 ± 0.115	1.074 ± 0.048	1.101 ± 0.059
250 B2	0.561 ± 0.183	0.775 ± 0.065	0.743 ± 0.038
253	1.097 ± 0.038	1.101 ± 0.046	1.068 ± 0.033
253 A2B1	0.876 ± 0.083	0.807 ± 0.029	0.834 ± 0.027
350	1.358 ± 0.021	1.353 ± 0.022	1.351 ± 0.019
500	1.427 ± 0.013	1.421 ± 0.022	1.411 ± 0.018

TABLE 5.14b

Measured Values of the Absorption Cross Section $\overline{v\Sigma_a}$
Derived from a Modified Age-Diffusion Analysis

Lattice Designator	Absorption Cross Section $\overline{v\Sigma_a}$, sec^{-1}		
	FRAUD	EXPO	STRIP
125	--	2617.4 ± 118.9	2730.5 ± 89.6
175	1337.2 ± 114.2	1195.1 ± 88.8	1303.8 ± 82.8
175 A1	2359.9 ± 134.4	2217.7 ± 169.8	2645.7 ± 295.8
175 A1B1	2141.6 ± 70.4	2373.7 ± 119.1	2569.5 ± 190.8
250	707.2 ± 60.7	631.4 ± 45.9	559.5 ± 58.7
250 B1	567.1 ± 128.9	656.9 ± 52.3	737.5 ± 70.9
250 B2	615.9 ± 148.1	781.3 ± 86.5	780.0 ± 48.0
253	3667.0 ± 215.5	3618.5 ± 224.7	3394.3 ± 158.9
253 A2B1	4803.2 ± 704.8	4034.6 ± 194.5	4103.6 ± 176.7
350	1837.3 ± 58.4	1863.2 ± 60.2	1790.4 ± 37.1
500	927.9 ± 15.5	929.1 ± 26.1	942.6 ± 23.1

TABLE 5.15a

Measured Values of the Multiplication Factor k_∞
Derived from a Two-Group Analysis

Lattice Designator	Multiplication Factor k_∞		
	FRAUD	EXPO	STRIP
125	--	1.312 ± 0.034	1.315 ± 0.026
175	1.402 ± 0.071	1.392 ± 0.061	1.389 ± 0.051
175 A1	1.073 ± 0.029	1.086 ± 0.040	1.139 ± 0.062
175 A1B1	0.829 ± 0.015	0.908 ± 0.024	0.949 ± 0.034
250	1.393 ± 0.074	1.389 ± 0.062	1.367 ± 0.082
250 B1	1.052 ± 0.108	1.127 ± 0.044	1.146 ± 0.052
250 B2	0.693 ± 0.153	0.887 ± 0.057	0.861 ± 0.033
253	1.151 ± 0.032	1.155 ± 0.039	1.132 ± 0.029
253 A2B1	0.981 ± 0.074	0.922 ± 0.025	0.948 ± 0.023
350	1.329 ± 0.014	1.325 ± 0.014	1.322 ± 0.014
500	1.379 ± 0.012	1.375 ± 0.016	1.367 ± 0.014

TABLE 5.15b

Measured Values of the Absorption Cross Section $\overline{v\Sigma_a}$
Derived from a Two-Group Analysis

Lattice Designator	Absorption Cross Section $\overline{v\Sigma_a}$, sec^{-1}		
	FRAUD	EXPO	STRIP
125	--	3458.7 ± 157.0	3610.7 ± 121.9
175	1838.0 ± 153.7	1685.2 ± 120.3	1818.0 ± 111.1
175 A1	2733.6 ± 92.5	3052.6 ± 170.6	3333.6 ± 265.0
175 A1B1	3056.0 ± 187.7	2932.6 ± 228.9	3497.9 ± 395.8
250	1025.4 ± 93.9	920.2 ± 70.5	805.1 ± 89.3
250 B1	753.4 ± 185.7	895.7 ± 75.0	1002.2 ± 100.2
250 B2	768.6 ± 215.6	1013.5 ± 129.9	1009.8 ± 73.1
253	4867.5 ± 282.6	4824.0 ± 304.1	4554.0 ± 219.9
253 A2B1	6285.3 ± 1005.0	5242.7 ± 276.5	5372.5 ± 252.6
350	2189.2 ± 55.5	2213.5 ± 56.9	2169.7 ± 40.5
500	1159.3 ± 22.3	1167.1 ± 28.7	1170.8 ± 27.5

The uncertainties quoted are based only on those in the coefficients r and t and do not reflect the uncertainties in τ_o, β, and $\overline{vD}_o$.

5.3 TWO-REGION LATTICES

The analysis of pulsed source experiments in two-region lattices is described in Sec. 4.3. Two such lattices have been investigated in the course of this work and are designated as 175(2R) and 500(2R) (see Table 3.1 for a description of these lattices). The measured decay constants for these two lattices are tabulated in Tables 5.16 and 5.17 as a function of moderator height H_o.

The first step in the analysis, carried out here on the two-group model, is the determination of the parameters of the reference lattices which are the 175 and 500 lattices, respectively. The derived values of k_∞ and $\overline{v\Sigma}_a$ for these lattices are given in Tables 5.15a and 5.15b, and the calculated values of $\overline{vD}$, τ_o, and $\overline{v_1\Sigma}_1$ are tabulated in Appendix B.

Next, the measured values of λ in the two-region lattice are used in conjunction with the known properties of the reference lattice to obtain the radial geometric buckling of the reference portion of the two-region lattice. As noted in Sec. 4.3, the radial geometric buckling, α_b^2, is independent of the moderator height H_o. This feature is illustrated in Fig. 5.2 which shows the variation of α_b^2 as a function of H_o for the 500(2R) lattice based on the decay constants obtained from EXPO. The values of α_b^2 and α_b for the two lattices are listed in Table 5.18 for each of the three codes for the analysis of the decay constant.

The third step involves obtaining the square root of the radial geometric buckling of the test region, α_x, as the solution to the secular equation (Eq. (2.52)). The solutions α_x are tabulated in Table 5.18, along with the corresponding values of α_x^2. Necessary to the solution of the secular equation are the values of R_x, the boundary between the two regions, and R_b, the extrapolated radius of the lattice. These are:

$$\left.\begin{aligned} R_x &= 10.35 \text{ cm}, \\ R_b &= 47.58 \text{ cm}, \end{aligned}\right\} \quad 175(2R)$$

and,

$$\left.\begin{aligned} R_x &= 27.90 \text{ cm}, \\ R_b &= 62.82 \text{ cm}. \end{aligned}\right\} \quad 500(2R)$$

TABLE 5.16

Measured Fundamental Mode Decay Constant λ
as a Function of Moderator Height H_o
for the 175 (2R) Lattice

Moderator Height H_o, cm	Decay Constant λ, sec^{-1}		
	FRAUD	EXPO	STRIP
130.8	728.7 ± 4.3	715.0 ± 5.9	711.9 ± 4.8
108.3	794.1 ± 6.7	783.2 ± 7.8	775.1 ± 7.0
94.4	869.8 ± 7.4	862.3 ± 12.7	871.7 ± 8.2
82.9	983.8 ± 7.8	969.0 ± 13.4	971.4 ± 13.1
74.3	1094.6 ± 10.7	1083.4 ± 12.9	1076.4 ± 12.3
67.8	1227.7 ± 9.9	1198.5 ± 13.7	1194.9 ± 14.4
63.0	1295.7 ± 21.1	1280.4 ± 15.7	1286.4 ± 25.0
59.9	1340.9 ± 20.7	1338.2 ± 32.4	1337.6 ± 23.4
54.9	1461.9 ± 25.8	1453.2 ± 17.4	1451.7 ± 17.7
52.9	1576.6 ± 20.2	1559.9 ± 37.0	1578.6 ± 28.3

TABLE 5.17

Measured Fundamental Mode Decay Constant λ
as a Function of Moderator Height H_o
for the 500 (2R) Lattice

Moderator Height H_o, cm	Decay Constant λ, sec^{-1}		
	FRAUD[a]	EXPO[a]	STRIP[a]
129.9	393.2 ± 2.1	393.3 ± 3.4	394.3 ± 3.3
112.8	469.4 ± 3.9	465.1 ± 5.9	465.2 ± 4.3
98.9	529.2 ± 3.4	527.1 ± 4.5	527.0 ± 4.3
89.7	593.3 ± 4.6	593.4 ± 5.1	590.7 ± 3.8
82.4	656.5 ± 11.6	657.4 ± 9.5	656.4 ± 11.2
76.5	720.0 ± 10.8	716.5 ± 7.1	714.4 ± 10.7
71.4	747.7 ± 4.3	779.8 ± 9.8	779.3 ± 12.0
67.8	814.3 ± 20.6	811.9 ± 10.4	810.0 ± 7.5
63.8	879.3 ± 4.1	878.3 ± 8.6	878.4 ± 11.1
60.9	948.7 ± 13.7	933.7 ± 8.7	922.2 ± 8.7
58.1	986.6 ± 13.6	983.6 ± 9.0	982.4 ± 11.8

[a]These values were measured without the cadmium plate at the bottom of the tank.

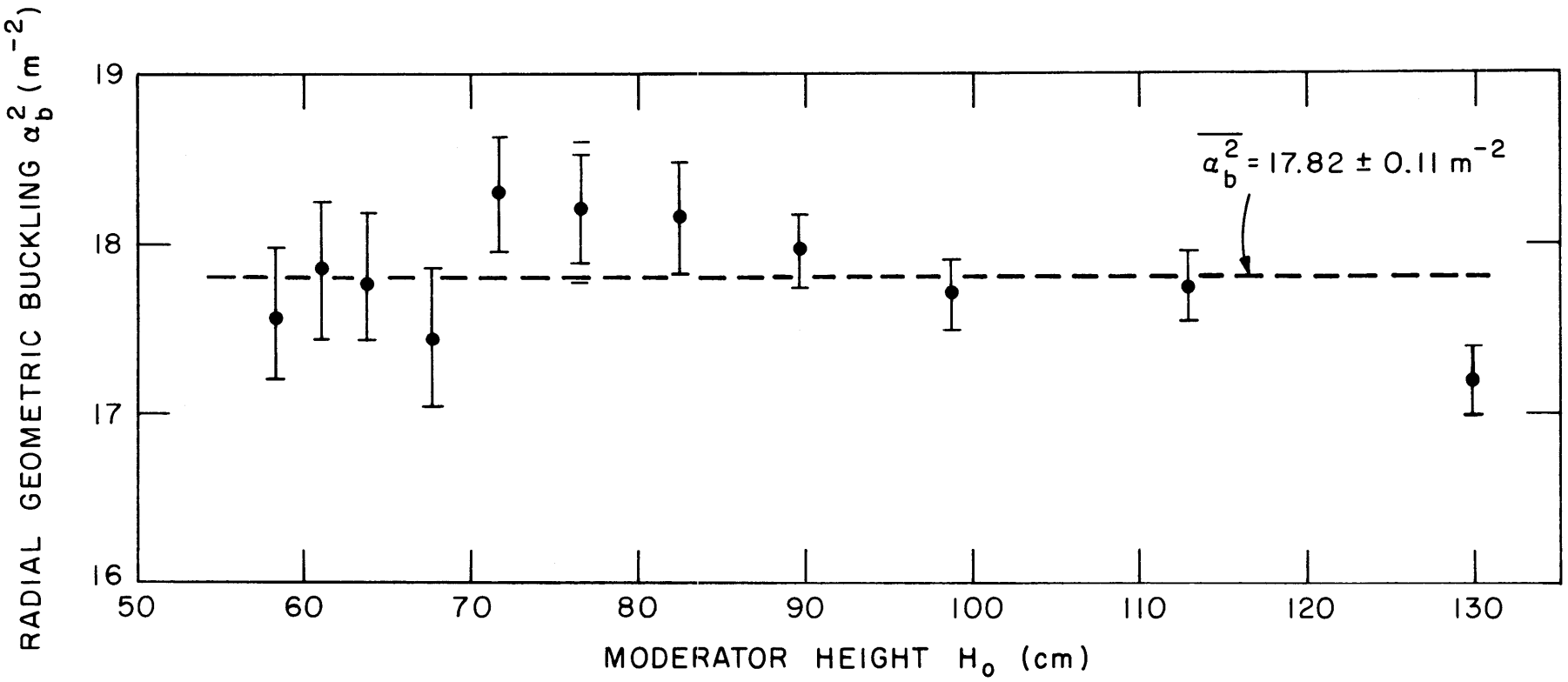

FIG. 5.2 MEASURED RADIAL GEOMETRIC BUCKLING α OF THE REFERENCE REGION FOR THE 500 (2R) LATTICE AS A FUNCTION OF MODERATOR HEIGHT H_o

TABLE 5.18

Values of the Radial Geometric Buckling
for the Reference and Test Regions of Two-Region Lattices

Lattice Designator	Computer Code	Reference Region		Test Region	
		α_b^2, m^{-2}	α_b, m^{-1}	α_x, m^{-1}	α_x^2, m^{-2}
175 (2R)	FRAUD	25.70 ± 0.16	5.069 ± 0.035	4.982 ± 0.034	24.82 ± 0.17
	EXPO	25.67 ± 0.15	5.067 ± 0.035	4.993 ± 0.034	24.93 ± 0.17
	STRIP	25.71 ± 0.17	5.070 ± 0.035	4.975 ± 0.034	24.75 ± 0.18
500 (2R)	FRAUD	17.72 ± 0.11	4.209 ± 0.036	3.328 ± 0.028	11.08 ± 0.09
	EXPO	17.82 ± 0.11	4.221 ± 0.036	3.308 ± 0.028	10.94 ± 0.09
	STRIP	17.81 ± 0.12	4.221 ± 0.036	3.306 ± 0.028	10.93 ± 0.09

The final step consists of least-squares fitting the measured values of λ in the two-region assembly and the corresponding values of the geometric buckling in the test region to obtain values of k_∞ and $\overline{\nu\Sigma}_a$ in the test region. The results are listed in Table 5.19, together with the associated uncertainties which are based on the standard deviations of the least-squares coefficients.

TABLE 5.19

Experimental Values of k_∞ and $\overline{\nu\Sigma}_a$
for the Test Region of Two-Region Lattices

Lattice Designator	Computer Code	Multiplication Factor k_∞	Absorption Cross Section $\overline{\nu\Sigma}_a$, sec^{-1}
175(2R)	FRAUD	1.344 ± 0.050	1652.9 ± 108.4
	EXPO	1.350 ± 0.035	1631.1 ± 71.9
	STRIP	1.341 ± 0.035	1695.9 ± 77.6
500(2R)	FRAUD	1.188 ± 0.018	1143.5 ± 53.7
	EXPO	1.175 ± 0.020	1128.1 ± 59.4
	STRIP	1.167 ± 0.021	1103.5 ± 62.6

5.4 ABSORBER-MODIFIED LATTICES

The first step in the analysis of pulsed source experiments on absorber-modified lattices is the determination of the least-squares coefficient r (Eq. (4.19a)) for the unmodified lattice and for each absorber-modified lattice. Then, a least-squares fit is made to an equation of the form:

$$ar = q + X_3. \tag{4.21}$$

The values of r used are experimental and the values of a and X_3 used are calculated. The negative of the least-squares value of q is the null-state (r=0) value of X_3. Finally, a new value of r^c is obtained according to the relation:

$$r^c = (1-\gamma_1)\overline{v\Sigma}_a - \frac{\gamma_1 q}{a^c}, \tag{4.24}$$

developed in Chap. IV.

Three unmodified lattices, 175, 250, and 253, have been studied with this technique. Two different concentrations of absorber were added to each of the first two lattices, and one concentration was added to the 253 lattice. A summary of these lattices is given in Table 3.1. The values of r, a, and X_3, based on a two-group model, are summarized in Table 5.20. Three values of r, based on each of the three computer codes, are quoted for each lattice. The variation of ar as a function of X_3 for the 250, 250B1, and 250B2 lattices is shown in Fig. 5.3, in which the values of r were obtained from the LSQHEB analysis of decay constants obtained from EXPO. Table 5.21 contains the new values of r^c obtained according to Eq. (4.24).

The new values of r^c are then used in conjunction with the unmodified lattice values of λ as a function of B^2 to obtain new values of s^c. The least-squares fit is carried out with the aid of LSQHEB and new values of k_∞ and $\overline{v\Sigma}_a$, evaluated from r^c and s^c, are given in Table 5.22. The quoted uncertainties are based on the standard deviations of r^c and s^c.

The possibility of obtaining an estimate of τ_o for the unmodified lattice has been advanced in Secs. 2.4 and 4.4. It depends on fitting the measured decay constants to a power series in the geometric buckling B^2:

$$\lambda' = r + tB^2 - uB^4, \tag{2.69}$$

and determining the null-state value of the coefficient t. The relation between τ_o and t^y is:

$$\tau_o = \frac{t^y}{\overline{v\Sigma}_a^y}, \tag{2.72}$$

where,

$$\overline{v\Sigma}_a^y = \frac{1}{a^y}\left[\frac{\sum_{i=0}^{2} \overline{v\Sigma}_{ai}^y \bar{n}_i^y V_i}{\overline{v\Sigma}_{ao}^y \bar{n}_o^y V_o} - q\right]. \tag{4.25}$$

TABLE 5.20

Values of r, a, and X_3
in Unmodified and Absorber-Modified Lattices

Lattice Designator	r (sec^{-1})			a (sec)	X_3
	FRAUD	EXPO	STRIP		
175	-719.8 ± 68.1	-641.5 ± 54.7	-687.5 ± 49.8	6.010×10^{-4}	0.0000
175 A1	-197.1 ± 79.4	-228.3 ± 103.3	-453.3 ± 177.2	5.904×10^{-4}	0.4279
175 A1B1	485.5 ± 40.6	303.6 ± 75.2	196.2 ± 116.7	5.859×10^{-4}	0.6280
250	-392.4 ± 39.1	-347.6 ± 30.1	-286.9 ± 38.0	1.248×10^{-3}	0.0000
250 B1	-33.2 ± 77.1	-105.9 ± 32.7	-136.8 ± 42.9	1.210×10^{-3}	0.2490
250 B2	239.8 ± 94.0	120.8 ± 59.9	147.4 ± 33.8	1.223×10^{-3}	0.4905
253	-689.6 ± 126.5	-706.5 ± 151.3	-562.2 ± 110.3	1.901×10^{-4}	0.0000
253 A2B1	166.3 ± 469.3	447.0 ± 134.3	322.0 ± 126.4	1.178×10^{-4}	0.1673

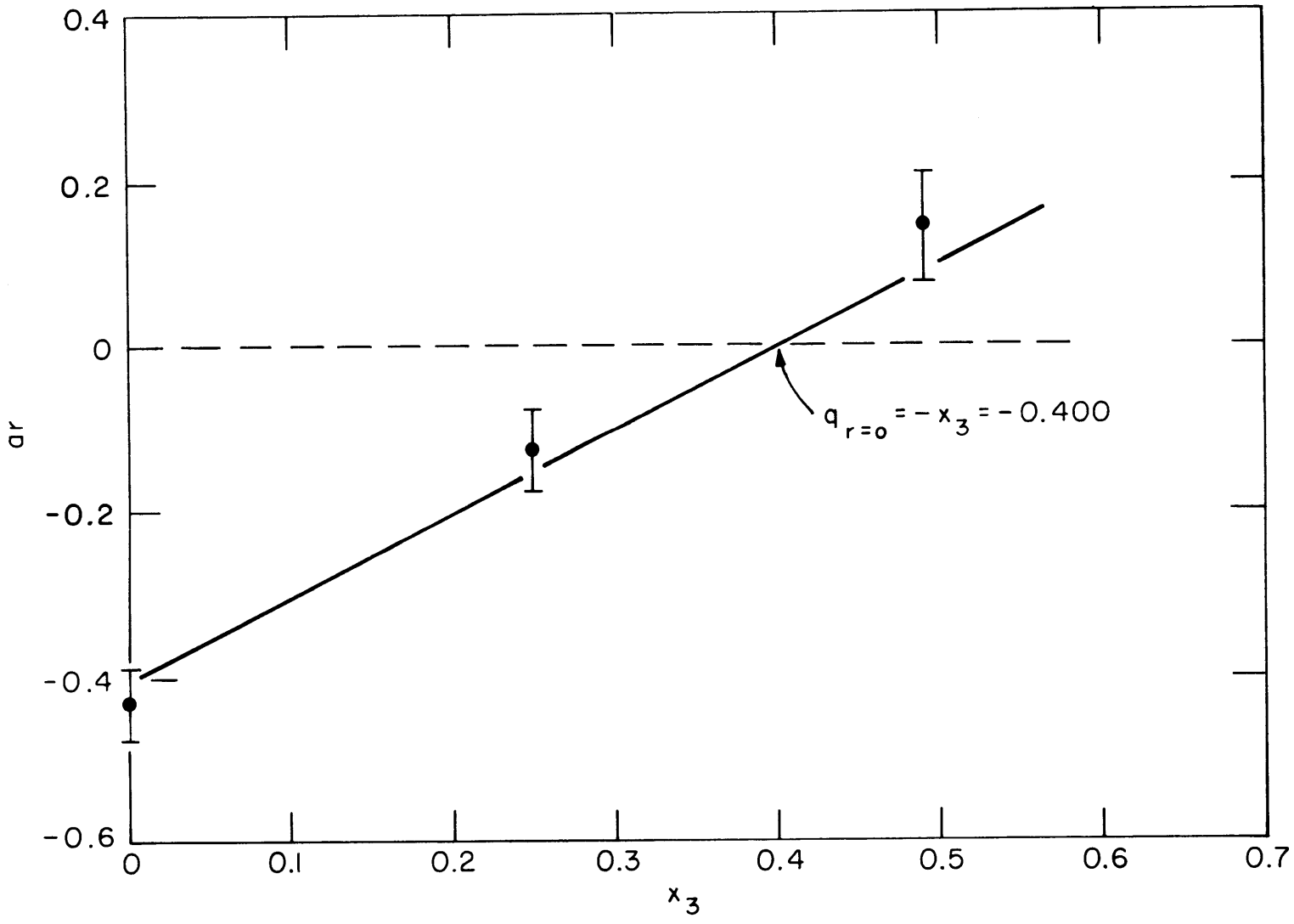

FIG. 5.3 THE QUANTITY ar AS A FUNCTION OF x_3 FOR THE 250 ABSORBER-MODIFIED LATTICES

TABLE 5.21

Least-Squares Values of q and New Values of r^c in Unmodified Lattices

Lattice Designator	Computer Code	q	r^c (sec^{-1})
175	FRAUD	-.3954 ± .0394	-644.7 ± 62.9
	EXPO	-.4219 ± .0421	-691.0 ± 67.6
	STRIP	-.4370 ± .0439	-714.8 ± 70.2
250	FRAUD	-.4184 ± .0790	-330.7 ± 62.3
	EXPO	-.4000 ± .0165	-316.6 ± 13.0
	STRIP	-.3528 ± .0295	-279.3 ± 23.3
253	FRAUD	-.1315 ± .0016	-633.3 ± 7.7
	EXPO	-.1081 ± .0232	-509.1 ± 109.1
	STRIP	-.1081 ± .0014	-512.8 ± 19.4

TABLE 5.22

New Experimental Values of the Multiplication Factor k_∞
and the Absorption Cross Section $\overline{v\Sigma_a}$
in Unmodified Lattices

Lattice Designator	Quantity	Computer Code		
		FRAUD	EXPO	STRIP
175	Multiplication Factor k_∞	1.399 ± 0.055	1.394 ± 0.054	1.390 ± 0.049
250		1.391 ± 0.101	1.387 ± 0.022	1.366 ± 0.041
253		1.143 ± 0.002	1.125 ± 0.028	1.124 ± 0.005
175	Absorption Cross Section $\overline{v\Sigma_a}$, sec^{-1}	1626.6 ± 65.8	1767.7 ± 70.6	1845.0 ± 72.0
250		862.3 ± 63.6	839.8 ± 16.0	785.5 ± 25.9
253		4725.3 ± 51.1	4382.3 ± 129.0	4444.5 ± 48.9

Because of the large uncertainty in the final result, this method of determining τ_o is not considered practical for the data at hand; and, therefore, the analysis is presented only for one set of absorber-modified lattices.

The determination of the coefficients r, t, and u is carried out with the LSQHEB code which performs a least-squares fit to the λ as a function of B^2 data in the manner described in Sec. 4.2. The resulting values of t for the 175, 175A1, and 175A1B1 lattices, with decay constants obtained from FRAUD, are listed in Table 5.23. In view of

TABLE 5.23

Experimental Values of the Coefficient t in Absorber-Modified Lattices

Lattice Designator	$t \times 10^{-5}$ ($cm^2 sec^{-1}$)
175	5.48 ± 1.79
175A1	2.92 ± 2.21
175A1B1	4.09 ± 0.91

the theoretically expected small variation of t as a function of added absorber and the relatively large variation obtained experimentally, the only realistic estimate of t^y is obtained from an average of the three values in Table 5.23, and, therefore:

$$t^y = (4.18 \pm 0.74) \times 10^5 \text{ cm}^2 \text{ sec}^{-1}.$$

With the values of a and q in Table 5.20 and Table 5.21, respectively, the null state absorption cross section is:

$$\overline{v\Sigma}_a^y = 2413.5 \pm 66.7 \text{ sec}^{-1},$$

and the final value of τ_o is 173 ± 22 cm^2.

5.5 EFFECTIVE RETURN COEFFICIENT

Measurements of the decay constant λ with and without the cadmium plate in the bottom of the lattice tank have been made in pure moderator and in the 500 lattice. The values of λ measured without the plate are listed in Tables 5.24 (moderator) and 5.25 (500 lattice).

The evaluation of β_a first requires the determination of the parameters of the medium with the cadmium plate at the bottom of the tank. These have been given in Tables 5.13 (moderator) and 5.15a and 5.15b (500 lattice). Next, the decay constants measured without the cadmium plate and the known parameters of the medium are used to evaluate the geometric buckling for the medium without the plate. Finally, the value of β_a is determined from the relation:

$$(B')^2 = \left(\frac{2.405}{R_o + d}\right)^2 + \left(\frac{\pi}{H_o + d + d\left(\frac{1+\beta_a}{1-\beta_a}\right)}\right)^2 . \qquad (2.84)$$

The variation of β_a as a function of $(B')^2$ is illustrated in Fig. 5.4 for both the moderator and the 500 lattice. The results shown are based on decay constants obtained from FRAUD. Certain of the data points are averages of two runs at a particular value of $(B')^2$. In all cases, the differences in the two values of β_a were less than the uncertainties in either value.

The final values of β_a, which are averages of the individual values of β_a over the range of geometric bucklings, are given in Table 5.26. The uncertainties quoted are the total errors which include contributions from statistical fluctuations in the observed values of λ and systematic errors in the values of d and H_o. The final value of β_a is taken to be the average of the lattice and moderator results:

$$\beta_a = 0.44 \pm 0.05,$$

and is the same for all three decay constant analysis codes.

TABLE 5.24

Measured Fundamental Mode Decay Constant λ
Without the Cadmium Plate at the Bottom of the Tank
as a Function of Moderator Height H_o for 99.47% Heavy Water at 25°C

Moderator Height H_o, cm	Decay Constant λ, sec^{-1}		
	FRAUD	EXPO	STRIP
130.5	435.3 ± 5.1	436.9 ± 8.1	427.9 ± 3.7
113.5	475.4 ± 7.8	469.0 ± 5.5	465.3 ± 5.1
99.4	498.4 ± 6.9	498.9 ± 5.7	493.3 ± 6.5
90.0	560.5 ± 1.8	549.2 ± 5.5	549.9 ± 5.7
83.0	577.5 ± 5.2	576.8 ± 7.4	572.6 ± 5.4
77.0	625.1 ± 3.1	620.6 ± 6.3	614.8 ± 5.6
71.8	676.3 ± 3.9	677.1 ± 8.9	666.7 ± 8.3
67.9	710.7 ± 4.9	699.7 ± 5.8	699.2 ± 6.4
64.3	742.2 ± 4.4	734.7 ± 8.0	735.4 ± 5.9
61.4	769.6 ± 14.8	765.7 ± 8.2	758.4 ± 7.4
59.5	780.9 ± 27.8	786.3 ± 17.1	779.7 ± 6.9

TABLE 5.25

Measured Fundamental Mode Decay Constant λ
Without the Cadmium Plate at the Bottom of the Tank
as a Function of Moderator Height H_o for the 500 Lattice

Moderator Height H_o, cm	Decay Constant λ, sec^{-1}		
	FRAU	EXPO	STRIP
129.9	317.6 ± 1.9	317.5 ± 2.1	316.8 ± 3.0
129.9	316.8 ± 3.4	318.1 ± 6.1	314.9 ± 2.4
114.0	358.7 ± 2.5	359.7 ± 4.3	354.9 ± 2.3
98.8	444.8 ± 2.9	442.1 ± 3.2	441.4 ± 2.5
90.7	495.4 ± 3.7	495.3 ± 4.6	492.0 ± 6.5
83.3	554.7 ± 6.1	552.3 ± 7.1	548.3 ± 4.2
82.4	558.4 ± 4.3	561.6 ± 5.4	555.2 ± 4.6
77.4	608.5 ± 7.3	604.7 ± 6.0	604.0 ± 7.1
76.5	623.4 ± 12.2	620.3 ± 4.5	618.9 ± 5.3
72.4	670.8 ± 5.1	674.6 ± 6.2	665.0 ± 12.4
71.4	675.7 ± 6.8	673.5 ± 5.3	673.5 ± 5.5
68.4	737.1 ± 4.1	741.4 ± 8.8	730.3 ± 7.9
67.4	740.2 ± 11.7	731.6 ± 9.5	729.4 ± 6.7
64.7	784.2 ± 13.1	780.4 ± 4.7	774.8 ± 6.9
63.8	784.2 ± 4.5	791.8 ± 8.4	782.3 ± 7.3
61.0	841.8 ± 7.1	841.7 ± 8.7	842.2 ± 10.2
58.1	895.2 ± 6.6	893.2 ± 11.6	886.5 ± 11.0

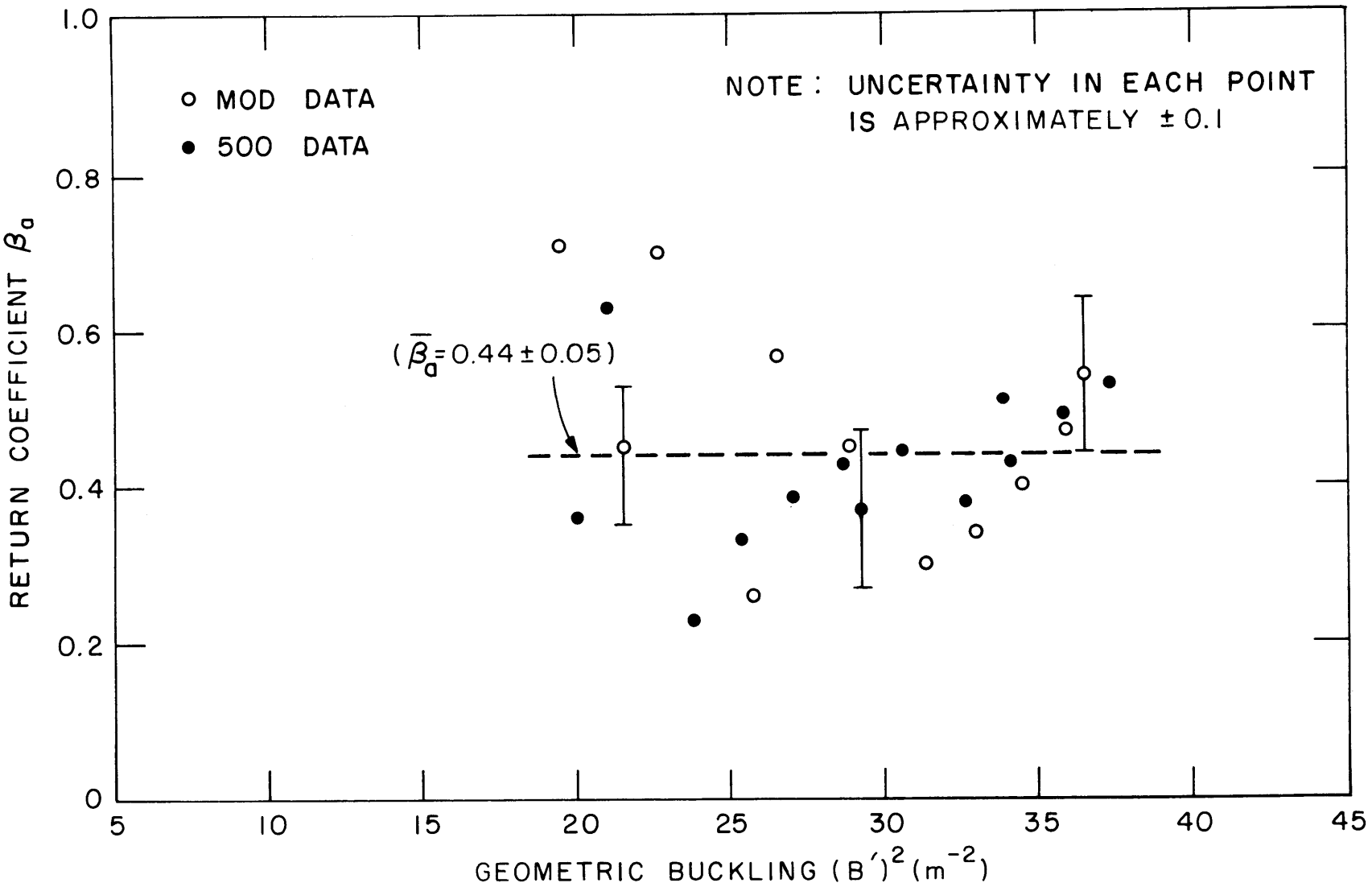

FIG. 5.4 EXPERIMENTAL VALUES OF THE RETURN COEFFICIENT β_a AS A FUNCTION OF GEOMETRIC BUCKLING $(B')^2$

TABLE 5.26

Experimental Values of the Return Coefficient β_a

Lattice Designator	Computer Code	Return Coefficient β_a
MOD	FRAUD	0.47 ± 0.08
	EXPO	0.50 ± 0.08
	STRIP	0.49 ± 0.08
500	FRAUD	0.42 ± 0.07
	EXPO	0.41 ± 0.07
	STRIP	0.40 ± 0.07

5.6 EVALUATION OF ERRORS

The determination of the total error in the measured lattice parameters, based on contributions from statistical fluctuations and systematic sources, is described in Sec. 4.6. Errors in the several parameters presumed known in the analysis can be taken into account according to the following relations:

$$(\Delta k_\infty)^2 = \sum_i \left(\frac{\partial k_\infty}{\partial \bar{X}_i}\right)^2 (\Delta X_i)^2, \tag{4.29a}$$

$$(\Delta \overline{v\Sigma}_a)^2 = \sum_i \left(\frac{\partial \overline{v\Sigma}_a}{\partial \bar{X}_i}\right)^2 (\Delta X_i)^2. \tag{4.29b}$$

The total error is then:

$$(\sigma k_\infty)^2 = (\Delta k_\infty)^2 + (\delta k_\infty)^2, \tag{4.30a}$$

$$(\sigma \overline{v\Sigma}_a)^2 = (\Delta \overline{v\Sigma}_a)^2 + (\delta \overline{v\Sigma}_a)^2, \tag{4.30b}$$

where δk_∞ and $\delta \overline{v\Sigma}_a$ represent the statistical errors.

The magnitude of the several contributions to the total error in k_∞ is illustrated by examining one lattice, the 500 lattice, in detail. The

final results, which are discussed and compared in the next section, are then reported on the basis of the total error.

The analysis employs the results of the two-group model and uses decay constants obtained from FRAUD. The values of the parameters presumed known and their associated uncertainties are transcribed from Appendix B:

$$\overline{vD}_o = (2.203 \pm 0.016) \times 10^5 \text{ cm}^2 \text{ sec}^{-1},$$

$$C = (4.58 \pm 0.28) \times 10^5 \text{ cm}^4 \text{ sec}^{-1},$$

$$\tau_o = 121 \pm 3 \text{ cm}^2,$$

$$\overline{v_1\Sigma}_1 = (4.37 \pm 0.87) \times 10^4 \text{ sec}^{-1},^*$$

$$\beta = (7.83 \pm 0.18) \times 10^{-3},$$

$$L^2 = 186.6 \pm 5.0 \text{ cm}^2.$$

Typical values of B^2 and λ in the center of the range of values are used:

$$\lambda = 658.4 \pm 9.0 \text{ sec}^{-1},$$

$$B^2 = 30.68 \pm 0.15 \text{ m}^{-2}.$$

Values of k_∞ and $\overline{v\Sigma}_a$ are given in Table 5.15. The various contributions to (Δk_∞) are summarized in Table 5.27. Summing the contributions to (Δk_∞) according to Eq. (4.29a) yields:

$$\Delta k_\infty = \left[\sum_i \left(\frac{\partial k_\infty}{\partial X_i} \right)^2 (\Delta X_i)^2 \right]^{1/2}$$

$$= 0.014.$$

Finally, the total error in k_∞ is evaluated from Eq. (4.30a):

$$\sigma k_\infty = \left[(\Delta k_\infty)^2 + (\delta k_\infty)^2 \right]^{1/2}$$

$$= 0.020.$$

---

* The large uncertainty in $v_1\Sigma_1$ is based on an estimated uncertainty of kT (more likely in the positive direction) in the lower limit of the fast energy group.

TABLE 5.27

Contributions to the Systematic Error in k_∞

Quantity X_i	$\frac{\partial k_\infty}{\partial X_i}$	Contribution
$\overline{\nu D}_o$	3.658×10^{-6}	0.0068
C	1.122×10^{-8}	0.0003
τ_o	3.139×10^{-3}	0.0094
$\overline{\nu_1 \Sigma}_1$	4.464×10^{-7}	0.0039
β	1.390	0.0002
L^2	4.659×10^{-5}	0.0002
B^2	3.811×10^{2}	0.0057

the total error in $\overline{\nu\Sigma}_a$ for the 500 lattice and for k_∞ and $\overline{\nu\Sigma}_a$ for the remaining lattices are evaluated in a similar manner.

5.7 DISCUSSION, CONCLUSIONS, AND COMPARISON OF RESULTS

5.7.1 Fundamental Mode Decay Constant

The experimental measurements of the neutron density as a function of time have been analyzed with three computer codes to obtain three values of the fundamental mode decay constant λ. Two of the codes, FRAUD and STRIP, were written as a part of this program, and the third, EXPO, was written as part of a previous report (M1). The measured values of λ for the several lattices investigated in the present work, based on each of the computer codes, are tabulated in Tables 5.1-5.12, 5.16, 5.17, 5.24, and 5.25. There is good agreement, within the quoted standard deviations, among the results of the three codes in over 90% of the cases.

The standard deviations of the decay constants obtained from STRIP and EXPO are, on the average, close to 1% although they sometimes become larger for larger values of λ. This increase arises

because, for a fixed number of counts in the most active channel, the number of decades over which the neutron density can be monitored decreases as the decay constant increases, with the result that fewer total counts are available for the analysis. The standard deviations of the decay constants obtained from FRAUD are generally smaller than 1%. This result is expected because FRAUD utilizes a greater range of the count rate data than either STRIP or EXPO.

A factor in the selection of a data analysis code is the amount of time required, both on the part of the computer, itself, and on the part of the user in preparing the data for the computer, to obtain the desired value of λ. The required computer times on the IBM-7094 are approximately 0.8, 1.0, and 3.0 minutes per case for STRIP, EXPO, and FRAUD, respectively. The order, in terms of increasing data preparation time, is EXPO, STRIP, and FRAUD.

Thus, no single code is best from all standpoints. However, in the absence of severe time limitations, the FRAUD code is preferable because of the expected greater confidence in the result. Furthermore, if time permits, all three codes should be employed in an analysis because a poor set of data can usually be detected by inconsistencies among the three values of λ.

5.7.2 Moderator Parameters

Experimental values of the moderator parameters $\overline{vD}_o$ and C for heavy water are listed in Table 5.13. The value of $\overline{vD}_o$ from FRAUD is repeated in Table 5.28 which summarizes experimental and theoretical determinations of $\overline{vD}_o$ and C by other workers. Table 5.28 also contains experimental values of $\overline{vD}_o$ corrected to 100% D_2O and 20°C according to the relations:

$$\frac{\Delta \overline{vD}_o}{\Delta T} = 0.0055 \text{ cm}^2/\text{sec°C},$$

$$\frac{1}{\overline{vD}_o} = \frac{f}{\overline{vD}_{D_2O}} + \frac{1 - f}{\overline{vD}_{H_2O}},$$

where f is the mole fraction of D_2O. The temperature correction is based on the measurements of Daughtry and Waltner (D4). The value

TABLE 5.28

Parameters of Heavy Water by the Pulsed Neutron Method

Author	D_2O Purity (mole %)	Temp. °C	Diffusion Coefficient, $\overline{vD}_o$ $cm^2sec^{-1}X10^{-5}$	Diffusion Cooling Coefficient, C $cm^4sec^{-1}X10^{-5}$	100% D_2O Diffusion Coefficient, $\overline{vD}_o$ $cm^2sec^{-1}X10^{-5}$	100% D_2O Diffusion Cooling Coefficient, C $cm^4sec^{-1}X10^{-5}$
Jones et al. (J1) 1965	99.80	21	1.966 ± 0.137	3.56 ± 1.08	1.978 ± 0.137	3.56 ± 1.08
Kussmaul and Meister (K4) 1963	99.82	21	2.000 ± 0.010	5.25 ± 0.25	2.011 ± 0.010	5.25 ± 0.25
Ganguly et al. (G2) 1963	99.88	20	2.068 ± 0.050	3.27 ± 0.21	2.080 ± 0.050	3.27 ± 0.21
Malaviya et al. (M1) 1964	99.60	20	1.967 ± 0.023	4.87 ± 0.31	2.003 ± 0.024	4.87 ± 0.31
Malaviya and Profio (M2) 1963	99.80	21	2.045 ± 0.044	4.71 ± 0.38	2.059 ± 0.044	4.71 ± 0.38
Parks and Bauman (P2) 1965	99.84	29	2.12 ± 0.02	8.1 ± 0.3	2.09 ± 0.02	8.1 ± 0.3
Westfall and Waltner (W3) 1962	99.81	29	2.040 ± 0.013	4.19 ± 0.18	2.014 ± 0.013	4.19 ± 0.18
Utzinger et al. (U1) 1965	99.85	22	2.020 ± 0.010		2.023 ± 0.010	
Honeck and Michael (H10)[a] 1963	100.0	20			2.057	4.73
THERMOS (H9)[a] 1961	100.0	20			2.114	
Radkowsky (R2)[a] 1950	100.0	20			2.10	
Present Work[b]	99.47	25	2.067 ± 0.018		2.088 ± 0.018	

(a) Theoretical
(b) Based on decay constants obtained from FRAUD

of $\overline{vD}_o$ for H_2O is $(3.598 \pm 0.010) \times 10^4$ cm^2 sec^{-1} which is based on a weighted average of the results reported in Refs. D6, G5, K3, L3, J1, and S3. The values of C are not corrected because the magnitude of the correction is much smaller than the reported uncertainties in C.

The corrected value of $\overline{vD}_o$ in the present work is $(2.088 \pm 0.018) \times 10^5$ cm^2 sec^{-1}, which disagrees with the weighted average of $(2.031 \pm 0.015) \times 10^5$ cm^2 sec^{-1} for the earlier measurements listed in Table 5.28, but agrees well with the recent experimental value of $(2.09 \pm 0.02) \times 10^5$ cm^2 sec^{-1} reported by Parks and Bauman (P2) and the theoretical values calculated by the methods of Honeck and Michael (H10) and Radkowsky (R2).

It was not possible to obtain a reliable value of C in the present work as evidenced by the large experimental errors reported in Table 5.13. A better estimate for C would have required measurements of λ in smaller assemblies (larger values of B^2) than those used here. At the largest value of B^2 given in Table 5.1, the contribution of the diffusion cooling term (CB^4) to the measured value of λ is only 1.1% of that of the diffusion term ($\overline{vD}_o$). Thus, diffusion cooling does not have a significant effect on the results reported in the present work.

5.7.3 Multiplication Factor (k_∞)

Experimental determinations of k_∞ are given in Tables 5.14a (modified age-diffusion model) and 5.15a (two-group model). Values are reported in triplicate; one for each of the three codes used to obtain a value of the decay constant. It is desired to select which, if any, code yields the best results and which, if any, theoretical model gives better agreement with values of k_∞ obtained by other means.

With the exception of the 175A1B1 lattice, the experimental values of k_∞ based on each of the three computer codes agree within the quoted standard deviations. This conclusion holds for both the modified age-diffusion model and the two-group model and is consistent with the observation in Sec. 5.7.1 that the three separate values of the decay constant agree within experimental error in over 90% of the cases. It seems reasonable, therefore, to select that value of k_∞ which has the smallest percentage standard deviation.

The choice of the theoretical model requires comparison with

values of k_∞ obtained by methods other than the pulsed source technique. Three methods of determining k_∞ for these lattices have been used for comparison with the pulsed source values.

(1) Addition of distributed thermal neutron absorbers. J. Harrington (H1) has developed a technique for determining k_∞ in absorber-modified subcritical lattices which is similar to the Hanford "null-reactivity" technique (H6). The measured value of the material buckling of the subcritical assembly is used to determine the amount of absorber required to reduce k_∞ to unity (null-state), and an equation similar to Eq. (2.65) is applied to derive values of k_∞:

$$k_\infty = \left(\frac{\eta}{\eta^y}\right)\left(\frac{\epsilon}{\epsilon^y}\right)\left(\frac{p}{p^y}\right)\left[1 + f\left(A_3^y - A_3\right) + f\sum_{i=1}^{2}\left(A_i^y - A_i\right)\right], \qquad (5.1)$$

where the symbols in Eq. (5.1) have been defined in Sec. 2.4. It should be pointed out, however, that the null states leading to Eqs. (5.1) and (2.65) differ by the factor $(1-\beta)$.

(2) Four-Factor Formula. If k_∞ is defined as the ratio of the total number of neutrons produced to the total number of neutrons destroyed, per unit time, in a system of infinite extent, k_∞ can be written as:

$$k_\infty = \eta\epsilon pf, \qquad (5.2)$$

where η is the number of fission neutrons produced per neutron absorbed, ϵ is the total number of fast neutrons produced per neutron resulting from fission, p is the probability that a fast neutron is not absorbed while slowing down to thermal energies, and f is the probability that a thermal neutron is absorbed in the fuel. The values of the four factors in Eq. (5.2) are usually determined by a combination of calculations and measurements as described in Ref. H1.

(3) Critical Equation. The relationship between k_∞ and the material buckling B_m^2, the critical equation, depends on the theoretical model used to describe the neutron slowing-down process. Two of the more common relations are:

$$k_\infty = \left(1+L^2B_m^2\right)\left(e^{B_m^2\tau_o}\right), \qquad (5.3a)$$

$$k_\infty = \left(1+L^2B_m^2\right)\left(1+B_m^2\tau_o\right), \qquad (5.3b)$$

which are based on age-diffusion theory and two-group theory, respectively. Values of k_∞ can be determined from these relations with calculated values of τ_o and L^2 and measured values of B_m^2.

The comparison of the several values of k_∞ is presented in Table 5.29. The first two columns contain the pulsed source values of k_∞, derived on age-diffusion and two-group theories, respectively, and selected in the manner described above. The uncertainties listed are the total errors which include contributions from statistical and known systematic sources. Columns 3 and 4 contain values of k_∞ obtained from Eqs. (5.1) and (5.2), respectively, and are taken from Ref. (H1). The values of k_∞ in the last two columns are evaluated from Eqs. (5.3a) and (5.3b) with the use of calculated values of τ_o and L^2 (see Appendix B) and measured values of B_m^2 (see Refs. H1 and H5). The uncertainties given for these latter values of k_∞ are based on the standard deviations in the measured values of B_m^2 and on estimated uncertainties of 2.5% and 3.0% in the calculated values of τ_o and L^2, respectively.

If the two pulsed neutron values of k_∞ are compared with the values obtained from their respective critical equations for each of the eleven lattices listed in Table 5.29, the results of the comparison can be divided into four categories:

(1) both pulsed neutron values are in good agreement, within the quoted uncertainties, with their respective critical equation values for four lattices (125, 175, 250, 350);

(2) the pulsed neutron values obtained from the two-group analysis agree well with the values obtained from the two-group critical equation for four lattices (175A1B1, 250B1, 253, 500) while the corresponding age-diffusion results do not;

(3) the pulsed neutron value obtained from the age-diffusion analysis agrees well with the value obtained from the age-diffusion critical equation for one lattice (175A1) while the corresponding two-group result does not;

(4) neither pulsed neutron value is in agreement with its respective critical equation value for two lattices (250B2, 253A2B1)

TABLE 5.29

Values of the Multiplication Factor k_∞

Lattice Designator	Source of Value for k_∞					
	Pulsed Source (Age-Diffusion)	Pulsed Source (Two-Group)	Added Absorber (Eq. 5.1)	Four-Factor Formula (Eq. 5.2)	Age-Diffusion Critical Equation (Eq. 5.3a)	Two-Group Critical Equation (Eq. 5.3b)
125	1.330 ± 0.035	1.315 ± 0.030		1.330 ± 0.027	1.338 ± 0.008	1.318 ± 0.008
175	1.437 ± 0.070	1.389 ± 0.054	1.416 ± 0.011	1.393 ± 0.026	1.419 ± 0.010	1.400 ± 0.010
175A1	1.006 ± 0.034	1.073 ± 0.033	1.004 ± 0.009	0.988 ± 0.018	1.004 ± 0.007	1.004 ± 0.007
175A1B1	0.704 ± 0.026	0.829 ± 0.022	0.871 ± 0.012	0.857 ± 0.017	0.831 ± 0.006	0.826 ± 0.006
250	1.445 ± 0.077	1.389 ± 0.064	1.429 ± 0.007	1.422 ± 0.028	1.432 ± 0.013	1.419 ± 0.013
250B1	1.074 ± 0.051	1.127 ± 0.047	1.148 ± 0.007	1.143 ± 0.023	1.142 ± 0.006	1.140 ± 0.006
250B2	0.743 ± 0.041	0.861 ± 0.037	0.963 ± 0.005	0.959 ± 0.020	0.963 ± 0.003	0.963 ± 0.003
253	1.097 ± 0.036	1.151 ± 0.036	1.187 ± 0.027	1.154 ± 0.023	1.190 ± 0.004	1.179 ± 0.004
253A2B1	0.834 ± 0.031	0.948 ± 0.028	1.003 ± 0.026	0.976 ± 0.020	1.002 ± 0.011	1.002 ± 0.011
350	1.351 ± 0.025	1.329 ± 0.021			1.331 ± 0.008	1.315 ± 0.008
500	1.427 ± 0.021	1.379 ± 0.020			1.390 ± 0.009	1.378 ± 0.009

although the two-group results are closer than the age-diffusion results in each case.

If the pulsed neutron values are compared with the values obtained from the method of added absorbers (Eq. (5.1)) and with the values obtained from the four-factor formula (Eq. (5.2)), similar results are obtained for each comparison. For all eleven lattices, the percentage uncertainty in the pulsed neutron value of k_∞ obtained from the two-group model is less than the corresponding value obtained from the age-diffusion model. It is concluded, therefore, that the two-group analysis is preferable to the age-diffusion analysis insofar as determining values of k_∞ in these lattices by the pulsed neutron technique is concerned. This conclusion is consistent with that reached by Meister (M3) who measured values of the decay constant in natural uranium, heavy water lattices and compared them with the results of simple two-group calculations based on lattice parameters obtained from previous exponential experiments; the agreement was good in the buckling range $B^2 < 25\,m^{-2}$.

A significant feature of Table 5.29 is the good agreement, within the quoted uncertainties, among the three steady-state values of k_∞ for all lattices except the 175A1B1 lattice. The pulsed neutron values of k_∞ obtained from the two-group analysis, with the exception of the three lattices previously noted, are also in agreement with the steady-state results. This lends confidence to all four methods for determining k_∞ in lattices of partially enriched uranium and heavy water.

Other workers have also obtained good agreement among two or more methods of determining k_∞ in heavy water lattices. Green (G7, G8) has calculated values of the material buckling B_m^2 from the two-group expression:

$$k_\infty = \left(1+L^2B_m^2\right)\left(1+\tau_0 B_m^2\right), \qquad (5.3b)$$

with values of k_∞ obtained from the four-factor formula and with calculated values of τ_0 and L^2 and has compared them to experimental values of B_m^2; the agreement between the derived bucklings and the experimental bucklings was good within the assumed experimental errors. Swedish workers (P4), on the other hand, prefer to compare the measured and calculated bucklings on the basis of a modified age-diffusion

theory. Crandall et al. (C2) have reported good agreement between measurements of k_∞ by the null reactivity technique (H6) in the PCTR and PLATR reactors and those obtained from two-group calculations with measured values of the material buckling.

The choice of the best method for determining k_∞ in subcritical lattices of uranium and heavy water is still an open question although certain conclusions may be drawn from the results presented here. The relatively larger (2.5% - 4.5%) uncertainties in some of the pulsed neutron results are attributed to statistical fluctuations in the measured values of the decay constant. If enough data (see Sec. 3.3 for a discussion of this point) are collected, the overall uncertainty in the pulsed neutron value of k_∞ may be reduced to about 1.5% (see, for example, the results for the 350 and 500 lattices in Table 5.29). This uncertainty is dominated by the uncertainties in the calculated values of the parameters presumed known in the analysis which, as shown in Sec. 5.6, contribute between 1.0% and 1.5% to the total uncertainty. Thus, until the uncertainties in τ_o and $\overline{vD}_o$ (and, to a lesser extent, in C, β, L^2, B^2, and $\overline{v_1\Sigma}_1$) can be reduced, the overall uncertainty in the pulsed neutron value of k_∞ cannot be reduced below 1.0%. The results of Harrington (H1) indicate that uncertainties between 1.9% and 2.0% are to be expected in values of k_∞ obtained from the four-factor formula and that uncertainties between 0.5% and 1.0% are possible with the method of added absorbers provided sufficient accuracy in the measurement of the material buckling is achieved. The uncertainties in the values of k_∞ calculated from the critical equation are between 0.3% and 1.1% for the results given in Table 5.29.

From the standpoint of the overall uncertainty in k_∞, the critical-equation analysis and added-absorber method yield the best precision. A disadvantage of the latter method is the extensive amount of time and effort required to achieve the stated accuracy. On the other hand, Crandall et al. (C2, C3) note that exponential-critical intercomparisons have demonstrated that small systematic differences exist between values of the material buckling measured in exponential and critical assemblies. They conclude that most of the differences are due to systematic changes in values of the radial buckling measured in the exponential assembly. This effect may also be present in the method of

added absorbers in which the "null-state" condition is determined from measurements of the material buckling as a function of the amount of added absorber. The determination of k_∞ from a critical equation, therefore, seems to offer some advantages over the method involving added absorbers. Here, however, the choice of the "appropriate" critical equation raises a new problem.

The pulsed neutron method provides results in a convenient way which may be compared with the results obtained from the critical equation. The precision of the (pulsed neutron) results should be as good as, or better than, that obtained with the four-factor formula. The pulsed neutron method requires less time to make the measurements and analyze the data than does the four-factor method. The method of added absorbers, as noted above, also suffers from the disadvantage of a time limitation, but it achieves somewhat better precision than the pulsed neutron method.

5.7.4 Absorption Cross Section ($\overline{v\Sigma}_a$) and Thermal Diffusion Area (L^2)

Tables 5.30 and 5.31 contain experimental and theoretical values of the absorption cross section $\overline{v\Sigma}_a$ and thermal diffusion area L^2 ($\equiv \overline{vD}_o/\overline{v\Sigma}_a$), respectively. The theoretical values of these quantities, based on the results of THERMOS, are taken from Table B.4. The experimental values of $\overline{v\Sigma}_a$ are taken from Tables 5.14b and 5.15b, and those of $\overline{vD}_o$ are taken from Table B.5.

With the exception of the 175A1 lattice, the values of $\overline{v\Sigma}_a$ and L^2 obtained from the two-group analysis are considerably closer to the theoretical values than are those obtained from the age-diffusion analysis. Furthermore, if an estimated 3% uncertainty is included in the theoretical values of L^2 (due to uncertainties in the nuclear cross sections used by THERMOS), the two-group pulsed source values of L^2 are in reasonable agreement with those from THERMOS. These observations reinforce the conclusion given in Sec. 5.7.3, with respect to values of k_∞, that the two-group analysis yields better results than the age-diffusion analysis. Consequently, the analysis of two-region lattices, absorber-modified lattices, and return coefficient measurements has been carried out on a two-group model.

TABLE 5.30

Values of the Absorption Cross Section $\overline{v\Sigma}_a$

Lattice Designator	Source of Value for $\overline{v\Sigma}_a$ (sec^{-1})		
	Pulsed Source (Age-Diffusion)	Pulsed Source (Two-Group)	Theoretical (THERMOS)
125	2730.6 ± 89.6	3610.7 ± 121.9	3376.6
175	1303.8 ± 82.8	1818.0 ± 111.1	1716.4
175A1	2359.9 ± 134.4	2733.6 ± 92.5	2442.1
175A1B1	2141.6 ± 70.4	3056.0 ± 187.7	2834.5
250	631.4 ± 45.9	920.2 ± 70.5	840.9
250B1	656.9 ± 52.3	895.7 ± 75.0	1076.0
250B2	780.0 ± 48.0	1009.8 ± 73.1	1265.2
253	3667.0 ± 215.5	4867.5 ± 282.6	5312.5
253A2B1	4103.6 ± 176.7	5372.5 ± 252.6	6611.0
350	1790.4 ± 38.1	2189.2 ± 56.5	2530.3
500	927.9 ± 16.5	1159.3 ± 23.4	1182.4

TABLE 5.31

Values of the Thermal Diffusion Area L^2

Lattice Designator	Source of Value for L^2 (cm^2)		
	Pulsed Source (Age-Diffusion)	Pulsed Source (Two-Group)	Theoretical (THERMOS)
125	93.2 ± 4.1	70.5 ± 2.7	76.7
175	175.0 ± 11.1	125.5 ± 7.7	135.6
175A1	102.4 ± 5.8	88.5 ± 3.0	98.5
175A1B1	114.6 ± 3.7	80.3 ± 4.9	86.5
250	342.3 ± 24.9	234.8 ± 18.0	260.9
250B1	331.9 ± 26.4	243.4 ± 20.4	206.3
250B2	278.8 ± 17.2	215.4 ± 15.6	177.4
253	73.4 ± 4.3	55.2 ± 3.2	50.7
253A2B1	66.4 ± 2.9	40.5 ± 1.9	42.2
350	132.8 ± 2.8	108.6 ± 3.8	99.7
500	237.4 ± 4.2	190.0 ± 3.8	186.6

5.7.5 Two-Region Lattices

The values of k_∞ and $\overline{\nu\Sigma}_a$ in the test region of two-region lattices are given in Table 5.19. They are repeated, along with values of L^2, in Table 5.32 which provides a comparison of these values with those obtained by other means. Values of k_∞ based on Eq. (5.2) have previously been given for a lattice composed entirely of the test region of the 175(2R) lattice by D'Ardenne (D3) and of the 500(2R) lattice by Weitzberg (W2). The theoretical values of $\overline{\nu\Sigma}_a$ and L^2 are evaluated from the results of THERMOS (see Table B.4). The uncertainties listed for the pulsed source results are the total uncertainties.

The pulsed source and steady-state values of k_∞ are in excellent agreement within the quoted uncertainties. Agreement between theory and experiment for $\overline{\nu\Sigma}_a$ and L^2 is also good for the 175(2R) lattice but only fair for the 500(2R) lattice. Thus, it is concluded that values of k_∞ for the test region of two-region lattices can be obtained to satisfactory accuracy, and that it may be possible to measure $\overline{\nu\Sigma}_a$ and L^2 in these assemblies.

5.7.6 Absorber-Modified Lattices

The new values of k_∞ and $\overline{\nu\Sigma}_a$ obtained in the unmodified 175, 250, and 253 lattices, after analysis according to the method described in Sec. 4.4, are given in Table 5.22. They are compared in Table 5.33 with the corresponding values given in Tables 5.15a and 5.15b which were obtained by a two-group analysis of the unmodified lattices alone. In all cases, the uncertainties in the former values are reduced relative to those in the latter (the reduction is particularly good for the 250 and 253 lattices), thereby indicating the efficacy of the method. The reduction in uncertainty applies only to the statistical fluctuations in the data. The overall uncertainty, as noted in Sec. 5.7.3, cannot be reduced below the limits set by systematic sources of error. It is concluded, therefore, that pulsed neutron measurements on absorber-modified lattices yield improved values of k_∞ and $\overline{\nu\Sigma}_a$ relative to those obtained for the unmodified lattice alone and that they are worthwhile whenever steady-state measurements are made in absorber-modified lattices.

TABLE 5.32

Values of the Multiplication Factor k_∞, Absorption Cross Section $\overline{v\Sigma}_a$, and Thermal Diffusion Area L^2 in the Test Region of Two-Region Lattices

Lattice Designator	Source of Value for k_∞		Source of Value for $\overline{v\Sigma}_a$ (sec^{-1})		Source of Value for L^2 (cm^2)	
	Pulsed Source (Two-Group)	Four-Factor Formula (Equation (5.2))	Pulsed Source (Two-Group)	Theoretical (THERMOS)	Pulsed Source (Two-Group)	Theoretical (THERMOS)
175(2R)	1.350 ± 0.038	1.339 ± 0.020	1631.1 ± 73.2	1615.9	139.8 ± 6.3	143.6
500(2R)	1.188 ± 0.024	1.219 ± 0.014	1143.5 ± 55.3	1687.3	207.5 ± 10.0	140.6

TABLE 5.33

Comparison of Values of the Multiplication Factor k_∞
and Absorption Cross Section $\overline{v\Sigma}_a$
in Unmodified Lattices

Lattice Designator	Source of Value for k_∞		Source of Value for $\overline{v\Sigma}_a$ (sec^{-1})	
	Table 5.22 (new value)	Table 5.15a	Table 5.22 (new value)	Table 5.15b
175	1.390 ± 0.049	1.389 ± 0.051	1845.0 ± 72.0	1811.0 ± 111.1
250	1.387 ± 0.022	1.389 ± 0.062	839.8 ± 16.0	920.2 ± 70.5
253	1.143 ± 0.002	1.151 ± 0.032	4725.3 ± 51.3	4867.2 ± 282.6

The large uncertainty in the values of τ_o obtained from the analysis of absorber-modified lattices renders the method of little practical value, at least insofar as the data obtained in this work is concerned. This large uncertainty arises because of the large uncertainty in the least-squares coefficient t obtained from the three-parameter fit described in Sec. 4.2. The same conclusion can also be reached from an examination of the results of a three-parameter fit to the λ data as a function of B^2. If the values of k_∞ and $\overline{v\Sigma}_a$ derived for the 500 lattice from a three-parameter fit (see last part of Sec. 5.2) are compared to the corresponding values in Tables 5.14a and 5.14b derived from a two-parameter fit, it is seen that the two-parameter fit yields uncertainties which are 10% to 20% of those obtained from the three-parameter fit.

CHAPTER VI

SUMMARY AND RECOMMENDATIONS FOR FUTURE WORK

The results of the work are summarized in this chapter, and recommendations for future work are given.

6.1 SUMMARY

The time dependence of the neutron density in a multiplying medium irradiated by bursts of fast neutrons has been investigated theoretically and experimentally. The theoretical work has concentrated on the development of expressions relating the prompt neutron decay constant to the nuclear parameters of the medium derived according to several theoretical models. Thus, the decay of a thermalized pulse of neutrons has been treated by age-diffusion theory, a modified age-diffusion theory in which the slowing down time for neutrons produced in thermal fission is taken as finite, two-group theory, and multigroup theory. The effects of delayed neutrons, finite source burst width, and resonance fission have also been considered.

The expression for the prompt neutron decay constant has also been derived under several experimental situations. The parameters of the test region in a two-region assembly have been related to the decay constant for the two-region assembly on the assumption that the parameters of the reference region are known from previous pulsed neutron experiments on a lattice composed entirely of the reference region medium. The analysis of experiments on a lattice modified by the insertion of successive amounts of a distributed neutron absorber has indicated the possibility of obtaining values of the parameters of the unmodified lattice more accurately than would be possible with measurements on the unmodified lattice alone. Finally, the absence of a cadmium plate at the bottom of the lattice tank, normally inserted to complete the "black boundary" requirement, has been treated by means of an effective return coefficient.

The experimental program has consisted of thermal die-away measurements in a number of subcritical lattices of partially enriched uranium metal rods and heavy water (see Table 3.1). Measurements were made at several values of the moderator height in each lattice to vary the geometric buckling B^2. Three values of the fundamental mode decay constant λ, one from each of three computer codes, were obtained from each set of data. Agreement, within experimental error, among the three values was obtained in over 90% of the cases studied. The experimental values of λ and B^2 were analyzed on both the modified age-diffusion model and the two-group model to obtain the parameters k_∞ and $\overline{v\Sigma}_a$. The remaining quantities appearing in the expressions for λ, e.g., τ_o, $\overline{vD}$, β, T_o, L^2, and $\overline{v_1\Sigma}_1$, were presumed known on the basis of calculations described in Appendix B. Experimental values of the thermal diffusion area L^2 were also obtained from the ratio of $\overline{vD}$ to $\overline{v\Sigma}_a$.

Measurements of λ as a function of B^2 were also made in pure moderator. The data were analyzed according to the method described in Ref. (M1) to obtain values of the diffusion parameters of heavy water.

The conclusions drawn from the present work are summarized as follows: The values of k_∞ obtained with the pulsed neutron technique are in good agreement, within the quoted uncertainties, with those obtained with steady-state techniques, e.g., measurements of the material buckling (critical equation), method of added absorbers (H1), and the four-factor formula. The agreement is better for a two-group analysis of the pulsed neutron measurements than for a modified age-diffusion analysis. Furthermore, the percentage uncertainties in the two-group values of k_∞ are smaller than those in the corresponding age-diffusion values.

Uncertainties between 1.5% and 4.5% have been obtained in the values of k_∞ reported in this work. The smaller uncertainties are dominated by the contribution of known systematic sources of error which, at present, limit the precision of the pulsed neutron method to between 1.0% and 1.5%. The pulsed neutron method is attractive, therefore, as a means of comparison with the results of material buckling measurements. The accuracy of the pulsed neutron method should be as good as, or better than, that of the four-factor formula and it is

less time consuming. The added-absorber method also requires considerably more time than the pulsed neutron method although somewhat better precision is possible with the former method.

The values of $\overline{v\Sigma}_a$ and L^2 obtained with a two-group analysis of the pulsed neutron measurements are in reasonable agreement, within experimental error, with values obtained from the THERMOS code.

Analysis of pulsed neutron measurements in two-region assemblies indicates that this technique may be used to study these assemblies. The pulsed neutron values of k_∞ in the test region of two-region lattices agree well with steady-state values of k_∞ obtained by other workers in lattices composed entirely of the test region medium.

The proposed analysis of absorber-modified lattices has been applied to three such sets of lattices. In all cases, the uncertainties in the new values of k_∞ and $\overline{v\Sigma}_a$ are smaller than those obtained from an analysis of pulsed neutron measurements on the unmodified lattice alone.

Pulsed neutron measurements with and without a cadmium plate at the bottom of the lattice tank indicate that the return coefficient for thermal neutrons from the graphite-lined cavity below the lattice tank is 0.44 ± 0.05. This value is independent of the moderator height and is an average of measurements made in one lattice and in pure moderator.

6.2 RECOMMENDATIONS FOR FUTURE WORK

The values of k_∞ obtained in the present work agree well with values obtained from the two-group critical equation with measured values of the material buckling and calculated values of τ_o and L^2. It is recommended that the pulsed neutron technique be extended to future lattices studied on the M. I. T. Heavy Water Lattice Project to provide a comparison with measurements of the material buckling. The method should become a standard tool in the investigation of subcritical lattices of this type.

The ultimate precision of the pulsed neutron technique is limited by the contribution of known systematic sources of error to the total uncertainty. Thus, the overall uncertainty in k_∞ may be reduced by reducing the uncertainties in the parameters presumed known in the

analysis. The percentage uncertainty in the diffusion coefficient $\overline{vD}_o$ of 0.9% could be reduced by an extensive series of measurements of the diffusion parameters of heavy water. A more accurate measurement of the age to indium resonance in heavy water would be useful inasmuch as the present uncertainty in τ_o is 2.5%. Similar considerations apply, to a lesser extent, to the rest of the "known" parameters. It may be possible, therefore, to reduce the overall uncertainty in k_∞ to 1.0% or less if measurements along these lines are made.

Pulsed neutron measurements can be made without a cadmium plate at the bottom of the lattice tank provided the effective return coefficient discussed in Secs. 4.5 and 5.5 is included in the analysis of data. It would be desirable to make additional measurements of the return coefficient to reduce the uncertainty in the value reported here. The increase in the contribution of known systematic errors to the uncertainty in k_∞ caused by use of the return coefficient, however, is only 0.05%, indicating that the uncertainty in the return coefficient has a relatively small effect on the overall uncertainty in k_∞.

An extensive investigation of the various methods for determining a value of the decay constant from a set of experimental data was made before the methods described in Sec. 4.1 were selected. One method, which was tried and rejected, consisted of fitting the observed data to a sum of exponential functions plus a constant background term by means of an iterative, least-squares technique in the same way that EXPO makes a fit to a single exponential function plus constant background. The iteration in the former method often diverged or oscillated, most likely because the initial guesses for the decay constants and coefficients were not sufficiently good (S4). Another method, which may prove useful in the analysis of data obtained from pulsed neutron experiments, has been suggested by Gardner (G3). It involves the use of integral transforms to determine the values of the decay constants in a set of data. An advantage of this method is that it does not require initial guesses for the number and values of the decay constants.

The statistical uncertainties in the values of k_∞ and $\overline{v\Sigma}_a$ obtained with the pulsed neutron technique could be reduced if a pulsed neutron source stronger than the one used in this work were obtained. It would

be desirable to investigate the possibility of using a larger BF_3 detector than the one used here or of trying a different type of detector, e.g., fission chamber, solid state detector, etc. These modifications in the experimental equipment might also improve the statistical accuracy of the pulsed neutron technique.

It may be possible to extend the pulsed neutron technique to the study of miniature lattices. This would provide greater flexibility in the number of lattices which could be studied since, at present, pulsed neutron experiments can be made only on weekends and other periods of reactor shutdown. One of the problems which could be studied is the effect of diffusion cooling in multiplying media. Little work has appeared to date on this subject because the effect is small in most subcritical assemblies of practical size. An interesting experiment to study the effect of spectral hardening in the miniature lattice would be to measure the diffusion parameters ($\overline{vD}_o$ and C) in a mixture of heavy water and added absorber (copper rods, for example) and compare them with values of $\overline{vD}_o$ and C obtained in heavy water alone.

The λ data as a function of B^2 obtained in the present work was analyzed with a two-parameter fit to obtain values of k_∞ and $\overline{v\Sigma}_a$. If a sufficient number of values of λ is obtained for a particular lattice, say 30 to 40, it may be possible to make a three-parameter fit of reasonable accuracy to determine a value of $\overline{vD}_o$ for the lattice as well as values of k_∞ and $\overline{v\Sigma}_a$.

APPENDIX A

COMPUTER PROGRAMS

The computer codes used in the analysis of experimental data obtained from pulsed source measurements are described in this appendix. The basic mathematical tool employed is the technique of "least-squares fitting" with which it is assumed the reader is familiar. Excellent treatments of the subject may be found in the literature and the interested reader is referred to them (see, for example, the discussions in Refs. D7, F2, H8, S4, and W6). A general description of each code is given first, followed by the input quantities required, an IBM-FORTRAN II listing, and a sample input deck.

A.1 THE EXPO CODE

The EXPO code, which has been described in detail in Ref. M1, is one of the three techniques used to obtain a value of the fundamental mode decay constant from a measurement of the neutron density as a function of time following the introduction of burst of fast neutrons into the medium. It assumes that the observed data may be represented as the sum of a single exponential function plus background:

$$y(t) = ae^{-\lambda t} + b. \tag{A.1}$$

An initial guess, denoted by the subscript zero, is made for each of the three unknowns (a, λ, and b) and Eq. (A.1) is rewritten:

$$y(t) = (a_o+\delta a)e^{-(\lambda_o+\delta\lambda)t} + (b_o+\delta b), \tag{A.2}$$

where the quantities δa, $\delta\lambda$, and δb are the differences between the "true values" and the "guessed values." Equation (A.2) is then expanded in a Taylor Series about the guessed values:

$$y(t) = y_o(t) + \left(\frac{\partial y}{\partial a}\right)_o \delta a + \left(\frac{\partial y}{\partial \lambda}\right)_o \delta\lambda + \left(\frac{\partial y}{\partial b}\right)_o \delta b + \ldots \tag{A.3}$$

If the expansion in Eq. (A.3) is truncated after terms to first order,

Eq. (A.3) is linear in the correction factors δa, $\delta\lambda$, and δb, which may be determined by standard least-squares fitting techniques. The corrections are then added to their respective initial guesses to obtain second estimates of the quantities a, λ, and b and the above steps are repeated. The process continues until the ratio of each correction factor to its estimate satisfies an appropriate convergence criterion:

$$\frac{\delta a}{a_o} < \epsilon_a, \tag{A.4a}$$

$$\frac{\delta \lambda}{\lambda_o} < \epsilon_\lambda, \tag{A.4b}$$

$$\frac{\delta b}{b_o} < \epsilon_b. \tag{A.4c}$$

In practice, higher spatial modes, in addition to the fundamental mode, are excited by the pulsed source. These higher modes are shorter lived than the fundamental mode, so that data in early time channels are not adequately described by Eq. (A.1). However, after sufficient time, the higher modes have died out and Eq. (A.1) is a valid representation of the data. The condition that higher modes are no longer present is verified by successively dropping the early time channels and repeating the above analysis. When the fit values of a, λ, and b become constant (within statistical error) as a function of "waiting time" (or initial channel number), the observed data is assumed to follow the form given in Eq. (A.1).

A.2 THE STRIP CODE

The STRIP code was written to provide an independent check on the value of the fundamental mode decay constant obtained from EXPO. The values obtained from STRIP agree with those from EXPO, within standard deviations, in practically all cases and, in addition, STRIP requires approximately 20% less operating time on the IBM-7094 computer than EXPO.

A.2.1 Description of STRIP

The STRIP code assumes that the count rate data can be represented by a function of the form given in Eq. (A.1):

$$y(t) = ae^{-\lambda t} + b. \tag{A.1}$$

Subtracting an estimated value for the background from Eq. (A.1) and taking the natural logarithm of the difference yields:

$$\ell n[\, y(t)-b] = \ell n(a) - \lambda t. \tag{A.5}$$

Equation (A.5) is linear in the unknown parameters $\ell n(a)$ and λ which again may be determined along with their standard deviations by least-squares fitting techniques.

The fit values of a and λ coupled with the estimated value of b, however, may not be the "best" values for the particular data at hand because of (1) a poor guess for the background term, and/or (2) contamination of the early time data by higher spatial modes. These two difficulties are overcome by systematically varying the value of b subtracted from the data and by systematically varying the time range over which the fit to Eq. (A.5) is performed and computing the variance of fit associated with each set of parameters (a, λ, and b). The variance of fit is a measure of how well the fitted parameters match the experimental data and is defined as the sum of weighted residuals squared divided by the number of data points minus the number of degrees of freedom:

$$V = \frac{\sum_{i=1}^{M} W_i\left(C_i - ae^{-\lambda t_i} - b\right)^2}{M - 3}. \tag{A.6}$$

In Eq. (A.6), V is the variance of fit, C_i is the experimental count rate in the i^{th} channel, W_i is the weight assigned to the value of C_i, and M is the number of data points used in the fit. That set of parameters which results in the smallest value of V is taken to be the best set for the experimental data.

The manner in which the background and data time ranges are systematically varied is best understood with the aid of Fig. A.1, which is a schematic representation of a typical set of data. The data in channels earlier than channel N contain contributions from higher modes, and data in channels later than channel MM contain statistical fluctuations (arising as the count rate approaches the background value) which inhibit the accuracy of Eq. (A.5). Thus, in a typical analysis, a value

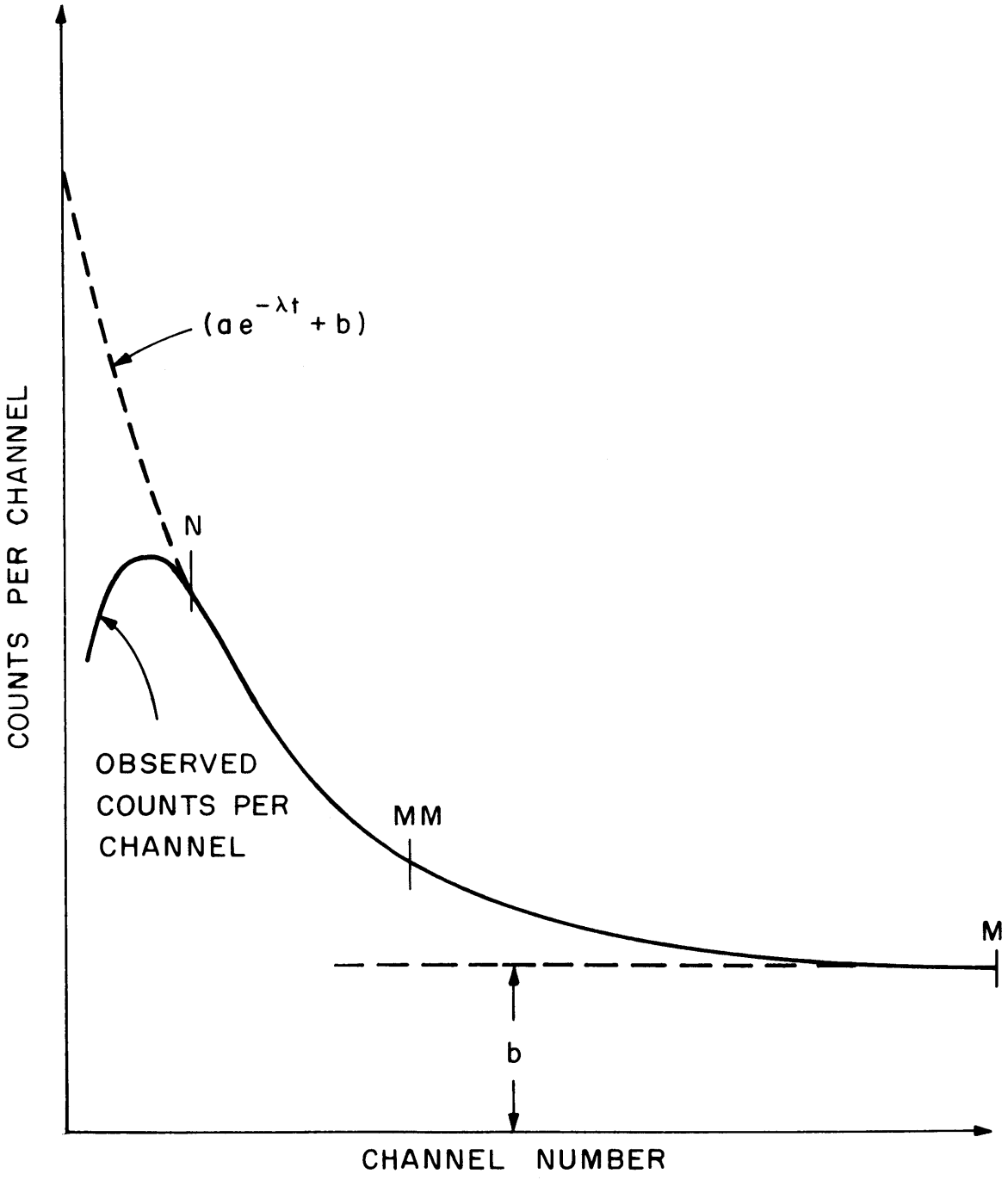

FIG. A.1 SCHEMATIC REPRESENTATION OF OBSERVED COUNTS PER CHANNEL AS A FUNCTION OF CHANNEL NUMBER FOR ANALYSIS WITH "STRIP"

for b is estimated (that value recorded in the pre-burst channel is generally used – see Sec. 3.2.4), and a value of MM is selected (that value for which the corresponding count rate is approximately twice the estimated background is generally used). A range of values is then assigned to N and a least-squares fit applied to the data between channels N and MM for each value of N in the assigned range. That value of N resulting in minimum V is taken to be the "waiting time" necessary for the higher modes to die out. In similar fashion, the values of MM (holding b and N fixed) and b (holding N and MM fixed) are successively varied and the minimum V in each range noted. If the values of MM and b selected in this manner differ appreciably from their initial estimates, the above process is repeated until the change in b is less than 1% and the change in MM is less than three channel numbers. In this way, the best values for the parameters a, λ, and b are ascertained.

It is noted that STRIP does not "search" for the minimum value of V but prints out the computed value of V corresponding to each variation in N, MM, or b. Thus, the user of the code should, himself, select the value of N corresponding to minimum V before continuing on to the variation of MM, and so on.

The input quantities to STRIP are explained in the next section which is followed by an IBM-FORTRAN II listing and sample input deck for the code.

A.2.2 Input Instructions for STRIP

Card 1 (Format(20I4)). The following quantities appear, in order, on this card:

NORUN is the designation for the set of data being analyzed;

M is the number of data points submitted;

MM is the number of the last channel used in the fit to Eq. (A.5);

MK is always equal to MM;

MMIN is the smallest value of MM used when MM is varied -- if MM is not varied, then MMIN is equal to MM;

N is the number of the first channel used in the fit to Eq. (A.5);

NK is always equal to N;

NMAX is the largest value of N used when N is varied – if N is not varied, then NMAX is equal to N;

K1 controls the format for reading in count rate data – the format is (1X, 7F9.0), (7(4X, F6.0)), or (8(5X, F5.0)), depending on whether K1 is positive, zero, or negative, respectively.

Card 2 (Format(1X, 7F9.0)). The following quantities appear, in order, on this card:

TAU is the counter deadtime in microseconds;

WIDTH is the channel width in microseconds;

GAP is the spacing between successive channels in microseconds;

PULSE is the number of pulses introduced into the assembly during the interval of the measurement;

DELAY is the preset target delay time setting in microseconds (see Sec. 3.2.4);

D is the delay time ratio (see Sec. 3.2.4);

SCALE is a scale factor which is used to change the magnitude of the internally computed weighting coefficients – a value of 1.0 is normally used.

Card 3 (Format(1X, 7F9.0)). The following quantities appear, in order, on this card:

BGINL is the smallest estimated background count rate per channel;

BGFNL is the largest estimated background count rate per channel – if the background is held constant, then BGFNL is equal to BGINL;

SIGBG is the estimated uncertainty in the background count rate;

DELBG is the incremental change in the background count rate per successive fit.

Card 4 (Format is defined by K1 on Card 1). The following quantities appear, in order, on this card:

CRAW(I) are the uncorrected counts per channel. They are read in on successive cards according to the specified format until M count rates have been stored in the memory of the computer. The uncorrected count rates are corrected internally for counter dead time according to the relation:

$$C(I) = \frac{CRAW(I)}{1.0 - (CRAW(I) \times TAU)/(PULSE \times WIDTH)} . \qquad (A.6)$$

A.2.3 LISTINGS FOR STRIP

COMPUTER PROGRAM STRIP

```
*      LIST8
*      LABEL
.STRIP
*      SYMBOL TABLE
C
C      THIS CODE MAKES A SEMI-LOG, LEAST SQUARES FIT TO A SET OF PULSED
C      NEUTRON DIE-AWAY DATA TO DETERMINE THE FUNDAMENTAL MODE DECAY
C      CONSTANT
C
       DIMENSION CRAW(3  ),T(300),C(300),CP(300),W(300),STOREL(300)
     1 FORMAT(20I4)
     2 FORMAT(1X,7F9.  )
   100 FORMAT(8(5X,F5.0),)
   101 FORMAT(7(4X,F6.0))
     3 FORMAT(2H1 )
     4 FORMAT(46H- HENRY E. BLISS*PULSED NEUTRON DATA REDUCTION)
     5 FORMAT(20H  RUN NUMBER      =  ,I4)
     6 FORMAT(1X,6P7F9.1)
     7 FORMAT(9H  NMAX = ,I3,7H  MM = ,I3,10H  BKGNB = ,F5.1)
     8 READ INPUT TAPE 4,1,NORUN,MORE,M,MM,MK,MMIN,N,NK,NMAX,K1
C      NORUN IS THE RUN NUMBER
C      MORE IS POSITIVE IF ANOTHER SET OF DATA IS TO FOLLOW
C      M IS THE NUMBER OF RAW DATA POINTS SUBMITTED
C      MM IS THE LAST CHANNEL USED IN THE DECAY CONSTANT ANALYSIS
C      MK IS ALWAYS EQUAL TO MM
C      MMIN IS THE CRITERION FOR DROPPING POINTS FROM THE END OF THE DATA
C      N IS THE FIRST CHANNEL USED IN THE ANALYSIS
C      NK IS ALWAYS EQUAL TO N
C      NMAX IS THE CRITERION FOR DROPPING POINTS FROM THE BEGINNING
C      K1 DETERMINES THE FORMAT FOR READING IN COUNT RATE DATA
       READ INPUT TAPE 4,2,TAU,WIDTH,GAP,PULSE,DELAY,D,SCALE
C      TAU IS THE COUNTER DEADTIME IN MICROSECONDS
C      WIDTH IS THE CHANNEL WIDTH IN MICROSECONDS
C      GAP IS THE SPACING BETWEEN SUCCESSIVE CHANNELS IN MICROSECONDS
C      PULSE IS THE NUMBER OF TARGET PULSES
C      DELAY IS THE TARGET DELAY TIME SETTING IN MICROSECONDS
C      D IS THE DELAY TIME RATIO
C      SCALE IS USED TO CHANGE THE MAGNITUDE OF THE WEIGHTING COUNTS
       READ INPUT TAPE 4,2,BGINL,BGFNL,SIGBG,DELBG
C      BGINL IS THE LOWEST ESTIMATE FOR THE CHANNEL BACKGROUND
C      BGFNL IS THE HIGHEST ESTIMATE FOR THE CHANNEL BACKGROUND
C      SIGBG IS THE ESTIMATED ERROR IN THE BACKGROUND
C      DELBG IS THE FACTOR BY WHICH THE BACKGROUND IS INCREASED IN
```

```
C     SUCCESSIVE FITS
      IF(K1)102,103,104
  102 READ 100,(CRAW(I), I=1,M)
      GO TO 105
  103 READ 101,(CRAW(I), I=1,M)
      GO TO 105
  104 READ 2,(CRAW(I), I=1,M)
C     CRAW(I) ARE THE RAW COUNT RATES IN COUNTS PER CHANNEL
  105 WRITE OUTPUT TAPE 2,3
      WRITE OUTPUT TAPE 2,4
      CALL CLOCK(2)
      WRITE OUTPUT TAPE 2,5,NORUN
      H = 1.0
      BKGND = BGINL
      S = WIDTH + GAP
      T(1) = (WIDTH*D - DELAY) + WIDTH/2.0
      DO 9 I = 2,M
    9 T(I) = T(1) + S*(FLOATF(I) - 1.0)
      DO 10 I = 1,M
      X1 = (CRAW(I)*TAU)/(PULSE*WIDTH)
   10 C(I) = CRAW(I)/(1.0 - X1)
   11 DO 12 I = N,MM
   12 CP(I) = C(I) - BKGND
      DO 20 I = N,MM
      IF(CP(I))13,13,14
   13 CP(I) = 0.0
      W(I) = 0.0
      GO TO 20
   14 W(I) = SCALE*(CP(I)**2)/(C(I) + SIGBG**2)
      CP(I) = LOGF(CP(I))
   20 CONTINUE
   21 SUM1 = 0.0
      SUM2 = 0.0
      SUM3 = 0.0
      SUM4 = 0.0
      SUM5 = 0.0
      DO 25 I = N,MM
      SUM1 = SUM1 + W(I)
      SUM2 = SUM2 + W(I)*T(I)
      SUM3 = SUM3 + W(I)*T(I)*T(I)
      SUM4 = SUM4 + W(I)*CP(I)
   25 SUM5 = SUM5 + W(I)*CP(I)*T(I)
      DETT = SUM1*SUM3 - SUM2*SUM2
      ACOET = (SUM4*SUM3 - SUM5*SUM2)/DETT
      ACOET = EXPF(ACOET)
      ALMDA = (SUM4*SUM2 - SUM5*SUM1)/DETT
      VAR = 0.0
      DO 30 I = N,M
      CP(I)=C(I) - BKGND
   30 VAR=VAR + (1.0/(C(I) + SIGBG**2))*((CP(I) - ACOET*EXPF(-ALMDA*T(I)
     1))**2)
      VAR = VAR*(1.0/FLOATF(M-N-1))
      DELAC = SQRTF((SUM3/DETT)*VAR)
      DELAC = DELAC*ACOET
      DELAL = SQRTF((SUM1/DETT)*VAR)
```

```
   IF(H)34,34,32
31 FORMAT(69HO  N   MM    M  BKGND     LAMBDA      SIGMA     COEFFT      SI
  1GMA  VARIANCE)
32 WRITE OUTPUT TAPE 2,31
   H = 0.0
33 FORMAT(3I4,0PF7.1,6P2F10.3,0P2F10.3,0PF10.5)
34 WRITE OUTPUT TAPE 2,33,N,MM,M,BKGND,ALMDA,DELAL,ACOET,DELAC,VAR
   IF(BKGND - BGFNL)40,41,41
4  BKGND=BKGND + DELBG
   GO TO 11
41 IF(N - NMAX)42,43,43
42 N=N + 1
   BKGND=BGINL
   GO TO 11
43 IF(MMIN-MM)44,45,45
44 MM=MM - 1
   BKGND=BGINL
   N=NK
   GO TO 11
45 IF(MORE)46,46,8
46 CALL EXIT
   END
```

STRIP SAMPLE INPUT DECK

```
5?1    1 127  80   80  35  21  21  21   1
2.0        80.0       10.0       30000.0   100.0      2.0        1.0
62.25      1.0        1.11       0.2
2254.      2688.      3208.      3449.     3797.      3902.      4052.
4265.      4158.      4141.      4074.     3993.      3881.      3693.
3345.      3371.      3184.      3195.     2891.      2882.      2739.
2312.      2441.      2398.      2198.     2036.      1952.      1828.
1826.      1642.      1451.      1469.     1362.      1299.      1267.
1144.      1137.      1086.      1004.     905.       833.       784.
775.       776.       643.       641.      671.       621.       569.
523.       511.       474.       427.      426.       429.       394.
356.       381.       343.       297.      319.       282.       276.
261.       233.       235.       270.      236.       203.       227.
183.       180.       160.       174.      170.       152.       161.
153.       123.       145.       140.      140.       128.       116.
118.       93.        116.       114.      103.       115.       103.
114.       88.        85.        86.       101.       89.        85.
92.        89.        77.        80.       78.        84.        85.
78.        78.        93.        79.       82.        71.        71.
76.        76.        69.        61.       80.        66.        65.
7?.        68.        72.        60.       76.        80.        70.
62.
```

A.3 THE FRAUD CODE

The objectives of the FRAUD code are (1) to obtain a more accurate value of the fundamental mode decay constant, (2) to obtain an estimate for the value of the next higher spatial mode decay constant, and (3) to provide an independent check on the value of the fundamental mode decay constant obtained from EXPO and STRIP.

A.3.1 Description of FRAUD

In Sec. 2.2.4, the thermal neutron density following injection of a burst of fast neutrons is derived as an infinite sum of exponential functions (plus a constant background):

$$y(t) = \sum_{i=1}^{\infty} \left(a_i e^{-\lambda_i t} \right) + b. \tag{A.7}$$

The values of λ_i increase monotonically with increasing values of the index i, so that after a sufficiently long time, the sum in Eq. (A.7) contains only one term (corresponding to i=1 and represented by Eq. (A.1)). However, owing to a particular detector location, the contribution of certain of the higher mode terms to Eq. (A.7) may be very small, so that the sum in Eq. (A.7) may be reduced to two terms over a considerable portion of the time range. This is illustrated schematically in Fig. A.2.

Thus, FRAUD assumes that the neutron density may be written as (after subtracting an estimated value for the background):

$$y(t) = a_1 e^{-\lambda_1 t} + a_2 e^{-\lambda_2 t}, \tag{A.8}$$

where $\lambda_2 > \lambda_1$. An initial estimate for the longer lived component in Eq. (A.8) allows it to be subtracted from the observed count rate:

$$y_2(t) = y(t) - a_1^1 e^{-\lambda_1^1 t} = a_2 e^{-\lambda_2 t}, \tag{A.9}$$

where the superscript 1 indicates that the values are first estimates of these quantities. Taking the natural logarithm of each side of Eq. (A.9) yields:

$$\ell n[\, y_2(t)] = \ell n(a_2) - \lambda_2 t. \tag{A.10}$$

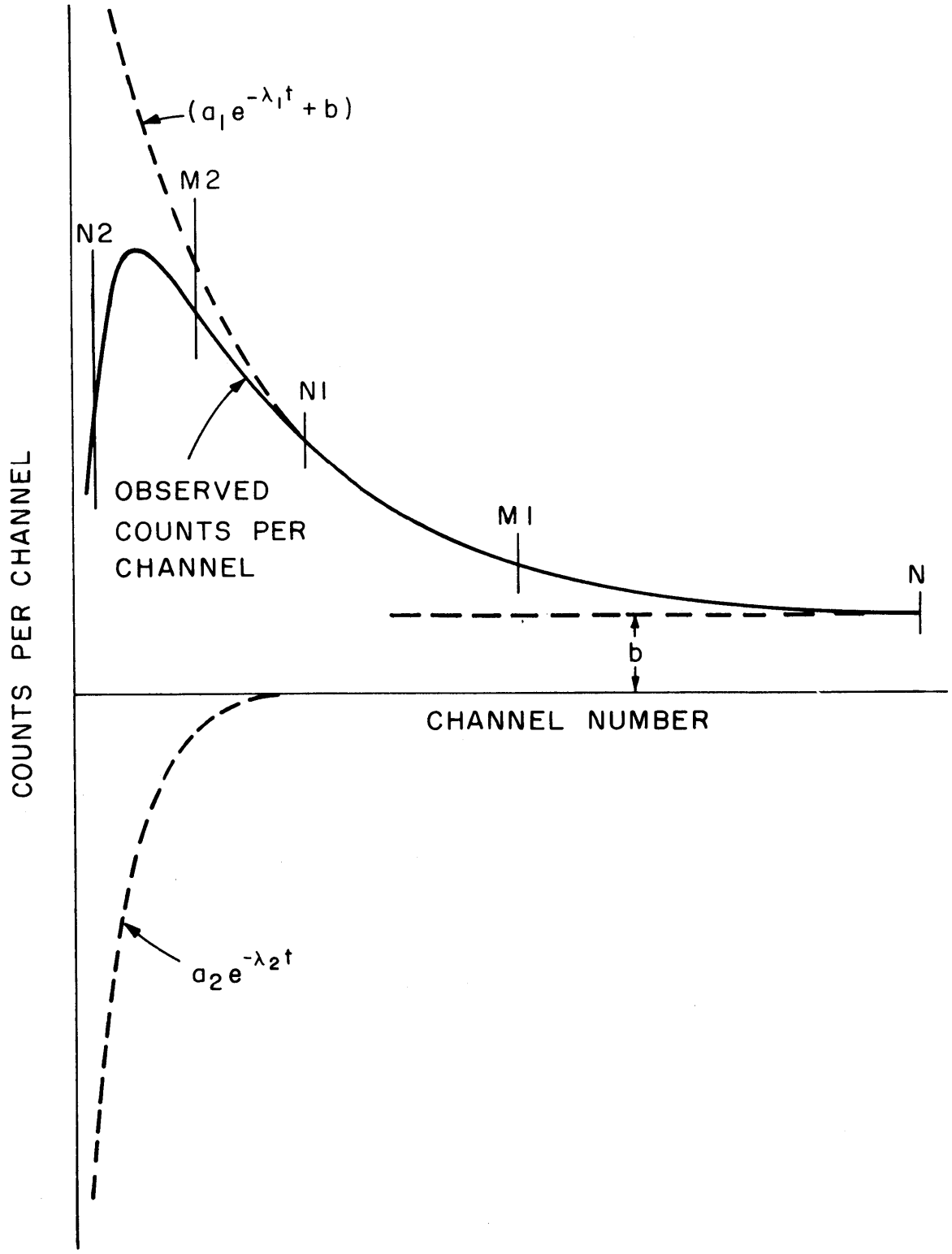

FIG. A.2 SCHEMATIC REPRESENTATION OF OBSERVED COUNTS PER CHANNEL AS A FUNCTION OF CHANNEL NUMBER FOR ANALYSIS WITH "FRAUD"

A first estimate of the higher mode parameters a_2 and λ_2 can then be obtained by least-squares fitting over the range of channels between N2 and M2 (see Fig. A.2). This estimate is then subtracted from the original data (Eq. (A.8)):

$$y_1(t) = y(t) - a_2^1 e^{-\lambda_2^1 t} = a_1 e^{-\lambda_1 t}, \tag{A.11}$$

which can be rewritten:

$$\ell n[y_1(t)] = \ell n(a_1) - \lambda_1 t. \tag{A.12}$$

The second estimate for the parameters a_1 and λ_1 is obtained from a least-squares fit to Eq. (A.12) over the channel range N1 to M1. This iteration procedure is continued until the percentage change in each parameter between successive iterations satisfies a pre-determined convergence criterion:

$$\left| \frac{a_{1,2}^{n+1} - a_{1,2}^{n}}{a_{1,2}^{n}} \right| < \epsilon_{a_{1,2}}, \tag{A.13a}$$

$$\left| \frac{\lambda_{1,2}^{n+1} - \lambda_{1,2}^{n}}{\lambda_{1,2}^{n}} \right| < \epsilon_{\lambda_{1,2}}. \tag{A.13b}$$

The best values for the unknown parameters are determined by systematic variation of M2, N1, M1, N2, and b (usually in that order) until the variance of fit is minimum. The procedure for varying these quantities is identical to that described in Sec. A.2.1.

A.3.2 Input Instructions for FRAUD

The input quantities for FRAUD are explained, not necessarily in order, in this section. The proper order can be found in the listing of the code in the next section.

Card 1 (Format(1X, 10I5)):

NORUN is the designation for the set of data being analyzed;

MORE is positive if another set of data follows;

ADD is not used by the program;

ITMAX is maximum number of iterations permitted;

N is the number of data points submitted.

Cards 2 and 3 (Format(1X, 7F9.2)). The quantities on this card are identical to those on Cards 2 and 3, respectively, of the STRIP input (see Sec. A.2.2).

Card 4 (Format (1X, 15I4)):

K1 is positive if values of the parameters are printed out after each iteration – otherwise, they are printed out only after convergence;

K2 and K3 control the print-out of corrected data, fit data, etc. – these quantities are printed out when K2=N2 and K3=M2 (if no print-out is desired, then K2=0; K3=0);

K4 and K5 control the formulation of the weighting coefficients – both K4 and K5 are usually set equal to -1;

K6 controls the format for reading in count rate data – the format is (1X, 7F9.0), (7(4X, F6.0)), or (8(5X, F5.0)), depending on whether K6 is positive, zero, or negative, respectively.

K7 and K8 are not used by the program.

Card 5 (Format (1X, 15I4)):

N1, M1, N2, and M2 are the starting channel numbers for each of the four ranges which are varied;

N1K, M1K, N2K, and M2K are always equal to N1, M1, N2, and M2, respectively;

N1MAX, M1MIN, N2MAX, and M2MIN are the final channel numbers for each of the four ranges which are varied – if a particular range is not varied, then the final number of the range is set equal to the starting number of the range.

Card 6 (Format(1X, 7F9.7)):

Q1 and DELQ1 are the initial guesses for the fundamental mode decay constant and its error;

A1 and DELA1 are the initial guesses for the fundamental mode coefficient and its error.

Card 7 (Format(1X, 7F9.7)):

EPSA1, EPSQ1, EPSA2, and EPSQ2 are the convergence criteria to be satisfied by the parameters.

Card 8 (Format determined by K6 on Card 4):

CRAW(I) are the uncorrected counts per channel. The N counts are read in on successive cards according to the above format.

A.3.3 LISTINGS FOR FRAUD

COMPUTER PROGRAM FRAUD

```
*       LIST8
*       LABEL
CFRAUD
*       SYMBOL TABLE
        DIMENSION CRAW(300),T(300),C(300),FIT(300),FIT1(300),FIT2(300),
       1HJOAN(300),C1(300),C2(300),W1(300),W2(300)
        COMMON NORUN,MORE,ADD,ITMAX,N,TAU,WIDTH,GAP,PULSE,DELAY,D,M1,M1K,M
       11MIN,M2,M2K,M2MIN,N2,N2K,N2MAX,EPSA1,EPSQ1,EPSA2,EPSQ2,BKGND,BGINL
       2,BGFNL,SIGBG,DELBG,CRAW,T,C,IT,A1,Q1,A2,Q2,AX1,QX1,AX2,QX2,K1,K2,K
       33,K4,K5,K6,K7,K8,VAR,VAR1,VAR2,FIT,FIT1,FIT2,DELA1,DELQ1,DELA2,DEL
       4Q2,SUMA1,SUMQ1,SUMA2,SUMQ2,DET1,DET2,C1,C2,W1,W2,HJOAN,N1,N1K,N1MA
       5X
C
C       THIS CODE FITS TWO HARMONICS TO A SET OF PULSED NEUTRON DIE-AWAY
C       DATA BY MEANS OF AN ITERATIVE,STRIPPING TECHNIQUE
C
     1  CALL DATA
     2  FORMAT(46H- HENRY E. BLISS*PULSED NEUTRON DATA REDUCTION)
     3  FORMAT(20H  RUN NUMBER      =  ,I5)
     4  FORMAT(129HOIT N2 M2 N1 M1 BKGND      LAMBDA1         SIGMA      COEFF
       1T1         SIGMA      LAMBDA2         SIGMA      COEFFT2         SIGMA
       2VARIANCE)
     5  FORMAT(2H  )
    25  FORMAT(2H1 )
        WRITE OUTPUT TAPE 2,25
        WRITE OUTPUT TAPE 2,2
        CALL CLOCK(2)
        WRITE OUTPUT TAPE 2,3,NORUN
        WRITE OUTPUT TAPE 2,4
        WRITE OUTPUT TAPE 2,5
        BKGND = BGINL
    28  DO 7 I=1,N
     7  C(I) = CRAW(I) - BKGND
     6  CALL FITT
        IF(N2-N2MAX)8,9,9
     8  N2=N2+1
        GO TO 6
     9  IF(M2MIN-M2)10,11,11
    10  M2=M2-1
        N2=N2K
        GO TO 6
    11  IF(N1-N1MAX)12,31,31
    12  N1=N1+1
```

```
    N2=N2K
   M2=M2K
   GO TO 6
31 IF(M1MIN-M1)32,13,13
32 M1=M1-1
   N1=N1K
   N2=N2K
   M2=M2K
   GO TO 6
13 IF(BKGND-BGFNL)14,15,15
14 BKGND = BKGND + DELBG
   M1 = M1K
   M2 = M2K
   N1=N1K
   N2 = N2K
   GO TO 28
15 IF(MORE)27,27,1
27 CALL EXIT
   END
```

```
      SUBROUTINE DATA
*     LIST8
*     LABEL
CDATA
*     SYMBOL TABLE
      DIMENSION CRAW(300),T(300),C(300),FIT(300),FIT1(300),FIT2(300),
     1HJOAN(300),C1(300),C2(300),W1(300),W2(300)
      COMMON NORUN,MORE,ADD,ITMAX,N,TAU,WIDTH,GAP,PULSE,DELAY,D,M1,M1K,M
     11MIN,M2,M2K,M2MIN,N2,N2K,N2MAX,EPSA1,EPSQ1,EPSA2,EPSQ2,BKGND,BGINL
     2,BGFNL,SIGBG,DELBG,CRAW,T,C,IT,A1,Q1,A2,Q2,AX1,QX1,AX2,QX2,K1,K2,K
     33,K4,K5,K6,K7,K8,VAR,VAR1,VAR2,FIT,FIT1,FIT2,DELA1,DELQ1,DELA2,DEL
     4Q2,SUMA1,SUMQ1,SUMA2,SUMQ2,DET1,DET2,C1,C2,W1,W2,HJOAN,N1,N1K,N1MA
     5X
C
C     THIS SUBROUTINE READS IN THE RAW DATA, COMPUTES CHANNEL TIMES, AND
C     AND CORRECTS FOR DEAD TIME AND BACKGROUND
C
  100 FORMAT(1X,10I5)
  101 FORMAT(1X,7F9.2)
  102 FORMAT(1X,15I4)
  103 FORMAT(1X,7F9.7)
  104 FORMAT(1X,7F9.0)
  105 FORMAT(8(5X,F5.0))
  106 FORMAT(7(4X,F6.0))
      READ INPUT TAPE 4,100,NORUN,MORE,ADD,ITMAX,N
C     NORUN IS THE RUN NUMBER
C     MORE IS POSITIVE IF ANOTHER SET OF DATA IS TO FOLLOW
C     ADD IS POSITIVE IF CONSECUTIVE CHANNELS ARE TO BE ADDED TOGETHER
C     TO IMPROVE THE FIT
C     ITMAX IS THE MAXIMUN NUMBER OF ITERATIONS PERMITTED
C     N IS THE NUMBER OF RAW DATA POINTS SUBMITTED
      READ INPUT TAPE 4,101,TAU,WIDTH,GAP,PULSE,DELAY,D
C     TAU IS THE COUNTER DEADTIME IN MICROSECONDS
C     WIDTH IS THE CHANNEL WIDTH IN MICROSECONDS
C     GAP IS THE SPACING BETWEEN SUCCESSIVE CHANNELS IN MICROSECONDS
C     PULSE IS THE NUMBER OF TARGET PULSES
C     DELAY IS THE TARGET DELAY TIME SETTING IN MICROSECONDS
C     D IS THE DELAY TIME RATIO
      READ INPUT TAPE 4,101,BGINL,BGFNL,SIGBG,DELBG
C     BGINL IS THE LOWEST ESTIMATE FOR THE CHANNEL BACKGROUND
C     BGFNL IS THE HIGHEST ESTIMATE FOR THE CHANNEL BACKGROUND
C     SIGBG IS THE ESTIMATED ERROR IN THE BACKGROUND COUNT RATE
C     DELBG IS THE FACTOR BY WHICH THE BACKGROUND IS INCREASED FOR THE
C     NEXT FIT
      READ INPUT TAPE 4,102,K1,K2,K3,K4,K5,K6,K7,K8
C     THE VARIOUS VALUES OF K ARE CONTROL FACTORS
C     IF K1 IS POSITIVE VALUES OF THE DECAY CONSTANTS, ETC. ARE PRINTED
C     OUT AFTER EACH ITERATION
C     IF K1 IS ZERO OR NEGATIVE THESE VALUES ARE PRINTED OUT ONLY AFTER
C     CONVERGENCE
C     K2 AND K3 CONTROL THE PRINT OUT OF THE CORRECTED DATA, FIT DATA,
C     ETC. - THESE VALUES ARE PRINTED OUT WHEN K2 = N2 AND K3 = M2
C     K4 AND K5 CONTROL THE FORMULATION OF THE WEIGHTING COEFFICIENTS
      READ INPUT TAPE 4,102,M1,M1K,M1MIN,M2,M2K,M2MIN,N1,N1K,N1MAX,N2,N2
     1K,N2MAX
```

```
C      M1 IS THE LAST DATA POINT USED IN THE FIRST HARMONIC FIT
C      M1K IS ALWAYS IDENTICAL TO M1
C      M1MIN IS THE CRITERION FOR DROPPING POINTS FROM THE END OF THE
C      FIRST HARMONIC DATA
C      M2 IS THE LAST POINT USED IN THE SECOND HARMONIC FIT
C      M2K IS ALWAYS IDENTICAL TO M2
C      M2MIN IS THE CRITERION FOR DROPPING POINTS FROM THE END OF THE
C      SECOND HARMONIC DATA
C      N1 IS THE FIRST POINT USED IN THE FIRST HARMONIC FIT
C      N1K IS ALWAYS IDENTICAL TO N1
C      N1MAX IS THE CRITERION FOR DROPPING POINTS FROM THE BEGINNING
C      N2 IS THE FIRST POINT USED IN THE SECOND HARMONIC FIT
C      N2K IS ALWAYS IDENTICAL TO N2
C      N2MAX IS THE CRITERION FOR DROPPING POINTS FROM THE BEGINNING
       READ INPUT TAPE 4,103,A1,Q1,DELA1,DELQ1
C      THESE ARE THE INITIAL GUESSES FOR THE FIRST HARMONIC COEFFICIENT,
C      DECAY CONSTANT, AND THEIR UNCERTAINTIES, RESPECTIVELY
       READ INPUT TAPE 4,103,EPSA1,EPSQ1,EPSA2,EPSQ2
C      THESE ARE THE CONVERGENCE CRITERIA TO BE USED IN THE ITERATIONS
       IF(K6)181,182,183
  181  READ INPUT TAPE 4,105,(CRAW(I), I=1,N)
       GO TO 190
  182  READ INPUT TAPE 4,106,(CRAW(I), I=1,N)
       GO TO 190
  183  READ INPUT TAPE 4,104,(CRAW(I), I=1,N)
C      CRAW(I) ARE THE RAW COUNT RATES IN COUNTS PER CHANNEL
  190  S=WIDTH + GAP
       T(1)=(WIDTH*D-DELAY) + WIDTH/2.0
       DO 171 I=2,N
  171  T(I)=T(1) + S*(FLOATF(I)-1.0)
       DO 172 I=1,N
       X1=(CRAW(I)*TAU)/(PULSE*WIDTH)
  172  CRAW(I) = CRAW(I)/(1.0 - X1)
       RETURN
       END
```

```
      SUBROUTINE FITT
*     LIST8
*     LABEL
CFITT
*     SYMBOL TABLE
      DIMENSION CRAW(300),T(300),C(300),FIT(300),FIT1(300),FIT2(300),
     1HJOAN(300),C1(300),C2(300),W1(300),W2(300)
      COMMON NORUN,MORE,ADD,ITMAX,N,TAU,WIDTH,GAP,PULSE,DELAY,D,M1,M1K,M
     11MIN,M2,M2K,M2MIN,N2,N2K,N2MAX,EPSA1,EPSQ1,EPSA2,EPSQ2,BKGND,BGINL
     2,BGFNL,SIGBG,DELBG,CRAW,T,C,IT,A1,Q1,A2,Q2,AX1,QX1,AX2,QX2,K1,K2,K
     33,K4,K5,K6,K7,K8,VAR,VAR1,VAR2,FIT,FIT1,FIT2,DELA1,DELQ1,DELA2,DEL
     4Q2,SUMA1,SUMQ1,SUMA2,SUMQ2,DET1,DET2,C1,C2,W1,W2,HJOAN,N1,N1K,N1MA
     5X
C
C     THIS SUBROUTINE CALLS THE FITTING SUBROUTINES AND TESTS THE RESULT
C     FOR PROPER CONVERGENCE
C
  199 FORMAT(5I3,0PF6.2,1P8E12.4,1PE12.5)
  221 FORMAT(59H0 CHANNEL    TIME       RAW DATA       COR DATA       FIT D
     1ATA)
  223 FORMAT(I9,0PF8.0,1P3E14.4)
      H1=0.0
      H2=0.0
      IT=1
  201 CALL FOXX1
      IF(IT-1)206,206,202
  202 IF(ABSF((AX2-A2)/A2) - EPSA2)203,203,205
  203 H2=1.0
      IF(ABSF((QX2-Q2)/Q2) - EPSQ2)206,206,205
  205 H2=0.0
  206 A2=AX2
      Q2=QX2
      IF(IT-1)225,225,208
  225 VAR2=0.0
      DO 226 I=N2,M2
      FIT2(I)=A2*EXPF(-Q2*T(I))
      FIT2(I)=-FIT2(I)
  226 VAR2=VAR2 + ((C2(I) - LOGF(FIT2(I)))**2)*W2(I)
      VAR2=VAR2*1.0/FLOATF(M2-N2-1)
      DELA2=SQRTF((SUMA2/DET2)*VAR2)
      DELA2=DELA2*A2
      DELA2=-DELA2
      DELQ2=SQRTF((SUMQ2/DET2)*VAR2)
  208 CALL FOXX2
      IF(ABSF((AX1-A1)/A1) - EPSA1)207,207,209
  207 H1=1.0
      IF(ABSF((QX1-Q1)/Q1) - EPSQ1)210,210,209
  209 H1=0.0
  210 A1=AX1
      Q1=QX1
  211 CALL FOXX3
  212 IF(H1)215,215,213
  213 IF(H2)215,215,218
  215 IF(K1)217,217,216
  216 WRITE OUTPUT TAPE 2,199,IT,N2,M2,N1,M1,BKGND,Q1,DELQ1,A1,DELA1,Q2,
```

```
   1DELQ2,A2,DELA2,VAR
217 IT = IT + 1
    IF(IT - ITMAX)201,201,218
218 WRITE OUTPUT TAPE 2,199,IT,N2,M2,N1,M1,BKGND,Q1,DELQ1,A1,DELA1,Q2,
   1DELQ2,A2,DELA2,VAR
    IF(N2 - K2)250,219,250
219 IF(M2 - K3)250,220,250
220 WRITE OUTPUT TAPE 2,221
222 WRITE OUTPUT TAPE 2,223,(I,T(I),CRAW(I),C(I),FIT(I), I = N2,M1)
250 RETURN
    END
```

```
      SUBROUTINE FOXX1
*     LIST8
*     LABEL
CFOXX1
*     SYMBOL TABLE
      DIMENSION CRAW(300),T(300),C(300),FIT(300),FIT1(300),FIT2(300),
     1HJOAN(300),C1(300),C2(300),W1(300),W2(300)
      COMMON NORUN,MORE,ADD,ITMAX,N,TAU,WIDTH,GAP,PULSE,DELAY,D,M1,M1K,M
     11MIN,M2,M2K,M2MIN,N2,N2K,N2MAX,EPSA1,EPSQ1,EPSA2,EPSQ2,BKGND,BGINL
     2,BGFNL,SIGBG,DELBG,CRAW,T,C,IT,A1,Q1,A2,Q2,AX1,QX1,AX2,QX2,K1,K2,K
     33,K4,K5,K6,K7,K8,VAR,VAR1,VAR2,FIT,FIT1,FIT2,DELA1,DELQ1,DELA2,DEL
     4Q2,SUMA1,SUMQ1,SUMA2,SUMQ2,DET1,DET2,C1,C2,W1,W2,HJOAN,N1,N1K,N1MA
     5X
C
C     THIS SUBROUTINE MAKES A LEAST SQUARES FIT TO THE SECOND HARMONIC
C     DATA
C
  300 DO 301 I=N2,M2
      HJOAN(I)=A1*EXPF(-Q1*T(I))
      C2(I)=C(I)-HJOAN(I)
  301 C2(I)=-C2(I)
      DO 306 I=N2,M2
      IF(C2(I))302,302,303
  302 W2(I)=0.0
      C2(I)=0.0
      GO TO 306
  303 IF(K4)305,305,304
  304 W2(I) = (C(I)**2)/(CRAW(I) + SIGBG**2)
      C2(I) = LOGF(C2(I))
      GO TO 306
  305 W2(I) = (C2(I)**2)/(CRAW(I) + SIGBG**2 + (EXPF(-2.0*Q1*T(I)))*(DEL
     1A1**2 + (A1*DELQ1*T(I))**2))
      C2(I) = LOGF(C2(I))
  306 CONTINUE
      SUM1=0.0
      SUM2=0.0
      SUM3=0.0
      SUM4=0.0
      SUM5=0.0
      DO 307 I = N2,M2
      SUM1=SUM1 + W2(I)
      SUM2=SUM2 + W2(I)*T(I)
      SUM3=SUM3 + W2(I)*(T(I)**2)
      SUM4=SUM4 + W2(I)*C2(I)
  307 SUM5 = SUM5 + W2(I)*C2(I)*T(I)
      DET2=(SUM1*SUM3) -(SUM2*SUM2)
      AX2 = (SUM4*SUM3 - SUM5*SUM2)/DET2
      AX2=EXPF(AX2)
      AX2=-AX2
      QX2 = (SUM4*SUM2 - SUM5*SUM1)/DET2
      SUMA2=SUM3
      SUMQ2=SUM1
      RETURN
      END
```

```
      SUBROUTINE FOXX2
*     LIST8
*     LABEL
CFOXX2
*     SYMBOL TABLE
      DIMENSION CRAW(300),T(300),C(300),FIT(300),FIT1(300),FIT2(300),
     1HJOAN(300),C1(300),C2(300),W1(300),W2(300)
      COMMON NORUN,MORE,ADD,ITMAX,N,TAU,WIDTH,GAP,PULSE,DELAY,D,M1,M1K,M
     11MIN,M2,M2K,M2MIN,N2,N2K,N2MAX,EPSA1,EPSQ1,EPSA2,EPSQ2,BKGND,BGINL
     2,BGFNL,SIGBG,DELBG,CRAW,T,C,IT,A1,Q1,A2,Q2,AX1,QX1,AX2,QX2,K1,K2,K
     33,K4,K5,K6,K7,K8,VAR,VAR1,VAR2,FIT,FIT1,FIT2,DELA1,DELQ1,DELA2,DEL
     4Q2,SUMA1,SUMQ1,SUMA2,SUMQ2,DET1,DET2,C1,C2,W1,W2,HJOAN,N1,N1K,N1MA
     5X
C
C     THIS SUBROUTINE MAKES A LEAST SQUARES FIT TO THE FIRST HARMONIC
C     DATA
C
      DO 401 I=N1,M1
      HJOAN(I)=-A2*EXPF(-Q2*T(I))
  401 C1(I)=C(I) +HJOAN(I)
      DO 406 I=N1,M1
      IF(C1(I))402,402,403
  402 C1(I)=0.0
      W1(I)=0.0
      GO TO 406
  403 IF(K5)405,405,404
  404 W1(I) = (C(I)**2)/(CRAW(I) + SIGBG**2)
      C1(I) = LOGF(C1(I))
      GO TO 406
  405 W1(I) = (C1(I)**2)/(CRAW(I) + SIGBG**2 + (EXPF(-2.0*Q2*T(I)))*(DEL
     1A2**2 + (A2*DELQ2*T(I))**2))
      C1(I) = LOGF(C1(I))
  406 CONTINUE
      SUM1=0.0
      SUM2=0.0
      SUM3=0.0
      SUM4=0.0
      SUM5=0.0
      DO 407 I=N1,M1
      SUM1=SUM1 + W1(I)
      SUM2=SUM2 + W1(I)*T(I)
      SUM3=SUM3 + W1(I)*(T(I)**2)
      SUM4=SUM4 + W1(I)*C1(I)
  407 SUM5 = SUM5 + W1(I)*C1(I)*T(I)
      DET1=(SUM3*SUM1) - (SUM2*SUM2)
      AX1 = (SUM4*SUM3 - SUM5*SUM2)/DET1
      AX1=EXPF(AX1)
      QX1 = (SUM4*SUM2 - SUM5*SUM1)/DET1
      SUMA1=SUM3
      SUMQ1=SUM1
      RETURN
      END
```

```
      SUBROUTINE FOXX3
*     LIST8
*     LABEL
CFOXX3
*     SYMBOL TABLE
      DIMENSION CRAW(300),T(300),C(300),FIT(300),FIT1(300),FIT2(300),
     1HJOAN(300),C1(300),C2(300),W1(300),W2(300)
      COMMON NORUN,MORE,ADD,ITMAX,N,TAU,WIDTH,GAP,PULSE,DELAY,D,M1,M1K,M
     11MIN,M2,M2K,M2MIN,N2,N2K,N2MAX,EPSA1,EPSQ1,EPSA2,EPSQ2,BKGND,BGINL
     2,BGFNL,SIGBG,DELBG,CRAW,T,C,IT,A1,Q1,A2,Q2,AX1,QX1,AX2,QX2,K1,K2,K
     33,K4,K5,K6,K7,K8,VAR,VAR1,VAR2,FIT,FIT1,FIT2,DELA1,DELQ1,DELA2,DEL
     4Q2,SUMA1,SUMQ1,SUMA2,SUMQ2,DET1,DET2,C1,C2,W1,W2,HJOAN,N1,N1K,N1MA
     5X
C
C     THIS SUBROUTINE CALCULATES THE VARIANCE OF FIT FOR EACH HARMONIC
C     AND CALCULATES THE GOODNESS OF FIT OF THE ASSOCIATED PARAMETERS
C
  500 DO 501 I=N2,N
      FIT1(I)=A1*EXPF(-Q1*T(I))
      FIT2(I)=A2*EXPF(-Q2*T(I))
  501 FIT(I)=FIT1(I) + FIT2(I)
      VAR=0.0
      DO 502 I=N2,N
  502 VAR=VAR + ((C(I) - FIT(I))**2)*1.0/(CRAW(I) + SIGBG**2)
      VAR=VAR*1.0/FLOATF(N  - N2 - 1)
      VAR1=0.0
      DO 503 I=N1,M1
  503 VAR1=VAR1 + ((C1(I) - LOGF(FIT1(I)))**2)*W1(I)
      VAR1=VAR1*1.0/FLOATF(M1 - N1 - 1)
      VAR2=0.0
      DO 504 I=N2,M2
      FIT2(I)=-FIT2(I)
  504 VAR2=VAR2 + ((C2(I) - LOGF(FIT2(I)))**2)*W2(I)
      VAR2=VAR2*1.0/FLOATF(M2 - N2 - 1)
      DELA1=SQRTF((SUMA1/DET1)*VAR1)
      DELA1=DELA1*A1
      DELQ1=SQRTF((SUMQ1/DET1)*VAR1)
      DELA2=SQRTF((SUMA2/DET2)*VAR2)
      DELA2=DELA2*A2
      DELA2=-DELA2
      DELQ2=SQRTF((SUMQ2/DET2)*VAR2)
      RETURN
      END
```

FRAUD SAMPLE INPUT DECK

```
  501     1     0    50  127
2.0       80.0       10.0       30000.0   100.0     2.0
62.25     62.00      1.11       1.80
  -1    0    0   -1   -1   +1
  73   73   73   11   11   11   16   16   16    1    1    8
10232.0   0.000681   77.0       0.000003
0.0010    0.0010     0.0050     0.0050
2254.     2688.      3208.      3449.     3797.     3902.     4052.
4205.     4158.      4141.      4074.     3993.     3881.     3693.
3545.     3371.      3184.      3195.     2891.     2882.     2739.
2612.     2441.      2398.      2198.     2036.     1952.     1828.
1826.     1642.      1451.      1469.     1362.     1299.     1267.
1144.     1137.      1086.      1004.     905.      833.      784.
775.      776.       643.       641.      671.      621.      569.
523.      511.       474.       427.      426.      429.      394.
326.      381.       343.       297.      319.      282.      276.
261.      233.       235.       270.      236.      203.      227.
183.      180.       160.       174.      170.      152.      161.
153.      123.       145.       140.      140.      128.      116.
118.      93.        116.       114.      103.      115.      103.
114.      88.        85.        86.       101.      89.       85.
92.       89.        77.        80.       78.       84.       85.
78.       78.        93.        79.       82.       71.       71.
76.       76.        69.        61.       80.       66.       65.
73.       68.        72.        60.       76.       80.       70.
62.
```

A.4 THE LSQHEB CODE

The LSQHEB code was written to facilitate the determination of the parameters k_∞ and $\overline{v\Sigma_a}$ from measured values of λ and B^2. It contains options which permit analysis of the data according to modified age-diffusion theory, two-group theory, two-group theory with the coefficient r held fixed, and age-diffusion theory with a power series expansion for the fast non-leakage probability.

A.4.1 Description of LSQHEB

The two-group analysis is described in some detail, followed by a summary of the modifications required to extend the analysis to the other options. For a more complete description of the operation of LSQHEB, reference is made to the listing in FORTRAN II in the next section.

The two-group expression for the i^{th} decay constant is:

$$\lambda_i = \frac{\overline{v\Sigma_a} + \overline{vD_o}B_i^2 - CB_i^4 - \overline{v\Sigma_a}(1-\beta)k_\infty P_1(B_i^2)}{1 + \alpha_{2G}(1+L^2B_i^2)\,P_1(B_i^2)}\,, \tag{A.14}$$

where

$$\alpha_{2G} = \frac{\overline{v\Sigma_a}}{\overline{v_1\Sigma_1}}\,, \tag{A.14a}$$

$$P_1(B_i^2) = \frac{1}{1 + \tau_o B_i^2}\,. \tag{A.14b}$$

The quantities $\overline{vD_o}$, C, α_{2G}, and τ_o are presumed known and Eq. (A.14) is rewritten:

$$\lambda_i' = \overline{v\Sigma_a} + \overline{v\Sigma_a}(1-\beta)\,k_\infty P_1(B_i^2), \tag{A.15}$$

where,

$$\lambda_i' = \lambda_i\left[1+\alpha_{2G}(1+L^2B_i^2)P_1(B_i^2)\right] - \overline{vD_o}B_i^2 + CB_i^4\,. \tag{A.15a}$$

Then, a least-squares fit is made to Eq. (A.15) with $P_1(B_i^2)$ taken as the independent variable. The weighting coefficients are calculated according to the relation:

$$W_i = \left(1/\sigma_{\lambda_i}\right)^2,$$

where σ_{λ_i} is the standard deviation of λ_i. Values of the "least-squares" coefficients $\overline{v\Sigma_a}$ and $\overline{v\Sigma_a}(1-\beta)k_\infty$ and associated uncertainties are then computed according to standard techniques which are described, for example, in Ref. H8. Thus, the parameter $\overline{v\Sigma_a}$ is obtained directly as a coefficient of the least-squares fit. A value of k_∞ may also be obtained (using a calculated value of β) as the ratio of the second to the first coefficient. However, the resulting uncertainty in k_∞ may be large if the uncertainty in either coefficient is large. A smaller uncertainty in the value of k_∞, particularly in cases of practical interest when k_∞ is near unity, results if Eq. (A.15) is put in slightly different form:

$$\lambda_i' = \overline{v\Sigma_a}[1-(1-\beta)k_\infty] - \overline{v\Sigma_a}(1-\beta)k_\infty[P_1(B_i^2)-1] = r - sP_1', \qquad (A.16)$$

and a new least-squares fit made. Then k_∞ is derived as:

$$k_\infty = \frac{1}{(1-\beta)(1+(r/s))} . \qquad (A.17)$$

Before the final values of k_∞ and $\overline{v\Sigma_a}$ are obtained, however, Eq. (A.14a) must be satisfied:

$$\overline{v\Sigma_a} = \alpha_{2G}\overline{v_1\Sigma_1} . \qquad (A.14a)$$

The fast group removal cross section is presumed known (see Sec. B.6) and, since α_{2G} is not known in advance, the procedure described above is repeated for a specified range of values of α_{2G}. Values of k_∞ and $\overline{v\Sigma_a}$ are printed out for each value of α_{2G}, and that set which results in satisfaction of Eq. (A.14a) is selected as the set yielding the best agreement with the experimental data.

The other options proceed in a similar manner, with the following changes made:

(1) Modified age-diffusion analysis

$$\lambda_i' = \lambda_i\left(1+\alpha_{FA}P_1(B_i^2)\right),$$

$$\alpha_{FA} = \overline{v\Sigma_a}(1-\beta)\,k_\infty T_o,$$

$$P_1(B_i^2) = e^{-B_i^2\tau_o};$$

(2) Two-group analysis with r fixed

Coefficient r taken as known according to procedure outlined in Sec. 4.4;

(3) Age diffusion analysis with power series expansion for fast non-leakage probability

$$\lambda_i' = r + tB_i^2 - uB_i^4,$$

$$t = \overline{v\Sigma_a}(1-\beta)k_\infty \tau_o,$$

$$u = \left(\frac{1}{2}\right)\overline{v\Sigma_a}(1-\beta)\, k_\infty \tau_o^2 .$$

The input data to LSQHEB, which consists of the measured decay constants λ_i, their associated uncertainties σ_{λ_i} and bucklings B_i^2, and the parameters presumed known, are described in the next section.

A.4.2 Input Instructions for LSQHEB

Card 1 (Format (15I5)). The following quantities appear, in order, on this card:

NORUN is the designation for the set of data being analyzed;

MORE is positive if another set of data follows;

N is the number of data points submitted.

Card 2 (Format (15I5)). The following quantities appear, in order, on this card:

K1 is positive if a modified age-diffusion analysis is used;

K2 is positive if a two-group analysis is used;

K3 is positive if a modified age-diffusion analysis with the fast non-leakage probability expanded in a power series is used;

K4 is positive if a two-group analysis is used with the coefficient r fixed;

K5 to K10 are not used by the program.

Card 3 (Format (7F10.5)). This card contains values of the decay constant Q(I) from I = 1 to N.

Card 4 (Format (7F10.5)). This card contains values of the standard deviation of the decay constants SIGQ(I) from I = 1 to N.

Card 5 (Format (7F10.5)). This card contains values of the buckling BB(I) from I = 1 to N.

Card 6 (Format (7F10.5)). The following quantities appear, in order, on this card:

BETA is the effective delayed neutron fraction;

TAU is the neutron age to thermal;

SIGTAU is the uncertainty in TAU;

VD is the diffusion coefficient;

C is the diffusion cooling coefficient.

Card 7 (Format (7F10.5)). The following quantities appear, in order, on this card:

ALMIN is the smallest value of α;

DELAL is the incremental change in α for the succeeding least-squares fit;

ALMAX is the largest value of α;

ZETA is the thermal diffusion area (L^2);

AFIX is the fixed value of r;

SGAFIX is the uncertainty is AFIX.

A.4.3 LISTINGS FOR LSQHEB

COMPUTER PROGRAM LSQHEB

```
*       LIST8
*       LABEL
CLSQHEB
*       SYMBOL TABLE
        DIMENSION W(50),Q(50),SIGQ(50),BB(50),P(50),PP(50),E(3,3),EE(3,3),
       1G(3),Y(3),QS(50),QQS(50)
        COMMON K1,K2,K3,K4,K5,K6,K7,K8,K9,K10,NORUN,MORE,N,W,SIGQ,P,PP,ALP
       1HA,BB,TAU,SIGTAU,Q,QS,VD,C,L1,A,SIGA,SIGB,B,BETA,DELAL,ALMAX,ZETA,
       2AFIX,SGAFIX,QQS,ALMIN
C
C       THIS CODE PERFORMS A LEAST-SQUARES FIT TO A SET OF LAMBDA AS A
C       FUCNTION OF B**2 DATA USING SEVERAL DIFFERENT MODELS
C
     1 FORMAT(2H0 )
     2 FORMAT(2H1 )
     3 FORMAT(2H- )
     4 FORMAT(75H- HENRY E. BLISS*DECAY CONSTANT VERSUS GEOMETRIC BUCKLIN
      1G LEAST SQUARES FIT)
     5 FORMAT(20H  LATTICE NUMBER  = ,I3)
     6 FORMAT(61H  FERMI AGE MODEL FOR FAST NON-LEAKAGE PROBABILITY - VD
      1KNOWN)
     7 FORMAT(117H0     VSA  SIGVSA   KINFIN   SIGK1   SIGK2  ALPHA     VAR
      1IANCE   COEFTM     SIGMA   COEFTN     SIGMA     TAU       VD       C)
     8 FORMAT(2F8.2,1X,3F8.4,F7.3,1PE12.4,0P4F9.2,F7.1,2F7.3)
     9 FORMAT(61H  TWO GROUP MODEL FOR FAST NON-LEAKAGE PROBABILITY - VD
      1KNOWN)
    10 FORMAT(124H0     VSA  SIGVSA   KINFIN   SIGK1   SIGK2  ALPHA   L**2
      1     VARIANCE   COEFTM     SIGMA   COETFN     SIGMA     TAU      VD
      2  C)
    11 FORMAT(2F8.2,1X,3F8.4,2F7.3,1PE12.4,0P4F9.2,F7.1,2F7.3)
    12 FORMAT(79H  EXPANSION OF FERMI SLOWING DOWN KERNAL IN POWER SERIES
      1 OF BUCKLING - VD KNOWN)
    13 FORMAT(124H0     VSA  SIGVSA   KINFIN   SIGK2  ALPHA     VARIANCE
      1   COEFTM        SIGMA       COEFTN        SIGMA       COEFTP        SI
      2GMA)
    15 FORMAT(70H  COEFFICIENT M FIXED - EXACT EXPRESSION FOR FERMI SLOWI
      1NG DOWN KERNAL)
    16 FORMAT(109H0     VSA  SIGVSA   KINFIN    SIGK  ALPHA     VARIANCE
      1  MFIX     SIGMA   COEFTN     SIGMA     TAU       VD       C)
    20 FORMAT(30H    LAMBDA      SIGMA  BUCKLING)
    21 FORMAT(2F10.2,F10.6)
    51 CALL DATA
    59 DO 60 I=1,N
```

```
 60 W(I)=(1.0/SIGQ(I))**2
    IF(K1)100,100,52
 52 PRINT 2
    PRINT 4
    CALL CLOCK(2)
    PRINT 5,NORUN
    PRINT 3
    PRINT 20
    PRINT 21, (Q(I),SIGQ(I),BB(I), I=1,N)
    PRINT 3
    PRINT 6
    PRINT 1
    PRINT 7
    PRINT 1
    DO 70 I=1,N
    P(I)=EXPF(-TAU*BB(I))
 70 PP(I)=P(I) - 1.0
 71 ALPHA=ALMIN
 72 DO 75 I=1,N
 75 QS(I)=Q(I)*(1.0 + ALPHA*P(I)) -1.0E5*(VD*BB(I) - C*BB(I)*BB(I))
    L1=0
    CALL FIT
    VSA=A
    SIGVSA=SIGA
    XK=-B/A
    XK=XK/(1.0 - BETA)
    SIGXK1=XK*SQRTF((SIGA/A)**2 + (SIGB/B)**2)
    L1=1
    CALL FIT
    SIGXK2=(XK**2)*ABSF(A/B)*SQRTF((SIGA/A)**2 + (SIGB/B)**2)
    VAR=0.0
    DO 80 I=1,N
    HA=VSA*XK*(1.0 - BETA)*P(I)
 80 VAR=VAR + W(I)*(Q(I) - (VSA + 1.0E5*(VD*BB(I) - C*BB(I)*BB(I)) - H
   1A)/(1.0 + ALPHA*P(I)))**2
    PRINT 8,VSA,SIGVSA,XK,SIGXK1,SIGXK2,ALPHA,VAR,A,SIGA,B,SIGB,TAU,VD
   1,C
    ALPHA=ALPHA + DELAL
    IF(ALPHA - ALMAX)72,72,100
100 IF(K2)127,127,101
101 PRINT 2
    PRINT 4
    CALL CLOCK(2)
    PRINT 5,NORUN
    PRINT 3
    PRINT 20
    PRINT 21, (Q(I),SIGQ(I),BB(I), I=1,N)
    PRINT 3
    PRINT 9
    PRINT 1
    PRINT 10
    PRINT 1
109 DO 110 I=1,N
    P(I)=1.0/(1.0 + TAU*BB(I))
110 PP(I)=P(I) - 1.0
```

```
113 ALPHA=ALMIN
114 DO 115 I=1,N
115 QS(I)=Q(I)*(1.0 + ALPHA*P(I)*(1.0 + ZETA*BB(I))) - 1.0E5*(VD*BB(I)
   1 - C*BB(I)*BB(I))
    L1=0
    CALL FIT
    VSA=A
    SIGVSA=SIGA
    XK=-B/A
    XK=XK/(1.0 - BETA)
    SIGXK1=XK*SQRTF((SIGA/A)**2 + (SIGB/B)**2)
    L1=1
    CALL FIT
    SIGXK2=(XK**2)*ABSF(A/B)*SQRTF((SIGA/A)**2 + (SIGB/B)**2)
    VAR=0.0
    DO 120 I=1,N
120 VAR=VAR + W(I)*(Q(I) - (VSA + 1.0E5*(VD*BB(I) - C*BB(I)*BB(I)) - V
   1SA*XK*(1.0 - BETA)*P(I))/(1.0 + ALPHA*P(I)*(1.0 + ZETA*BB(I))))**2
    PRINT 11,VSA,SIGVSA,XK,SIGXK1,SIGXK2,ALPHA,ZETA,VAR,A,SIGA,B,SIGB,
   1TAU,VD,C
    ALPHA=ALPHA + DELAL
    IF(ALPHA - ALMAX)114,114,127
127 IF(K3)150,150,130
130 PRINT 2
    PRINT 4
    CALL CLOCK(2)
    PRINT 5,NORUN
    PRINT 3
    PRINT 20
    PRINT 21, (Q(I),SIGQ(I),BB(I), I=1,N)
    PRINT 3
    PRINT 12
    PRINT 1
    PRINT 13
    PRINT 1
    L1=0
    CALL FIT1
150 IF(K4)180,180,171
171 PRINT 2
    PRINT 4
    CALL CLOCK(2)
    PRINT 5,NORUN
    PRINT 3
    PRINT 20
    PRINT 21, (Q(I),SIGQ(I),BB(I), I=1,N)
    PRINT 3
    PRINT 15
    PRINT 1
    PRINT 16
    PRINT 1
    CALL FIT2
180 IF(MORE)181,181,51
181 CALL EXIT
    END
```

```
      SUBROUTINE DATA
*     LIST8
*     LABEL
CDATA
*     SYMBOL TABLE
      DIMENSION W(50),Q(50),SIGQ(50),BB(50),P(50),PP(50),E(3,3),EE(3,3),
     1G(3),Y(3),QS(50),QQS(50)
      COMMON K1,K2,K3,K4,K5,K6,K7,K8,K9,K10,NORUN,MORE,N,W,SIGQ,P,PP,ALP
     1HA,BB,TAU,SIGTAU,Q,QS,VD,C,L1,A,SIGA,SIGB,B,BETA,DELAL,ALMAX,ZETA,
     2AFIX,SGAFIX,QQS,ALMIN
   30 FORMAT(15I5)
   31 FORMAT(7F10.5)
      READ 30,NORUN,MORE,N
      READ 30,K1,K2,K3,K4,K5,K6,K7,K8,K9,K10
      READ 31,(Q(I), I=1,N)
      READ 31,(SIGQ(I), I=1,N)
      READ 31,(BB(I), I=1,N)
      READ 31,BETA,TAU,SIGTAU,VD,C
      READ 31,ALMIN,DELAL,ALMAX,ZETA,AFIX,SGAFIX
      RETURN
      END
```

```
      SUBROUTINE FIT
*     LIST8
*     LABEL
CFIT
*     SYMBOL TABLE
      DIMENSION W(50),Q(50),SIGQ(50),BB(50),P(50),PP(50),E(3,3),EE(3,3),
     1G(3),Y(3),QS(50),QQS(50)
      COMMON K1,K2,K3,K4,K5,K6,K7,K8,K9,K10,NORUN,MORE,N,W,SIGQ,P,PP,ALP
     1HA,BB,TAU,SIGTAU,Q,QS,VD,C,L1,A,SIGA,SIGB,B,BETA,DELAL,ALMAX,ZETA,
     2AFIX,SGAFIX,QQS,ALMIN
      IF(ALPHA - ALMIN)301,301,305
  301 SUM1=0.0
      SUM2P=0.0
      SUM2PP=0.0
      SUM3P=0.0
      SUM3PP=0.0
      DO 302 I=1,N
      SUM1=SUM1 + W(I)
      SUM2P=SUM2P + W(I)*P(I)
      SUM2PP=SUM2PP + W(I)*PP(I)
      SUM3P=SUM3P + W(I)*P(I)*P(I)
  302 SUM3PP=SUM3PP + W(I)*PP(I)*PP(I)
  305 SUM4=0.0
      DO 306 I=1,N
  306 SUM4=SUM4 + W(I)*QS(I)
      SUM5=0.0
      IF(L1)307,307,310
  307 DO 308 I=1,N
  308 SUM5=SUM5 + W(I)*QS(I)*P(I)
      SUM2=SUM2P
      SUM3=SUM3P
      GO TO 315
  310 DO 311 I=1,N
  311 SUM5=SUM5 + W(I)*QS(I)*PP(I)
      SUM2=SUM2PP
      SUM3=SUM3PP
  315 DET=SUM1*SUM3 - SUM2*SUM2
      A=(SUM4*SUM3 - SUM2*SUM5)/DET
      B=(SUM1*SUM5 - SUM2*SUM4)/DET
      VAR=0.0
      IF(L1)316,316,318
  316 DO 317 I=1,N
  317 VAR=VAR + W(I)*((QS(I) - A - B*P(I))**2)
      GO TO 320
  318 DO 319 I=1,N
  319 VAR=VAR + W(I)*((QS(I) - A - B*PP(I))**2)
  320 VAR=VAR/FLOATF(N - 2)
      SIGA=SQRTF((SUM3/DET)*VAR)
      SIGB=SQRTF((SUM1/DET)*VAR)
      RETURN
      END
```

```
      SUBROUTINE FIT1
*     LIST8
*     LABEL
CFIT1
*     SYMBOL TABLE
      DIMENSION W(50),Q(50),SIGQ(50),BB(50),P(50),PP(50),E(3,3),EE(3,3),
     1G(3),Y(3),QS(50),QQS(50)
      COMMON K1,K2,K3,K4,K5,K6,K7,K8,K9,K10,NORUN,MORE,N,W,SIGQ,P,PP,ALP
     1HA,BB,TAU,SIGTAU,Q,QS,VD,C,L1,A,SIGA,SIGB,B,BETA,DELAL,ALMAX,ZETA,
     2AFIX,SGAFIX,QQS,ALMIN
   40 FORMAT(39H0 OVERFLOW IN LEAST SQUARES DETERMINANT)
   41 FORMAT(39H0 LEAST SQUARES DETERMINANT IS SINGULAR)
   14 FORMAT(0P2F8.2,1PE12.4,1PE10.2,0PF7.3,1P7E11.3)
   15 FORMAT(0P2F8.2,1PE12.4,1PE10.2,0P3F7.3,1P7E10.3)
      DO 135 I=1,3
      DO 135 J=1,3
  135 E(I,J)=0.0
      DO 136 I=1,N
      E(1,1)=E(1,1) + W(I)
      E(1,2)=E(1,2) + W(I)*BB(I)
      E(1,3)=E(1,3) + W(I)*(BB(I)**2)
      E(2,3)=E(2,3) + W(I)*(BB(I)**3)
  136 E(3,3)=E(3,3) + W(I)*(BB(I)**4)
      E(2,1)=E(1,2)
      E(2,2)=E(1,3)
      E(3,1)=E(1,3)
      E(3,2)=E(2,3)
      ALPHA=ALMIN
  137 DO 138 I=1,N
  138 P(I)=EXPF(-TAU*BB(I))
  139 DO 140 I=1,3
  140 Y(I)=0.0
  141 DO 142 I=1,N
  143 QS(I)=Q(I)*(1.0 + ALPHA*P(I)) - 1.0E5*(VD*BB(I) - C*BB(I)*BB(I))
  146 Y(1)=Y(1) + W(I)*QS(I)
      Y(2)=Y(2) + W(I)*QS(I)*BB(I)
  142 Y(3)=Y(3) + W(I)*QS(I)*BB(I)*BB(I)
      D1=1.0
      DO 144 I=1,3
      DO 144 J=1,3
  144 EE(I,J)=E(I,J)
      M=XSIMEQF(3,3,1,EE,Y,D1,G)
      GO TO (152,150,151),M
  150 PRINT 40
      GO TO 165
  151 PRINT 41
      GO TO 165
  152 DET=D1
      COEFTM=EE(1,1)
      COEFTN=EE(2,1)
      COEFTP=EE(3,1)
      VAR=0.0
      DO 160 I=1,N
  160 VAR=VAR + W(I)*((QS(I) - COEFTM - COEFTN*BB(I) - COEFTP*BB(I)*BB(I
     1))**2)
```

```
      VAR=VAR/FLOATF(N - 3)
      SIGM=SQRTF(((E(2,2)*E(3,3) - E(2,3)*E(3,2))/DET)*VAR)
      SIGN=SQRTF(((E(1,1)*E(3,3) - E(1,3)*E(3,1))/DET)*VAR)
      SIGP=SQRTF(((E(1,1)*E(2,2) - E(1,2)*E(2,1))/DET)*VAR)
      XM=(SIGM/COEFTM)**2
      XN=(SIGN/COEFTN)**2
      XP=(SIGP/COEFTP)**2
      XTAU=(SIGTAU/TAU)**2
  170 VSA=COEFTM + COEFTN/TAU
      SIGVSA=SQRTF((SIGM**2) + ((COEFTN/TAU)**2)*(XN + XTAU))
      XK=1.0/(1.0 + (COEFTM*TAU)/COEFTN)
      XK=XK/(1.0 - BETA)
      SIGXK=(XK**2)*ABSF((COEFTM*TAU)/COEFTN)*SQRTF(XM + XN + XTAU)
      PRINT 14,VSA,SIGVSA,XK,SIGXK,ALPHA,VAR,COEFTM,SIGM,COEFTN,SIGN,COE
     1FTP,SIGP
  164 ALPHA=ALPHA + DELAL
      IF(ALPHA - ALMAX)139,139,165
  165 RETURN
      END
```

```
      SUBROUTINE FIT2
*     LIST8
*     LABEL
CFIT2
*     SYMBOL TABLE
      DIMENSION W(50),Q(50),SIGQ(50),BB(50),P(50),PP(50),E(3,3),EE(3,3),
     1G(3),Y(3),QS(50),QQS(50)
      COMMON K1,K2,K3,K4,K5,K6,K7,K8,K9,K10,NORUN,MORE,N,W,SIGQ,P,PP,ALP
     1HA,BB,TAU,SIGTAU,Q,QS,VD,C,L1,A,SIGA,SIGB,B,BETA,DELAL,ALMAX,ZETA,
     2AFIX,SGAFIX,QQS,ALMIN
   17 FORMAT(2F8.2,1X,2F8.4,F7.3,1PE12.4,0P4F9.2,F7.1,2F7.3)
      ALPHA=ALMIN
  201 SUM1=0.0
      SUM2=0.0
      SUM3=0.0
      DO 205 I=1,N
      P(I)=1.0/(1.0 + TAU*BB(I))
  205 PP(I)=P(I) - 1.0
      DO 206 I=1,N
      SUM1=SUM1 + W(I)
      SUM2=SUM2 + W(I)*PP(I)
  206 SUM3=SUM3 + W(I)*PP(I)*PP(I)
  207 SUM4=0.0
      DO 208 I=1,N
      QS(I)=Q(I)*(1.0 + ALPHA*P(I)*(1.0 + ZETA*BB(I))) - 1.0E5*(VD*BB(I)
     1 - C*BB(I)*BB(I))
  208 SUM4=SUM4 + W(I)*QS(I)*PP(I)
      B=(SUM4 - AFIX*SUM2)/SUM3
      VAR=0.0
      DO 210 I=1,N
      BBAR=(QS(I) - AFIX)/PP(I)
  210 VAR=VAR + W(I)*((B - BBAR)**2)
      VAR=VAR/FLOATF(N - 1)
      SIGB=SQRTF(VAR/SUM1)
      VAR=0.0
      DO 211 I=1,N
  211 VAR=VAR + W(I)*(Q(I) - (VSA + 1.0E5*(VD*BB(I) - C*BB(I)*BB(I)) - V
     1SA*XK*(1.0 - BETA)*P(I))/(1.0 + ALPHA*P(I)*(1.0 + ZETA*BB(I))))**2
      VSA=AFIX - B
      XK=1.0/(1.0 - (AFIX/B))
      XK=XK/(1.0 - BETA)
      SIGVSA=SQRTF((SGAFIX**2) + (SIGB**2))
      SIGXK=(XK**2)*ABSF(AFIX/B)*SQRTF((SGAFIX/AFIX)**2 + (SIGB/B)**2)
      PRINT 17,VSA,SIGVSA,XK,SIGXK,ALPHA,VAR,AFIX,SGAFIX,B,SIGB,TAU,VD,C
      ALPHA=ALPHA + DELAL
      IF(ALPHA - ALMAX)207,207,215
  215 RETURN
      END
```

LSQHEB SAMPLE INPUT DECK

```
    5     1    11
   +1    +1    +1    +1     0     0     0     0     0     0
676.6       747.5       816.2       922.5       1009.8      1125.1      1207.8
1449.5      1591.6      746.9       1309.0
4.30        4.16        3.70        4.60        8.25        6.59        7.94
39.21       34.80       6.33        15.87
0.003100    0.003303    0.003458    0.003662    0.003926    0.004323    0.004580
0.005259    0.005781    0.003188    0.004926
0.00783     125.0       3.0         2.339       4.86
0.0         0.001       0.20        135.6       -631.5      62.9
```

APPENDIX B

CALCULATION OF LATTICE PARAMETERS

Values of some of the parameters appearing in the various expressions for the fundamental mode decay constant can be predicted theoretically, either for comparison with experimentally obtained values or for treating them as known in the analysis of experimental data. A description of the methods used to calculate these parameters is given in this appendix together with the values obtained.

B.1 FERMI AGE (τ_o)

The Fermi age for neutrons is defined as one-sixth of the mean square distance traveled by a neutron from the point of its production (zero age) to the point at which its age is τ. Experimentally, the neutron age in a particular medium (usually a moderator) is determined from observations of the neutron density at a particular energy as a function of position from a source of fast neutrons imbedded in the medium. Indium, which has a strong, isolated absorption resonance at 1.46 ev (H11) is commonly used as a detector material. The age to thermal energies is then obtained by adding a correction factor (based on a calculation) to the observed age to indium resonance.

The age cannot be measured in this way in a multiplying medium because it is impossible for a detector foil to distinguish between neutrons from the source and neutrons resulting from multiplication within the medium. But, if the volume fractions of fuel and other non-moderator constituents are small, then it is reasonable to apply correction factors to the measured value for the age in pure moderator to determine a value for the age in a multiplying medium. The following treatment, which is based on that given in Ref. G1, allows the experimentally determined age in pure D_2O to be corrected for effects due to aluminum cladding, uranium fuel, light water contamination, and density changes.

For a medium containing more than one kind of material, the age

can be written as:

$$\tau = \int_{E}^{E_o} \frac{1}{3\xi\Sigma_s\Sigma_t} \frac{dE}{E}, \tag{B.1}$$

where,

$$\Sigma_t = \Sigma_s\left(1 - \frac{2}{3}\sum_{i=1}^{M} C_i/A_i\right), \tag{B.2a}$$

$$\Sigma_s = \sum_{i=1}^{M} \Sigma_{si}, \tag{B.2b}$$

$$\xi = \frac{\sum_{i=1}^{M} \Sigma_{si}\xi_i}{\sum_{i=1}^{M} \Sigma_{si}}, \tag{B.2c}$$

$$C_i = \frac{N_i\sigma_{si}}{\Sigma_s}. \tag{B.2d}$$

In Eqs. (B.2a) - (B.2d), M is the number of components in the mixture, the subscripts s and t refer to scattering and transport, respectively, and the symbols A and N refer to atomic weight and number density, respectively. If the scattering cross sections all have the same energy dependence, Eq. (B.1) may be rewritten:

$$\frac{1}{\tau} = 3\xi\Sigma_s\Sigma_t \int_{E}^{E_o} F^2(E) \frac{dE}{E}, \tag{B.3}$$

where the function F(E) represents the energy dependence of the scattering cross sections. For a single species, assuming the scattering cross section is independent of energy (F(E) = 1), we have:

$$\frac{1}{\tau_i} = 3\xi_i\Sigma_{si}\Sigma_{ti} \ln\frac{E_o}{E}. \tag{B.4}$$

Equation (B.4) can be used to estimate the age in a material for which no experimental information is available (e.g., Fe, Al, U, etc.).

If Eqs. (B.2a) - (B.2d) are substituted into Eq. (B.3), it can be shown, after some algebraic manipulation, that:

$$\frac{10^4}{\tau} = \sum_{j=1}^{M} \sum_{i \geq j}^{M} A_{ij} c_i c_j, \tag{B.5}$$

where,

$$A_{ii} = \frac{1}{\tau_i}, \tag{B.6a}$$

$$A_{ij} = \frac{1}{\sqrt{\tau_i \tau_j}} \left[\left(\frac{1 - (2/3A_i)}{1 - (2/3A_j)} \right) \left(\frac{\xi_j}{\xi_i} \right) \right]^{1/2}$$

$$+ \frac{1}{\sqrt{\tau_i \tau_j}} \left[\left(\frac{1 - (2/3A_j)}{1 - (2/3A_i)} \right) \left(\frac{\xi_i}{\xi_j} \right) \right]^{1/2}, \tag{B.6b}$$

$$c_i = V_i \frac{\rho_i}{\rho_{io}}. \tag{B.6c}$$

In Eq. (B.6c), V_i is the volume fraction of the i^{th} component of the mixture, ρ_i is the density of the i^{th} component, and ρ_{io} is the density of the i^{th} component at the temperature for which τ_i was measured or calculated (Eq. (B.4)). The coefficients A_{ij} have been evaluated for a number of materials (G1, R1) and are listed in Table B.1 to facilitate the use of Eq. (B.5). The values for V_i may be found in the annual reports of the M. I. T. Lattice Project (H3, H4). It should be noted that a value of the age calculated from Eq. (B.4) will be somewhat in error owing to neglect of such effects as chemical binding. However, provided the volume fractions of the non-moderator constituents are a few percent or less, the effect on Eq. (B.5) may be neglected. Furthermore, the value of 125 ± 3 cm^2 for the age in pure D_2O, which is based on an experimental determination of 109 ± 3 cm^2 (W1) as the age to 1.46 ev and a correction of 16 cm^2 to thermal energies, should be changed if a newer and more accurate measurement of the age to 1.46 ev is published.

The treatment so far has taken into account only elastic scattering. The threshold for inelastic scattering in uranium is approximately 300 kev which indicates that some fission neutrons may begin the slowing down process with a partially degraded energy spectrum; hence,

TABLE B.1

Values of the Coefficients A_{ij} for Use in Eq. (B.5)[a]

Density[c] gm/cc	j \ i	H_2O	D_2O	Al	U	Cu
1.0	H_2O	323	–	–	–	–
1.1	D_2O	400	80	–	–	–
2.7	Al	110	29	0.93	–	–
18.7	U	500	120	4.9	2.4	–
8.9	Cu[b]	468	177	9.7	17.6	21.5

(a) The values for H_2O, D_2O, Al, and U are reproduced from Ref. G1.

(b) The values for Cu have been calculated from Eqs. (B.6a) and (B.6b).

(c) All calculations are based on the densities listed and all measurements are corrected to these densities.

the value of the age should be decreased slightly to take into account inelastic scattering. Galanin (G1) suggests the following formula to treat this effect:

$$\tau = \tau_o\left[1 - \left(1 - \frac{\tau_1}{\tau_o}\right)\left(\frac{\sigma_i}{\sigma_i+\sigma_e}\right)P\right], \qquad (B.7)$$

where τ_o is the age for a neutron which has not undergone an inelastic collision, τ_1 is the age for a neutron which has done so, σ_i and σ_e are the inelastic and elastic scattering cross sections, respectively, for uranium, and P is the probability that a neutron produced in a uranium rod will undergo a collision before leaving the rod. The values of the constants used in Eq. (B.7) are listed in Table B.2

The final values for the age as calculated with Eqs. (B.5) and (B.7) are given in Table B.3 for the lattices investigated in this work. The method described in this section for determining the age in a heavy water lattice is similar to that used by other workers, for example, at the Chalk River (G8) and Savannah River (D9) Laboratories and at A. B. Atomenergi (P4). The value of the age in a heavy water lattice is

TABLE B.2

Values of the Constants Used in Eq. (B.7)

Constant	Value	Source
σ_i	2.07 ± 0.51b	R1
σ_e	1.89 ± 0.04b	R1
τ_1/τ_o	0.7	G1
$P_{0.250}$ [(a)]	0.0812	R1
$P_{0.750}$	0.2102	R1
$P_{1.010}$	0.2648	R1

(a) The subscript on P refers to the rod diameter in inches.

TABLE B.3

Calculated Values of the Neutron Age τ_o

Lattice Designator	Neutron Age, cm^2
125	129 ± 3
175	125 ± 3
175A1	125 ± 3
175A1B1	125 ± 3
250	123 ± 3
250B1	123 ± 3
250B2	123 ± 3
253	128 ± 3
253A2B1	128 ± 3
350	123 ± 3
500	121 ± 3
175(2R)[(a)]	125 ± 3
	125 ± 3
500(2R)	122 ± 3
	121 ± 3
MOD	125 ± 3

(a) See footnote (b) to Table 3.1.

not very different from that in pure heavy water provided the volume fraction of the non-moderator constituents in the lattice is small. Differences in the calculated values of the age among different laboratories result primarily because of differences in the value of the age in pure heavy water; e.g., 120 cm^2 at Savannah River (D9) and 130 cm^2 at A. B. Atomenergi (P4).

B.2 EFFECTIVE DELAYED NEUTRON FRACTION (β)

It has been shown in Chaps. II and IV that the effect of delayed neutrons may be neglected for the lattices studied in this work provided the multiplication factor used refers only to "prompt" neutrons:

$$k_p = k_\infty(1-\beta). \tag{B.8}$$

Values of k_∞ are inferred from measured values of the prompt neutron multiplication factor by dividing by the quantity $(1-\beta)$ where β is the effective fraction of neutrons whose appearance in the assembly is delayed relative to that of the prompt neutrons.

The parameter β is widely used in kinetics work and considerable effort has been expended in obtaining theoretical and experimental values for it. Malaviya (M1) has surveyed the various determinations of β and recommends a value of $\beta = (0.783 \pm 0.018) \times 10^{-2}$ as appropriate for systems of partially enriched uranium metal and heavy water.

B.3 ABSORPTION CROSS SECTION ($\overline{v\Sigma}_a$)

One of the parameters which is readily obtained from a set of pulse neutron experiments is the product of neutron velocity and macroscopic absorption cross section, weighted by the neutron density and averaged over a unit cell:

$$\overline{v\Sigma}_a = \frac{\int_{\vec{r}} d\vec{r} \int_v dv\, v\Sigma_a(\vec{r}, v) n(\vec{r}, v)}{\int_{\vec{r}} d\vec{r} \int_v dv\, n(\vec{r}, v)} . \tag{B.9}$$

This quantity can be calculated with the aid of the THERMOS code (H9). The numerator and denominator of Eq. (B.9) are each evaluated separately by the code and the quantity $\overline{v\Sigma}_a$ is just the ratio of these two

quantities. In the case of the absorber modified lattices, it is necessary to use the TULIP code (H1) which normalizes the results of THERMOS calculations centered on a fuel rod and on an added absorber rod, respectively.

The calculated values of $\overline{v\Sigma}_a$ are listed in Table B.4 for the lattices studied in this work.

B.4 DIFFUSION COEFFICIENT ($\overline{vD}_o$)

The THERMOS and TULIP codes can also be used to calculate values of the velocity averaged diffusion coefficient in these lattices. This quantity is defined in a manner similar to that for the absorption cross section:

$$\overline{vD}_o = \frac{\int_{\vec{r}} d\vec{r} \int_v dv\, vD_o(\vec{r}, v) n(\vec{r}, v)}{\int_{\vec{r}} d\vec{r} \int_v dv\, n(\vec{r}, v)} . \qquad \text{(B.10)}$$

It is sometimes argued (M1) that the value obtained for this quantity from a pulsed neutron experiment on pure moderator can be taken as the value for a lattice with the same moderator provided that: (1) the macroscopic transport cross sections of fuel and moderator are similar; and (2) that the volume fraction of fuel is small. Although both criteria are satisfied by the heavy water lattices studied at M.I.T., the assumption that $\overline{vD}_o$ remains constant from pure moderator to a lattice is not valid because the addition of fuel (or other strong absorber) may significantly harden the neutron spectrum relative to that existing in pure moderator. This effect causes $\overline{vD}_o$ to increase when an absorbing material is added to a moderating medium.

The calculation of $\overline{vD}_o$ with the aid of THERMOS is slightly more involved than the corresponding calculation of $\overline{v\Sigma}_a$. We define the following integrals:

$$I_{1j} = \int d\vec{r}_j \int dv\, n(\vec{r}_j, v), \qquad \text{(B.11a)}$$

$$I_{2j} = \int d\vec{r}_j \int dv\, vn(\vec{r}_j, v), \qquad \text{(B.11b)}$$

$$I_{3j} = \frac{\int d\vec{r}_j \int dv\ vD_o(\vec{r}_j, v)\ n(\vec{r}_j, v)}{\int d\vec{r}_j \int dv\ vn(\vec{r}_j, v)}\ , \qquad \text{(B.11c)}$$

where the index j refers to a particular constituent of the unit cell. Since the contribution by the non-moderator constituents is small, we can approximate the numerator of Eq. (B.10) for these constituents by:

$$\int d\vec{r}_j \int dv\ vD_o(\vec{r}_j, v)\, n(\vec{r}_j, v) \approx \frac{I_{2j}}{3[\bar{\Sigma}_{sj}(1-\bar{\mu}_j)+\bar{\Sigma}_{aj}]}\ . \qquad \text{(B.12)}$$

The integral I_{3j} for a water moderator is evaluated directly by the EDIT subroutine (M.I.T. version) in THERMOS. Hence, for M homogeneous regions in the unit cell (with the M^{th} region being moderator) Eq. (B.10) becomes:

$$\overline{vD}_o = \frac{\sum_{j=1}^{M-1}\left(\frac{I_{2j}}{3[\bar{\Sigma}_{sj}(1-\bar{\mu}_j)+\bar{\Sigma}_{aj}]}\right) + I_{2M}I_{3M}}{\sum_{j=1}^{M} I_{1j}}\ . \qquad \text{(B.13)}$$

The values of $\overline{vD}_o$ calculated according to Eq. (B.13) are given in Table B.4. All values are based on a moderator temperature of 20°C and the D_2O purities listed in Table 3.1. The last column in Table B.4 contains the theoretical values of L^2 ($= \overline{vD}_o/\overline{v\Sigma}_a$), the thermal diffusion area.

In analyzing the data obtained in this investigation, the intent has been to work with experimental values of quantities whenever possible. However, experimental determinations of $\overline{vD}_o$ in these lattices have not, as yet, been reported and thus one must either consider $\overline{vD}_o$ as an unknown quantity to be determined from the pulsed neutron experiment or treat $\overline{vD}_o$ as known on a "quasi-experimental" basis. The latter method was used in the data analysis and it is described below.

By "quasi-experimental" is meant the correction of the experimental value of $\overline{vD}_o$ in pure moderator by the theoretical value from THERMOS which takes spectral hardening into account. Thus, if we use the superscripts e and t to represent experimental (or "quasi-experimental") and theoretical, respectively, and the subscripts m

TABLE B.4

Values of the Absorption Cross Section $\overline{v\Sigma}_a$, Diffusion Coefficient $\overline{vD}_o$, and Thermal Diffusion Area L^2 Calculated by THERMOS[a]

Lattice Designator	D_2O Purity Mole %	Absorption Cross Section $\overline{v\Sigma}_a$, sec^{-1}	Diffusion Coefficient $\overline{vD}_o$, $cm^2 sec^{-1} \times 10^{-5}$	Thermal Diffusion Area L^2, cm^2
125	99.60	3376.6	2.590	76.70
175	99.53	1716.4	2.327	135.6
175A1	99.53	2442.1	2.406	98.52
175A1B1	99.53	2834.5	2.452	86.51
250	99.56	840.9	2.194	260.9
250B1	99.56	1076.0	2.220	206.3
250B2	99.56	1265.2	2.244	177.4
253	99.51	5312.5	2.694	50.71
253A2B1	99.51	6611.0	2.789	42.19
350	99.47	2530.3	2.370	93.66
500	99.47	1182.4	2.206	186.6
175(2R)[b]	99.53	1615.9	2.320	143.6
		1716.4	2.327	135.6
500(2R)[b]	99.47	1687.3	2.370	140.5
		1182.4	2.206	186.6
MOD	99.47	31.62	2.063	6524.0

(a) All calculations are based on a moderator temperature of 20°C.

(b) See footnote (b) to Table 3.1.

and ℓ to represent moderator and lattice, respectively, we may write:

$$\overline{vD}^{e}_{\ell} = \overline{vD}^{e}_{m} + \overline{vD}^{t}_{\ell} - \overline{vD}^{t}_{m}. \tag{B.14}$$

That the theoretical correction should be linear may be seen from Fig. B.1 in which the values of $\overline{vD}_o$ calculated by THERMOS are plotted as a function of fuel to moderator volume ratio for each of two different enrichments. It is evident that the predicted variation of $\overline{vD}_o$ as a function of V_f/V_m is linear. Thus, by assuming that the slopes of the curves in Fig. B.1 remain constant for small changes in temperature and D_2O purity, it is possible to obtain $\overline{vD}^{e}_{\ell}$ by correcting $\overline{vD}^{e}_{m}$ (the experimental value of vD_o in pure moderator) to the appropriate temperature and purity and applying the spectral change computed by THERMOS.

The results obtained for $\overline{vD}^{e}_{\ell}$ are listed in Table B.5. A value is quoted for each of the three computer codes (FRAUD, EXPO, and STRIP) used to determine a value for the fundamental mode decay constant. The corrections for D_2O temperature and purity were given earlier in Sec. 5.7. They are repeated here:

$$\frac{\Delta\overline{vD}^{e}_{m}}{\Delta T} = 0.0055 \text{ cm}^2/\text{sec } ^\circ\text{C}, \tag{B.15a}$$

$$\frac{1}{\overline{vD}^{e}_{m}} = \frac{f}{\overline{vD}^{e}_{D_2O}} + \frac{1-f}{\overline{vD}^{e}_{H_2O}}, \tag{B.15a}$$

where $\overline{vD}^{e}_{D_2O}$ and $\overline{vD}^{e}_{H_2O}$ are the experimental values of $\overline{vD}_o$ in pure D_2O and H_2O, respectively, and f is the mole fraction of D_2O.

B.5 SLOWING DOWN TIME (T_o)

An important parameter appearing in an age-diffusion analysis of the pulsed source experiment is the fission neutron slowing down time, T_o. It is defined as the elapsed time between the production of a high energy ($\approx$2 Mev) fission neutron and its appearance as a thermal neutron in a system of infinite extent. Such a definition is rather arbitrary, depending on when a neutron is considered to be "thermalized." An analogous problem arises in multigroup theory when one decides

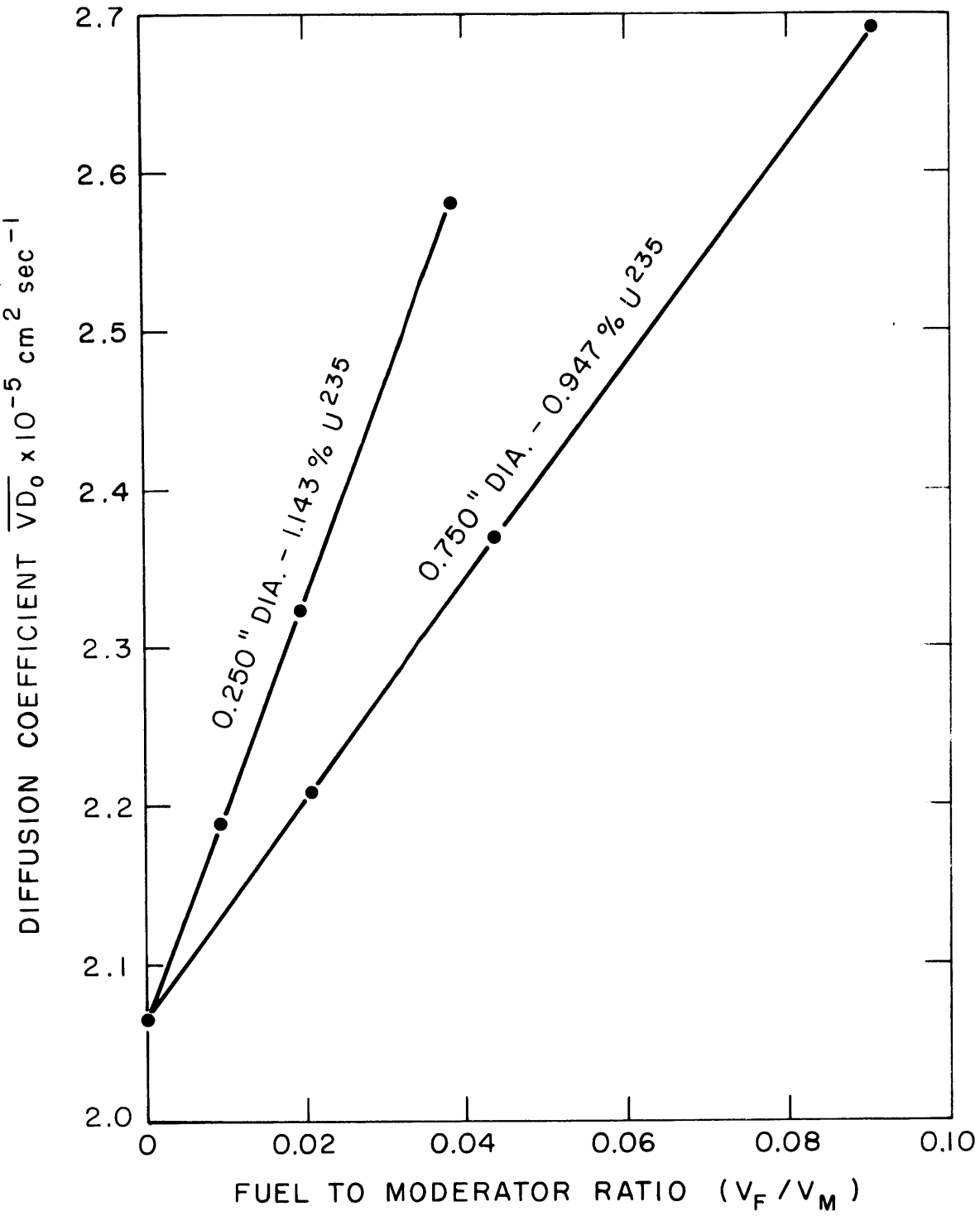

FIG. B.1 THEORETICAL VALUES OF THE DIFFUSION COEFFICIENT, $\overline{VD_o}$, AS A FUNCTION OF FUEL TO MODERATOR VOLUME RATIO, V_F/V_M

TABLE B.5

Corrected Experimental Values of the Diffusion Coefficient $\overline{vD}_o$

Lattice Designator	Temperature (°C)	D_2O Purity (Mole %)	Diffusion Coefficient $\overline{vD}_o$, $cm^2 sec^{-1} \times 10^{-5}$		
			FRAUD	EXPO	STRIP
125	27	99.60	2.603	2.574	2.545
175	27	99.53	2.339	2.310	2.281
175A1	25	99.53	2.418	2.389	2.360
175A1B1	23	99.53	2.454	2.425	2.396
250	24	99.56	2.190	2.161	2.132
250B1	23	99.56	2.210	2.180	2.152
250B2	23	99.56	2.233	2.204	2.175
253	24	99.51	2.690	2.661	2.632
253A2B1	24	99.51	2.785	2.756	2.727
350	26	99.47	2.378	2.349	2.320
500	24	99.47	2.203	2.174	2.145
175(2R)[a]	23	99.53	2.310	2.281	2.252
			2.317	2.288	2.259
500(2R)[a]	25	99.47	2.373	2.344	2.315
			2.209	2.180	2.151
MOD	25	99.47	2.067	2.039	2.018

(a) See footnote (b) to Table 3.1.

arbitrarily on the energy boundary between groups.

One way of determining a value of T_o divides the time range into two parts. The first part is called the moderating time and is defined as the time required for a fission neutron to slow down to the cutoff of the moderating region (customarily taken to be the cadmium cutoff at 0.4 ev). Above this energy the effect of chemical binding on the slowing down process can be neglected and a straightforward relation between the moderating time and cutoff velocity results (L1):

$$T_m = \frac{2}{\xi \Sigma_s}\left[\frac{1}{v_m} - \frac{1}{v_o}\right] \approx \frac{2}{\xi \Sigma_s v_m}, \qquad \text{(B.16)}$$

since $v_o \gg v_m$ where v_o is the initial velocity. A value for T_m can also be obtained experimentally by observing the time dependence of capture gamma rays from cadmium following the introduction of a fast neutron burst. The experimental value of 10.5 ± 1.0 μsec (P6) in D_2O is slightly smaller than the value of 12.9 μsec obtained from Eq. (B.16). The difference is not considered significant in view of the much longer time spent in the thermalization region to be discussed next.

The second part of the slowing down time is called the thermalization time and is defined as the time required for a fission neutron to slow down from the cutoff of the moderating region to the thermal energy region. An analytical description of the neutron slowing down process in this region is extremely difficult because of effects such as chemical binding which decrease the effective mass of the scattering nuclei and permit up- as well as down-scattering.

The neutron temperature concept, first used in pulsed-source work by von Dardel (D1), has gained wide acceptance as an experimental means for studying the thermalization process. In this approximation, it is assumed that the neutrons entering the thermalization region have a Maxwellian energy distribution characterized by a temperature θ_m which is greater than the moderator temperature θ_o; the distribution then cools exponentially to the moderator temperature. Thus, we may write:

$$\theta(t) = \theta_o + (\theta_m - \theta_o)e^{-t/T_{th}}, \qquad \text{(B.17)}$$

where the quantity T_{th} is called the thermalization time constant. On

this model, the neutron pulse takes an infinite length of time to achieve equilibrium with the moderator atoms. The thermalization time constant may be considered as a measure of the time required to attain equilibrium and, hence, we have:

$$T_o = T_m + T_{th}. \tag{B.18}$$

The addition of T_m and T_{th} to obtain T_o is slightly inconsistent in that T_m is an average time while T_{th} is a relaxation time. But, since the magnitude of the effect on the prompt neutron decay constant is only a few per cent, this inconsistency may be neglected.

Experimentally, estimates of T_{th} can be obtained by measuring the time dependence of neutron transmission through 1/v absorbers of varying thicknesses. Such data on heavy water is sparse although a value of 33 ± 4 μsec has recently been reported by Moller (M4). Von Dardel (D2) has previously obtained a value of 60 ± 15 μsec(*).

One can also turn to a theoretical model to estimate T_{th}. Nelkin (N1) introduced the concept of the mean square energy transfer, M_2, defined by:

$$M_2 = \int_0^\infty dE \int_0^\infty dE'(E'-E)^2 \Sigma_s(E\rightarrow E') M(E), \tag{B.19}$$

where M(E) is the Maxwellian energy distribution, and showed that M_2 could be related to T_{th}^o:

$$T_{th}^o = \frac{3\sqrt{\pi}}{2v_o M_2}, \tag{B.20}$$

where the superscript "o" refers to an infinite medium. A relation between T_{th}^o and T_{th} has been derived (A1):

$$\frac{1}{T_{th}} = \frac{\overline{v}DB^2}{3} + \frac{1}{T_{th}^o}, \tag{B.21}$$

which slightly decreases the value of the thermalization time constant

(*) This value and its associated uncertainty are estimates based on a plot of neutron temperature as a function of time which appears in Ref. D2.

in a finite medium relative to that in an infinite medium. The correction factor amounts to no more than 2% in the systems studied here and may be neglected relative to the uncertainties in T^o_{th}.

Beckurt's (B2) treatment of diffusion cooling leads to an expression for T^o_{th} in terms of the diffusion and diffusion cooling coefficients:

$$T^o_{th} = \frac{6C}{(\overline{vD}_o)^2} . \qquad \text{(B.22)}$$

In the absence of consistent experimental values for T^o_{th}, Eq. (B.22) is preferred because it is based on parameters directly obtainable from a pulsed neutron experiment on pure moderator. As pointed out in Sec. 5.7, it was not possible to obtain a reasonable value of C in this work. But, a reasonable estimate for C can be obtained from a weighted average of the first five values listed in Table 5.28, all of which are reported at similar D_2O temperatures and purities. With the value obtained in the present work, the diffusion parameters of 100% D_2O at 20°C are:

$$\overline{vD} = (2.088 \pm 0.018) \times 10^5 \text{ cm}^2\text{sec}^{-1},$$

$$C = (4.53 \pm 0.27) \times 10^5 \text{ cm}^4\text{sec}^{-1},$$

which, when inserted in Eq. (B.22), yields:

$$T^o_{th} = 63 \pm 4 \ \mu\text{sec}.$$

If we use the experimental value of 10.5 ± 1 μsec quoted earlier for the moderation time, T_m, we obtain an estimate for the total neutron slowing down time in 100% D_2O at 20°C:

$$T_o = T_m + T^o_{th} = 74 \pm 4 \ \mu\text{sec}.$$

Since the parameter T_o appears in the expression for the decay constant only when there is neutron multiplication in the assembly, it is desirable to obtain values of T_o in these assemblies. As a first approximation, one might use the above value of T_o on the basis that the spectral hardening caused by absorption in fuel and other absorbers is not significant. As illustrated in Table B.4, the presence of fuel and added absorber can increase $\overline{vD}_o$ by as much as 35% in the lattices studied here so that spectral hardening is significant. One would

therefore expect the neutron slowing down time to decrease somewhat as the amount of spectral hardening increases. A better approximation is to assume that the ratio $C/\overline{vD}_o$ remains constant with changes in the spectrum. This is equivalent to saying that the percentage decrease in neutron leakage because of diffusion cooling is not influenced by changes in the neutron spectrum. Then the decrease in T_o, as reflected in a smaller value of the thermalization time constant, can be obtained from the calculated increase in $\overline{vD}_o$ (relative to the value in pure moderator).

The constancy of $C/\overline{vD}_o$ in the presence of increasing absorption cannot be verified experimentally because little, if any, effort has been made to date to obtain values of C in multiplying assemblies. The reason is that the contribution of the diffusion cooling term to the decay constant is extremely small (less than 1%) in subcritical assemblies of practical size. There has been some recent experimental and theoretical work on the changes in $\overline{vD}_o$ and C with moderator temperature in pure moderator. An increase in moderator temperature causes the average neutron velocity to increase by shifting the entire spectrum to higher velocities while an increase in 1/v absorption increases the average neutron velocity by depressing the lower velocity portion of the spectrum. Although the means by which the spectrum is hardened are different in the two cases, it is not clear that the change in C should be different in the two cases. Thus, it is assumed that data on the variation of the ratio $C/\overline{vD}_o$ with temperature in pure moderator can be taken as indicative of the variation of $C/\overline{vD}_o$ with the amount of absorption in multiplying assemblies. Experimental and theoretical determinations of $\overline{vD}_o$ and C as functions of temperature are listed in Table B.6. The last column gives calculated values of $C/\overline{vD}_o$. Over a wide range of experimental temperatures, it is seen that $C/\overline{vD}_o$ remains constant within the limits of experimental error. The calculations of Honeck and Michael (H10) also confirm this result although their values of C are lower, in general, than the experimental values. The constancy of $C/\overline{vD}_o$ with spectrum changes appears to be a justifiable assumption and we write the thermalization time constant for a lattice as:

$$\left(T^o_{th}\right)_\ell = \left(T^o_{th}\right)_m \frac{\overline{vD}_m}{\overline{vD}_\ell}, \qquad \text{(B.23)}$$

TABLE B.6

Values of the Diffusion Coefficient $\overline{vD}_o$, Diffusion Cooling Coefficient C, and the Ratio $(C/\overline{vD}_o)$ as Functions of Temperature in Pure D_2O

Author	Temperature (°C)	Diffusion Coefficient $\overline{vD}_o$, $cm^2 sec^{-1} \times 10^{-5}$	Diffusion Cooling Coefficient C, $cm^4 sec^{-1} \times 10^{-5}$	The Ratio $C/\overline{vD}_o$ cm^2
(a) Daughtry and Waltner (D4)	25	1.983 ± 0.029	4.65 ± 0.54	2.34 ± 0.27
	50	2.189 ± 0.035	6.39 ± 0.74	2.92 ± 0.34
	75	2.331 ± 0.040	7.08 ± 0.85	3.04 ± 0.36
	100	2.473 ± 0.045	7.47 ± 1.02	3.02 ± 0.41
	125	2.582 ± 0.050	7.43 ± 1.16	2.88 ± 0.49
	150	2.714 ± 0.056	7.69 ± 1.32	2.83 ± 0.49
	170	2.906 ± 0.063	8.83 ± 1.53	3.04 ± 0.53
	200	3.053 ± 0.070	9.26 ± 1.76	3.03 ± 0.58
	225	3.246 ± 0.078	10.16 ± 2.05	3.13 ± 0.63
	250	3.517 ± 0.088	12.41 ± 2.43	3.53 ± 0.69
(b) Honeck and Michael (H10)	20	2.054	4.73	2.30
	77	2.354	5.31	2.26
	127	2.658	6.05	2.28
	177	3.011	7.43	2.47

(a) Experimental
(b) Theoretical

where the subscripts ℓ and m refer to lattice and moderator, respectively.

The final values for T_o, based on Eqs. (B.18) and (B.23), are given in Table B.7. Values of the diffusion cooling coefficient, C, are also given.

B.6 FAST REMOVAL CROSS SECTION ($\overline{v_1\Sigma}_1$)

The fast removal cross section, $\overline{v_1\Sigma}_1$, appears in the expression for the prompt neutron decay constant when a two-group analysis of the pulsed neutron source experiment is used. As in the case of the slowing down time, this quantity has not been measured experimentally. In fact, it is often treated as a parameter which is adjusted to "force" agreement between theory and experiment. Since the ratio of fast to thermal neutron lifetimes is usually only a few percent in the assemblies studied here, it seems reasonable to calculate $\overline{v_1\Sigma}_1$ on the basis of a simple model. It can be shown that the fast removal cross section in two-group theory is given by the following expression (K1):

$$\overline{v_1\Sigma}_1 = \frac{\overline{v_1\Sigma}_{s1}}{\frac{1}{\xi}\ln\frac{E_o}{E_c}}, \tag{B.24}$$

where E_o and E_c are the upper and lower limits, respectively, of the fast energy group. The quantity $\overline{v_1\Sigma}_{s1}$ is averaged over the neutron density:

$$\overline{v_1\Sigma}_{s1} = \frac{\int_{E_c}^{E_o} v(E)\,\Sigma_{s1}(E)\,n(E)\,dE}{\int_{E_c}^{E_o} n(E)\,dE}. \tag{B.25}$$

If we assume that, over the energy range of the fast group, $\Sigma_s(E)$ is constant and the neutron flux exhibits the familiar 1/E-dependence, Eq. (B.25) becomes:

TABLE B.7

Values of the Diffusion Cooling Coefficient C, Thermalization Time Constant T^o_{th}, and Fission Neutron Slowing Down Time T_o

Lattice Designator	Diffusion Cooling Coefficient C, $cm^4 sec^{-1} \times 10^{-5}$	Thermalization Time Constant T^o_{th}, μsec	Slowing Down Time T_o, μsec
125	5.43 ± 0.33	50 ± 4	60 ± 4
175	4.86 ± 0.30	56 ± 4	66 ± 4
175A1	4.99 ± 0.30	54 ± 4	64 ± 4
175A1B1	5.11 ± 0.31	53 ± 4	64 ± 4
250	4.56 ± 0.28	60 ± 4	70 ± 4
250B1	4.60 ± 0.28	59 ± 4	70 ± 4
250B2	4.65 ± 0.28	59 ± 4	69 ± 4
253	5.61 ± 0.34	48 ± 4	59 ± 4
253A2B1	5.81 ± 0.35	47 ± 4	58 ± 4
350	4.94 ± 0.30	55 ± 4	66 ± 4
500	4.58 ± 0.28	59 ± 4	70 ± 4
175(2R)[(a)]	4.86 ± 0.30	57 ± 4	67 ± 4
	4.86 ± 0.30	57 ± 4	67 ± 4
500(2R)[(a)]	4.93 ± 0.30	55 ± 4	66 ± 4
	4.58 ± 0.28	59 ± 4	70 ± 4
MOD	4.43 ± 0.27	63 ± 4	74 ± 4

(a) See footnote (b) to Table 3.1.

$$\overline{v_1\Sigma}_{s1} = \frac{\Sigma_{s1} \int_{E_c}^{E_o} v(E) \frac{\phi_o}{v(E)\,E}\, dE}{\int_{E_c}^{E_o} \frac{\phi_o}{v(E)\,E}\, dE}$$

$$= \frac{v_c \Sigma_{s1}}{2} \ln \frac{E_o}{E_c} . \qquad \text{(B.26)}$$

Inserting Eq. (B.26) in Eq. (B.24), we obtain the desired expression:

$$\overline{v_1\Sigma}_1 = \frac{\xi v_c \Sigma_{s1}}{2} . \qquad \text{(B.27)}$$

The lower limit of the fast group is usually taken to be 5 kT (0.126 ev) which corresponds to a neutron velocity of 4.91×10^5 cm/sec. For 99.47% D_2O, we have the following constants:

$$\xi = 0.521,$$
$$\Sigma_{s1} = 0.353 \text{ cm}^{-1},$$

which yields:

$$\overline{v_1\Sigma}_1 = 4.44 \times 10^4 \text{ sec}^{-1}.$$

For a medium composed of more than one material, it is assumed that $\overline{v_1\Sigma}_1$ can be obtained by suitable averaging of ξ and Σ_{s1} over the constituents of the medium. The final values of ξ, Σ_{s1}, and $\overline{v_1\Sigma}_1$ are listed in Table B.8.

TABLE B.8

Values of the Average Change in Lethargy ξ, Fast Scattering Cross Section Σ_{s1}, and Fast Removal Cross Section $\overline{v_1\Sigma_1}$

Lattice Designator	Average Change in Lethargy ξ	Fast Scattering Cross Section Σ_{s1}, cm^{-1}	Fast Removal Cross Section $\overline{v_1\Sigma_1}$, $sec^{-1} \times 10^{-4}$
125	0.494	0.348	4.23
175	0.505	0.350	4.34
175A1	0.496	0.353	4.30
175A1B1	0.491	0.355	4.28
250	0.510	0.352	4.41
250B1	0.509	0.352	4.40
250B2	0.506	0.353	4.39
253	0.468	0.353	4.06
253A2B1	0.458	0.356	4.01
350	0.491	0.353	4.26
500	0.504	0.353	4.37
175(2R)[(a)]	0.505	0.350	4.34
	0.505	0.350	4.34
500(2R)[(a)]	0.494	0.353	4.28
	0.504	0.353	4.37
MOD	0.512	0.353	4.44

(a) See footnote (b) to Table 3.1.

APPENDIX C

DETERMINATION OF HIGHER MODE DECAY CONSTANTS AND COEFFICIENTS

The FRAUD code, which has been described in Secs. 4.1.2 and A.3, assumes that the neutron density as a function of time following the injection of a burst of fast neutrons may be represented as the sum of two exponential functions (after subtracting the constant background):

$$n(t) = A_1 e^{-\lambda_1 t} + A_2 e^{-\lambda_2 t}. \tag{C.1}$$

The purpose of this appendix is to test the validity of this assumption by including values of λ_2 in the least-squares fit of the λ as a function of B^2 data and to compare the experimental values of the ratio (A_2/A_1) to the theoretical values of this quantity derived from the analysis presented in Chap. II. The following discussion is based on results from the 500 lattice.

C.1 THE NEXT HIGHER MODE DECAY CONSTANT

The inclusion of a value of the next higher mode decay constant λ_2 (denoted here by λ_{nm}), obtained from FRAUD in the λ as a function of B^2 least-squares fit, requires that the corresponding value of the separation constant B_2^2 (denoted by B_{nm}^2) be determined. First, from an examination of the expression for λ_{nm} derived in Chap. II,

$$\lambda_{nm} = \overline{v\Sigma_a} + \overline{vD}B_{nm}^2 - \overline{v\Sigma_a}(1-\beta)\, k_\infty P_1(B_{nm}^2), \tag{C.2}$$

it is evident that the magnitude of λ_{nm} increases as the magnitude of B_{nm}^2 increases ($P_1(B_{nm}^2$ decreases as B_{nm}^2 increases) and hence, the next higher mode value of λ_{nm} obtained from FRAUD ($\equiv\lambda_2$) corresponds to the next smallest value of B_{nm}^2 ($\equiv B_2^2$). For a medium of cylindrical shape, the expression for B_{nm}^2 is:

$$B_{nm}^2 = \left(\frac{\alpha_n}{R}\right)^2 + \left(\frac{m\pi}{H}\right)^2, \tag{C.3}$$

where,

$$m = 1, 2, 3, \ldots$$
$$\alpha_n = 2.405, 5.520, \ldots \quad . \tag{C.3a}$$

The smallest value of B^2_{nm} ($\equiv B^2_{11}$) has been defined previously as the geometric buckling of the medium. Depending on the relative values of R and H, the next smallest value of B^2_{nm} is either B^2_{12} or B^2_{21}. However, from the expression for the spatial dependence of the nm^{th} mode,

$$F_{nm}(r, z) = J_o(\alpha_n r) \sin\left(\frac{m\pi z}{H}\right), \tag{C.4}$$

it is evident that, at the location of the detector (r=0; z=H/2), the contribution to the neutron density by the nm^{th} mode is zero for even values of m. Therefore, the value of λ_2 obtained from FRAUD corresponds either to B^2_{21} or B^2_{13}.

Figure C.1 shows the variation of B^2_{nm} as a function of moderator height H for the 500 lattice (R = 62.66 cm). Separate curves are shown for B^2_{11}, B^2_{21}, and B^2_{13}. For values of H greater than 112 cm, $B^2_{13} < B^2_{21}$, and for values of H less than 112 cm, $B^2_{21} < B^2_{13}$. This result is incorporated in Table C.1 which lists the experimental values of λ_1 and λ_2 along with the corresponding values of B^2_1 ($\equiv B^2_{11}$) and B^2_2 ($\equiv B^2_{21}$ or B^2_{13}).

The decay constants λ_1 and λ_2 were analyzed according to the two-group method described in Sec. 4.2. The results were:

$$k_\infty = 1.385 \pm 0.023,$$
$$\overline{v\Sigma_a} = 1088.4 \pm 38.1 \text{ sec}^{-1}.$$

The uncertainties are based on the standard deviations of the least-squares coefficients. For comparison, the values of k_∞ and $\overline{v\Sigma_a}$ obtained from an analysis of the fundamental mode decay constants only are transcribed from Tables 5.15a and 5.15b:

$$k_\infty = 1.379 \pm 0.012,$$
$$\overline{v\Sigma_a} = 1159.3 \pm 22.3 \text{ sec}^{-1}.$$

The variation of the measured decay constants listed in Table C.1

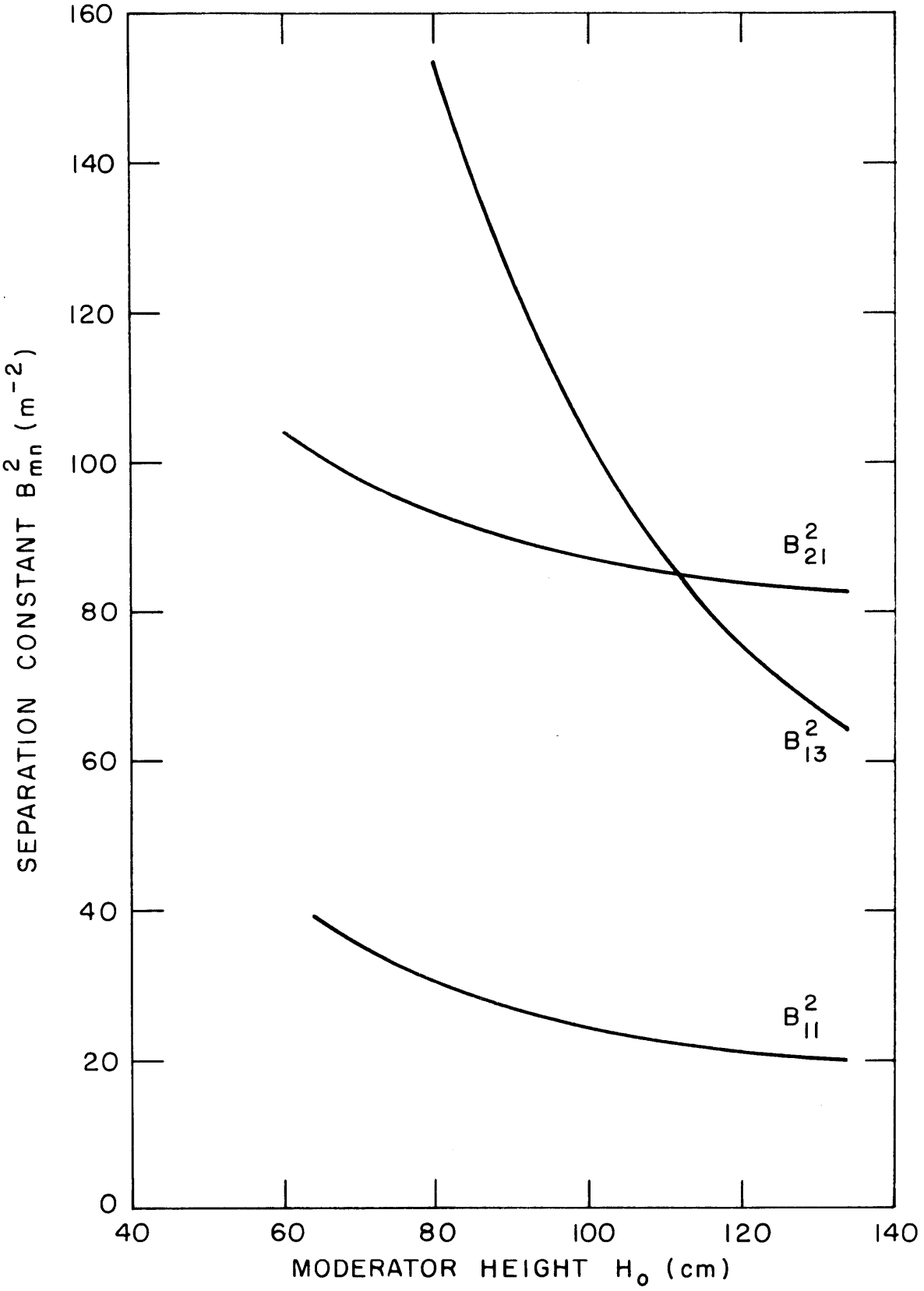

FIG. C.1 THE SEPARATION CONSTANT B^2_{mn} AS A FUNCTION OF MODERATOR HEIGHT H_o FOR THE 500 LATTICE

TABLE C.1

Measured Fundamental and Next Higher Mode Decay Constants λ_1 and λ_2, Coefficients A_1 and A_2, and Calculated Separation Constants B_1^2 and B_2^2 as Functions of Moderator Height H for the 500 Lattice

Moderator Height H, cm	Fundamental Mode			Next Higher Mode		
	Decay Constant λ_1, sec^{-1}	Coefficient A_1	Separation Constant B_1^2, m^{-2}	Decay Constant λ_2, sec^{-1}	Coefficient A_2	Separation Constant B_2^2, m^{-2}
132.0	324.3 ± 1.5	10314 ± 60	20.36	1578.6 ± 20.9	-16297 ± 364	65.60
115.0	382.3 ± 3.7	10660 ± 170	22.16	1913.9 ± 49.4	-17728 ± 1541	81.80
101.2	450.6 ± 3.5	9921 ± 144	24.34	2176.7 ± 172.8	-15040 ± 2595	86.88
91.7	517.1 ± 3.9	9940 ± 143	26.44	2513.1 ± 199.2	-16870 ± 6318	88.98
84.6	587.5 ± 6.4	10362 ± 230	28.49	2036.0 ± 54.1	-9049 ± 482	91.03
78.6	658.4 ± 9.0	12371 ± 343	30.68	2066.7 ± 829.4	-9567 ± 9020	93.22
73.4	723.7 ± 3.3	9734 ± 68	33.02	2237.2 ± 38.5	-7767 ± 173	95.56
69.7	782.7 ± 6.8	9489 ± 181	35.02	2107.5 ± 174.7	-5664 ± 837	97.76
65.9	857.6 ± 10.5	9101 ± 275	37.43	2412.9 ± 142.3	-6812 ± 739	99.97
63.2	928.1 ± 4.6	10479 ± 91	39.41	2311.6 ± 60.8	-6939 ± 244	101.95
60.5	969.3 ± 9.2	9542 ± 167	41.66	2556.5 ± 66.2	-6547 ± 244	104.20

as a function of separation constant is shown in Fig. C.2. The solid line is the fitted expression for λ based on values of λ_1 only, and the dashed line is the fitted expression based on values of λ_1 and λ_2.

C.2 THE RATIO (A_2/A_1)

The fitted coefficients A_1 and A_2 obtained from FRAUD are also tabulated in Table C.1. It is desired to compare the experimental ratio (A_2/A_1) with that predicted theoretically. The definition of the nm^{th} mode coefficient is repeated from Chap. II:

$$A_{nm} = C_{nm} F_{nm}(r, z) e^{-(\Lambda_{nm} - \lambda_{nm})T_o}, \tag{C.5}$$

where,

$$C_{nm} = \frac{\int_{r,z} S'(r, z) F_{nm}(r, z)\, dr\, dz}{\int_{r,z} F_{nm}^2(r, z)\, dr\, dz}, \tag{C.5a}$$

$$\Lambda_{nm} = \langle vD \rangle B_{nm}^2 + \langle vD \rangle \left\langle \frac{\Sigma_a}{D} \right\rangle, \tag{C.5b}$$

$$T_o = \frac{\tau_o}{\langle vD \rangle}. \tag{C.5c}$$

If Eqs. (C.5b), (C.5c), and (C.2) are inserted in Eq. (C.5), the ratio (A_2/A_1) may be written as:

$$\frac{A_{nm}}{A_{11}} = \frac{C_{nm}}{C_{11}} \frac{F_{nm}}{F_{11}} e^{-\tau_o\left(B_{nm}^2 - B_{11}^2\right)} e^{-\overline{v\Sigma_a}(1-\beta)k_\infty T_o (P_{nm} - P_{11})}. \tag{C.6}$$

The evaluation of the source expansion coefficients C_{nm} and C_{11} is carried out using Eq. (C.5a) with the expression for $S'(r, z)$ derived in Sec. 2.2.1. The integral in the numerator of Eq. (C.5a) is evaluated numerically. Values of $(F_{nm}(r,z)/F_{11}(r,z))$ and B_{nm}^2 are calculated from Eqs. (C.4) and (C.3), respectively, and the determination of the rest of the quantities in Eq. (C.6) has been described previously.

Figure C.3 illustrates the variation of the ratios (A_{21}/A_{11}) and (A_{13}/A_{11}) as functions of the moderator height evaluated from Eq. (C.6). Also shown are the experimental values of the ratio (A_2/A_1) calculated from the results given in Table C.1.

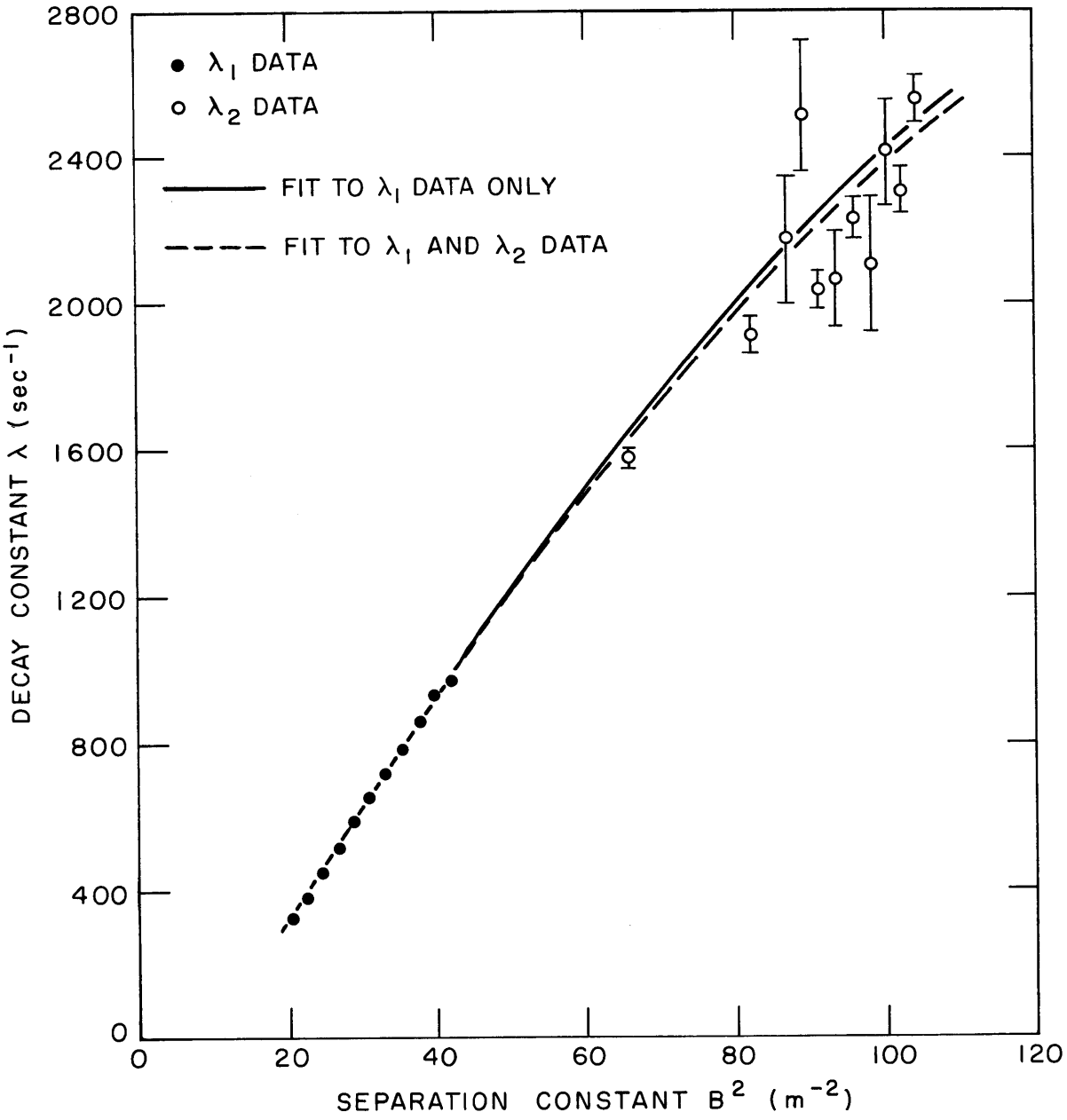

FIG. C.2 MEASURED DECAY CONSTANTS λ_1 AND λ_2 AS FUNCTIONS OF SEPARATION CONSTANTS B_1^2 AND B_2^2 FOR THE 500 LATTICE

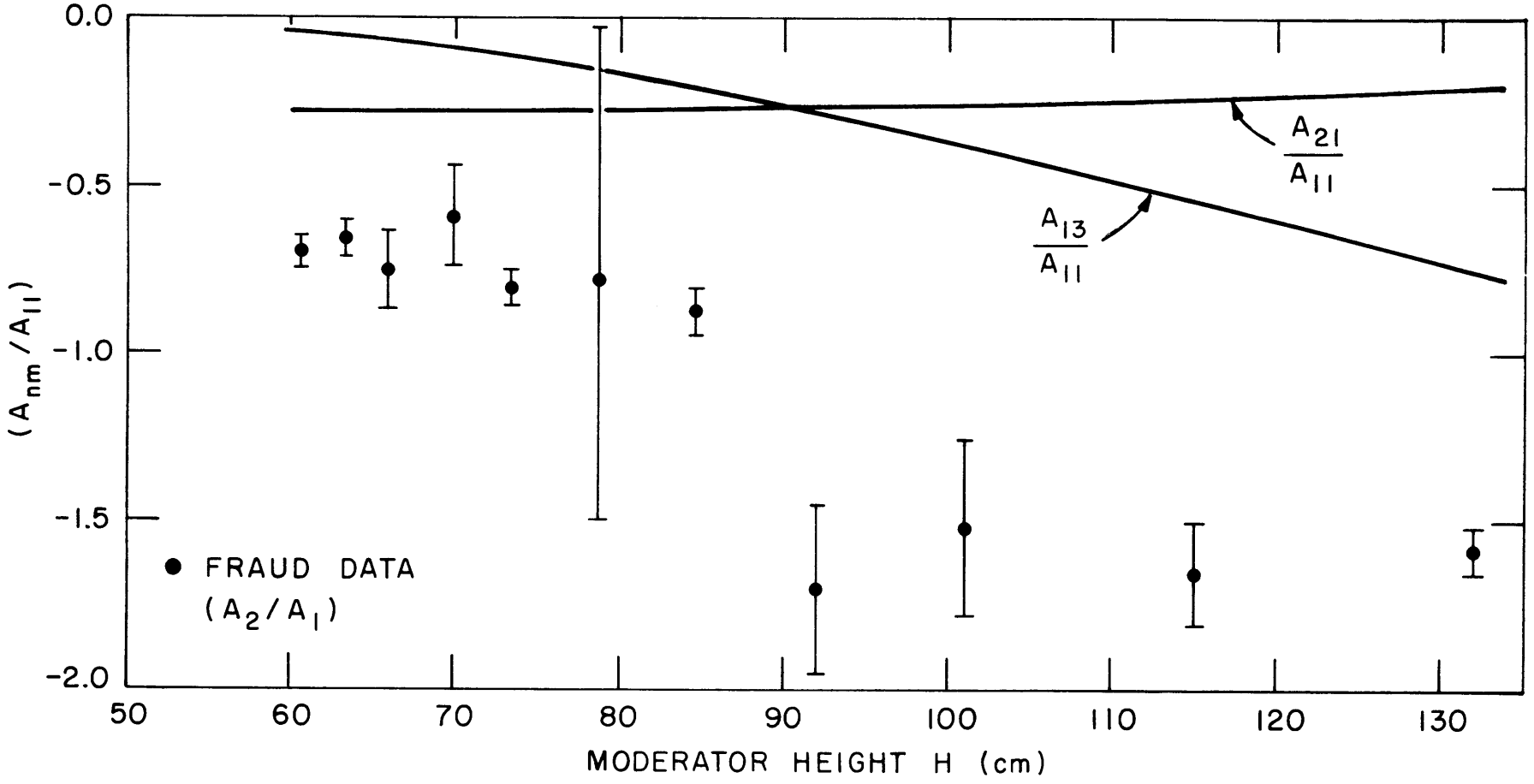

FIG. C.3 THE RATIO A_{nm}/A_{11} AS A FUNCTION OF MODERATOR HEIGHT H FOR THE 500 LATTICE

C.3 DISCUSSION

The comparison of the values of k_∞ based on λ_1 alone and that based on λ_1 and λ_2 reveals excellent agreement within the quoted uncertainties. A similar comparison of the two values of $\overline{\nu\Sigma_a}$ shows agreement just outside the quoted uncertainties. However, the uncertainties in the latter values of k_∞ and $\overline{\nu\Sigma_a}$ are approximately twice those of the former; and hence, for the data at hand, there is no advantage to including values of λ_2 in the least-squares fit.

At the same time, it can be concluded that Eq. (C.1) is a reasonable approximation to the observed neutron density as a function of time over part of the range of the data. However, the relatively large uncertainties in λ_2 (compared to those in λ_1) and the amount of scatter in the values of λ_2 about the fit expression for λ indicate that the contribution of the next higher mode to the neutron density is small enough to render impractical the inclusion of values of λ_2 in the analysis of pulsed source experiments at M. I. T.

The poor agreement between the experimental and theoretical values of (A_2/A_1) is hardly surprising in view of the approximations involved in deriving the expression for the distribution of source neutrons $S(r,z)$ and in using continuous slowing-down theory. However, it is encouraging that the theoretically predicted negative value of the coefficient A_2 is verified experimentally in every case.

APPENDIX D

REFERENCES

A1 Amaldi, E., "The Production and Slowing Down of Neutrons," Handbuch der Physik, edited by S. Flügge, 38, No. 2 (Berlin, Germany: Springer-Verlag, 1958).

B1 Bauman, N. P., "Determination of Diffusion Coefficients for Thermal Neutrons in D_2O at 20, 100, 165 and 200°C," Nuclear Sci. Eng., 14, 179 (1962).

B2 Beckurts, K. H., "Measurements with a Pulsed Neutron Source," Nuclear Sci. Eng., 2, 516 (1957).

B3 Brown, P. S., T. J. Thompson, I. Kaplan, and A. E. Profio, "Measurements of the Spatial and Energy Distribution of Thermal Neutrons in Uranium, Heavy Water Lattices," NYO-10205, MITNE-17 (August, 1962).

C1 Corngold, N., P. Michael, and W. Wollman, "The Time Decay Constants in Neutron Thermalization," Nuclear Sci. Eng., 15, 13 (1963).

C2 Crandall, J. L., et al., "Efficacy of Experimental Physics Studies on Heavy Water Lattices," Heavy Water Lattices: Second Panel Report, Report of a Panel Held in Vienna, 18-22 February, 1963, Technical Report Series No. 20, 503 (Vienna: IAEA, September, 1963).

C3 Crandall, J. L., et al., "Lattice Studies and Critical Experiments in D_2O Moderated Systems," Proceedings of the Third International Conference on the Peaceful Uses of Atomic Energy, 3, 126 (1964).

D1 Von Dardel, G. F., "The Interaction of Neutrons with Matter Studied with a Pulsed Neutron Source," Trans. Roy. Inst. Technology, No. 75 (Stockholm, 1954).

D2 Von Dardel, G. F., and N. G. Sjöstrand, "Diffusion Parameters of Thermal Neutrons in Water," Phys. Review, 96, 1245 (1954).

D3 D'Ardenne, W. H., T. J. Thompson, D. D. Lanning, and I. Kaplan, "Studies of Epithermal Neutrons in Uranium, Heavy Water Lattices," MIT-2344-2, MITNE-53 (August, 1964).

D4 Daughtry, J. W. and A. W. Waltner, "Diffusion Parameters of Heavy Water," Proceedings of a Symposium on Pulsed Neutron Research, Karlsruhe, 10-14 May 1965,1, 65 (Vienna: IAEA, August, 1965).

D5 Daughtry, J. W., and A. W. Waltner, "Temperature Dependence of Thermal Neutron Properties of D_2O," Trans. Am. Nucl. Soc., 7, No. 2, 232 (November, 1964).

D6 De Juren, J. A., "Spectral Correction Analysis of Pulsed Neutron Decay Data," Trans. Am. Nucl. Soc., 7, No. 2, 230 (November, 1964).

D7 Deming, W. E., Statistical Adjustment of Data (New York, N. Y.: Dover Publications, Inc., 1964).

D8 Donahue, D. J., D. D. Lanning, R. A. Bennett, and R. E. Heineman, "Determination of k_∞ from Critical Experiments with the PCTR," Nuclear Sci. Eng., 4, 297 (1958).

D9 Driggers, F. E., "BSQ, An IBM-704 Code to Calculate Heavy Water Lattice Parameters," Heavy Water Lattices: Second Panel Report, Report of a Panel Held in Vienna, 18-22 February, 1963, Technical Report Series No. 20, 551 (September, 1963).

F1 Foulke, L. R., "A Modal Expansion Technique for Space-Time Reactor Kinetics," Ph.D. Thesis, M.I.T. Dept. of Nuclear Engineering (September, 1966).

F2 Friedlander, G., and J. W. Kennedy, Nuclear and Radiochemistry (New York, N. Y.: John Wiley and Sons, Inc., 1955).

G1 Galanin, A. D., Thermal Reactor Theory (New York, N. Y.: Pergamon Press, 1960).

G2 Ganguly, N. K., F. C. Cobb, and A. W. Waltner, "The Diffusion Parameters of Heavy Water," Nuclear Sci. Eng., 17, 223 (1963).

G3 Gardner, D. G., and J. C. Gardner, "Analysis of Multicomponent Decay Curves by Use of Fourier Transforms," Proceedings of a Symposium on Applications of Computers to Nuclear and Radiochemistry, Gatlinburg, Tennessee, 17-19 October, 1962, NAS-NS-3107 (March, 1963).

G4 Glasstone, S. and M. C. Edlund, The Elements of Nuclear Reactor Theory (Princeton, New Jersey: D. Van Nostrand Company, Inc., 1952).

G5 Gon, E., L. Lidofsky, and H. Goldstein, "Pulsed-Source Measurements of Neutron-Diffusion Parameters in Water," Trans. Am. Nucl. Soc., 8, No. 1, 274 (June, 1965).

G6 Gosnell, J., Sc.D. Thesis, M.I.T. Nucl. Eng. Dept. (forthcoming).

G7 Green, R. E., et al., "Highlights of Chalk River Work on the Physics of Heavy Water Lattices Since the 1959 IAEA Panel," Heavy Water Lattices: Second Panel Report, Report of a Panel Held in Vienna, 18-22 February, 1963, Technical Report Series No. 20, 51 (Vienna: IAEA, September, 1963).

G8 Green, R. E., et al., "Lattice Studies at Chalk River and their Interpretation," Proceedings of the Third International Conference on the Peaceful Uses of Atomic Energy, 3, 89 (1964).

H1 Harrington, J., D. D. Lanning, I. Kaplan, and T. J. Thompson, "Use of Neutron Absorbers for the Experimental Determination of Lattice Parameters in Subcritical Assemblies," MIT-2344-6, MITNE-69 (February, 1966).

H2 Thompson, T. J., I. Kaplan, and A. E. Profio, "Heavy Water Lattice Project Annual Report," NYO-9658 (September, 1961).

H3 Lanning, D. D., I. Kaplan, and F. M. Clikeman, Heavy Water Lattice Project Annual Report," MIT-2344-3, MITNE-60 (September, 1964).

H4 Thompson, T. J., I. Kaplan, F. M. Clikeman, and M. J. Driscoll, "Heavy Water Lattice Project Annual Report," MIT-2344-4, MITNE-65 (September, 1965).

H5 "Heavy Water Lattice Project Annual Report," September, 1966 (forthcoming).

H6 Heinemann, R. E., et al., "Experience in the Use of the Physical Constants Testing Reactor," Proceedings of the Second International Conference on the Peaceful Uses of Atomic Energy, 12, 650 (1958).

H7 Hildebrand, F. B., Advanced Calculus for Applications (Englewood Cliffs, N. J.: Prentice Hall, Inc., 1962).

H8 Hildebrand, F. B., Introduction to Numerical Analysis (New York, N. Y.: The Maple Press Co., 1956).

H9 Honeck, H. C., "THERMOS, A Thermalization Transport Theory Code for Reactor Lattice Calculations," BNL-5826 (September, 1961).

H10 Honeck, H. C., and P. Michael, "A Remark on the Measurement of the Diffusion Coefficient for Thermal Neutrons," Nuclear Sci. Eng., 16, 140 (1963).

H11 Hughes, D. J., and R. B. Schwartz, "Neutron Cross Sections," BNL-325 (Second edition, July 1958).

J1 Jones, H. G., A. Robeson, and G. N. Salaita, "Diffusion Parameters of Mixtures of Light and Heavy Water at Several Temperatures," Trans. Am. Nucl. Soc., 8, No. 2, 431 (November, 1965).

K1 Kaplan, I., and A. Travelli, "Notes for Nuclear Reactor Physics I," M.I.T. Nucl. Eng. Dept. (October, 1964).

K2 Klose, H., M. Küchle, and W. Reichardt, "Pulsed Neutron Measurements on Graphite," Proceedings of the Brookhaven Conference on Neutron Thermalization, BNL-719 (C-32), 3, 935 (1962).

K3 Küchle, M., "Measurement on the Temperature Dependence of Neutron Diffusion in Water and Diphenyl by the Impulse Method," Nukleonik, 2, 131 (1960).

K4 Kussmaul, G., and H. Meister, "Thermal Neutron Diffusion Parameters of Heavy Water," Journal of Nuclear Energy A/B, 17, 411 (1963).

L1 Lamarsh, J. R., Introduction to Nuclear Reactor Theory (Reading, Massachusetts: Addison-Wesley Publishing Company, Inc., 1966).

L2 Lanning, D. D., (Personal communication).

L3 Lopez, W. M., and J. R. Beyster, "Measurement of Neutron Diffusion Parameters in Water by the Pulsed Source Method," Nuclear Sci. Eng., 12, 190 (1962).

M1 Malaviya, B. K., I. Kaplan, T. J. Thompson, and D. D. Lanning, "Studies of Reactivity and Related Parameters in Slightly Enriched Uranium, Heavy Water Lattices," MIT-2344-1, MITNE-49 (May, 1964).

M2 Malaviya, B. K., and A. E. Profio, "Measurement of the Diffusion Parameters of Heavy Water by the Pulsed-Neutron Technique," Trans. Am. Nucl. Soc., 6, No. 1, 58 (June, 1963).

M3 Meister, H., "Pulsed Neutron Experiments on Subcritical Heavy Water Natural Uranium Lattices," Journal of Nuclear Energy A/B, 17, 97 (1963).

M4 Möller, E., "Neutron Moderation Studied by the Time-Dependent Reaction Rate Method," Proceedings of a Symposium on Pulsed Neutron Research, Karlsruhe, 10-14 May, 1965, 1, 155 (Vienna: IAEA, August, 1965).

M5 Morse, P. M. and H. Feshbach, Methods of Theoretical Physics, Part I (New York, N. Y.: McGraw-Hill Book Company, Inc., 1953).

N1 Nelkin, M., "The Diffusion Cooling of Neutrons in Finite Media," Journal of Nuclear Energy A/B, 8, 48 (1958).

N2 Nelkin, M., "The Decay of the Thermalized Neutron Pulse," Nuclear Sci. Eng., 7, 210 (1960).

P1 Palmedo, P. F., I. Kaplan, and T. J. Thompson, "Measurements of the Material Bucklings of Lattices of Natural Uranium Rods in D_2O," NYO-9660, MITNE-13 (January, 1962).

P2 Parks, P. B., and N. P. Bauman, "Pulsed Measurements of Neutron-Diffusion Parameters in D_2O," Trans. Am. Nucl. Soc., 8, No. 2, 436 (November, 1965).

P3 Peak, J., I. Kaplan, and T. J. Thompson, "Theory and Use of Small Subcritical Assemblies for the Measurement of Reactor Parameters," NYO-10204, MITNE-16 (April, 1962).

P4 Pershagen, B., "Heavy Water Lattice Calculations in Sweden," Heavy Water Lattices: Second Panel Report, Report of a Panel Held in Vienna, 18-22 February, 1963, Technical Report Series No. 20, 257 (Vienna: IAEA, September, 1963).

P5 Pilat, E. E., Ph.D. Thesis, M.I.T. Nucl. Eng. Dept. (forthcoming).

P6 Profio, A. E., and J. D. Eckard, "Investigations of Neutron Moderation with a Pulsed Source," Nuclear Sci. Eng., 19, 321 (1964).

R1 "Reactor Physics Constants," ANL-5800 (Second edition, July, 1963).

R2 Radkowsky, A., "Temperature Dependence of Thermal Transport Mean Free Path from Experimental Data on Scattering Cross Section of Water," ANL-4476 (1950).

S1 Sefchovich, E., Sc.D. Thesis, M.I.T. Nucl. Eng. Dept. (forthcoming)

S2 Simms, R., I. Kaplan, T. J. Thompson, and D. D. Lanning, "Analytical and Experimental Investigations of the Behavior of Thermal Neutrons in Lattices of Uranium Metal Rods in Heavy Water," NYO-10211, MITNE-33 (October, 1963).

S3 Starr, E., and J. Koppel, "Determination of Diffusion Hardening in Water," Nuclear Sci. Eng., 14, 224 (1962).

S4 Stevenson, P. C., "Processing of Counting Data," NAS-NS-3109 (September, 1965).

U1 Utzinger, E., W. Herr, and H. R. Lutz, "Pulsed-Source Experiments with Multiplying and Non-Multiplying Heavy Water Systems," Proceedings of a Symposium on Pulsed Neutron Research, Karlsruhe, 10-14 May, 1965, 2, 119 (Vienna: IAEA, August, 1965).

W1 Wade, J. W., "Neutron Age in Mixtures of D_2O and H_2O," Nuclear Sci. Eng., 4, 12 (1958).

W2 Weitzberg, A., I. Kaplan, and T. J. Thompson, "Measurements of Neutron Capture in U-238 in Lattices of Uranium Rods in Heavy Water," NYO-9659, MITNE-11 (January, 1962).

W3 Westfall, F. R., and A. W. Waltner, "Measurements of Natural Uranium Heavy-Water Lattices by the Pulsed Neutron Technique," Trans. Am. Nucl. Soc., 5, No. 2, 386 (November, 1962).

W4 Wolberg, J. R., T. J. Thompson, and I. Kaplan, "A Study of the Fast Fission Effect in Lattices of Uranium Rods in Heavy Water," NYO-9661, MITNE-15 (February, 1962).

W5 Woodruff, G. L., I. Kaplan, and T. J. Thompson, "A Study of the Spatial Distribution of Fast Neutrons in Lattices of Slightly Enriched Uranium Rods Moderated by Heavy Water," MIT-2344-5, MITNE-67 (November, 1965)

W6 Worthing, A. G., and J. Geffner, Treatment of Experimental Data (New York, N. Y.: John Wiley and Sons, Inc., 1943).